PFC/RR-81-27

DOE UC-20 C, D, E

TRITIUM PERMEATION MODELLING OF A CONCEPTUAL FUSION REACTOR DESIGN

D. R. Hanchar
M. S. Kazimi

July 1981

Plasma Fusion Center
and the
Deparment of Nuclear Engineering
Massachusetts Institute of Technology
Cambridge, Massachusetts 02139

Prepared for
E.G. & G. Idaho, Inc.
and
The U.S. Department of Energy
Idaho Operations Office
under
DOE Contract #DE-AP07-79ID00019

PUBLICATIONS UNDER CONTRACT #K-1702

ON FUSION SAFETY

1. M. S. Kazimi et al., "Aspects of Environmental Safety Analysis of Fusion Reactors," MITNE-212, Dept. of Nuclear Engineering, M.I.T., October 1977.

2. R. W. Sawdye, J. A. Sefcik, M. S. Kazimi, "Reliability Requirements for Admissible Radiological Hazards from Fusion Reactors," Trans. Am. Nucl. Soc. 27, 65-66, November 1977.

3. D. A. Dube, M. S. Kazimi and L. M. Lidsky, "Thermal Response of Fusion Reactor Containment to Lithium Fire," 3rd Top. Meeting in Fusion Reactor Technology, May 1978.

4. R. W. Sawdye and M. S. Kazimi, "Application of Probabilistic Consequence Analysis to the Assessment of Potential Radiological Hazards of Potential Hazards of Fusion Reactors," MITNE-220, Dept. of Nuclear Engineering, M.I.T., July 1978.

5. D. A. Dube and M. S. Kazimi, "Analysis of Design Strategies for Mitigating the Consequences of Lithium Fire within Containment of Controlled Thermonuclear Reactors," MITNE-219, Dept. of Nuclear Engineering, M.I.T., July 1978.

6. R. W. Sawdye and M. S. Kazimi, "Fusion Reactor Reliability Requirements Determined by Consideration of Radiological Hazards," Trans. Am. Nucl. Soc. 32, 66, June 1979.

7. R. W. Green and M. S. Kazimi, "Safety Considerations in the Design of Tokamak Toroidal Magnet Systems," Trans. ANS 32, 69, June 1979.

8. R. W. Green and M. S. Kazimi, "Aspects of Tokamak Toroidal Magnet Protection," PFC/TR-79-6, Plasma Fusion Center, M.I.T., July 1979.

9. S. J. Piet and M. S. Kazimi, "Uncertainties in Modeling of Consequences of Tritium Release from Fusion Reactors," PFC/TR-79-5, Plasma Fusion Center, M.I.T., July 1979.

10. M. J. Young and S. J. Piet, "Revisions to AIRDOS-II," PFC/TR-79-8, Contract #K-1702, Plasma Fusion Center, M.I.T., August 1979.

11. S. J. Piet and M. S. Kazimi, "Implications of Uncertainties in Modeling of Tritium Releases from Fusion Reactors," Proc. Tritium Technology in Fission, Fusion and Isotopic Applications, April 1980.

12. M. S. Tillack and M. S. Kazimi, "Development and Verification of the LITFIRE Code for Predicting the Effects of Lithium Spills in Fusion Reactor Containments, PFC/RR-80-11, Plasma Fusion Center, M.I.T., July 1980.

Publications Under Contract #K-1702 (continued)

13. M. S. Kazimi and R. W. Sawdye, "Radiological Aspects of Fusion Reactor Safety: Risk Constraints in Severe Accidents," J. of Fusion Energy, Vol. 1, No. 1, pp. 87-101, January 1981.

14. P. J. Krane and M. S. Kazimi, "An Evaluation of Accidental Water-Reactions with Lithium Compounds in Fusion Reactor Blankets," PFC/RR-81-26, Plasma Fusion Center, M.I.T., July 1981.

15. D. R. Hanchar and M. S. Kazimi, "Tritium Permeation Modelling of a Conceptual Fusion Reactor Design," PFC/RR-81-27, Plasma Fusion Center, M.I.T., July 1981.

TRITIUM PERMEATION MODELLING OF A CONCEPTUAL FUSION REACTOR DESIGN

ABSTRACT

The environmental and economic acceptability of presently conceived D-T fueled fusion power plants will depend in large part on the ability to contain and handle tritium within the reactor building and to control tritium releases to the environment without incurring exorbitant costs. In order to analyze the time evolution (from reactor start-up) of the inventories, a transient tritium permeation model was developed based on a simplified conceptual fusion reactor design. The major design constraints employed in the model for the fusion plant were the use of a solid breeder blanket, a low pressure purge gas in the blanket and a high pressure (helium) primary coolant. Both diffusive hold-up and solubility considerations were found to be important contributors to the solid breeder tritium inventory, while the fluid resistance to permeation offered by the primary coolant in the heat transfer loop, although included in the model, was found to be negligible compared to the resistance offered by the primary containment metal. Using the STARFIRE-Interim Reference Design system parameters as input, the model predicted a total tritium inventory of approximately 4.5 kg after 18 days for the Li_2O breeder. The addition of oxygen (up to a partial pressure of 10^{-13} torr) to the primary coolant loop was required in order to keep the tritium losses through the heat exchanger (and hence, to the environment) to within the design goal of 0.1 Ci/day.

A steady-state tritium permeation model for determining fluid--or metal--limited transport was formulated and applied to the STARFIRE-Interim and GA Field-Reversed Mirror Reference Designs. It was shown that only with a reduction in tritium partial pressure in the main coolant loop caused by the presence of oxygen, would the transport properties of a helium coolant become important for tritium migration.

ACKNOWLEDGEMENTS

The authors express their gratitude to Professor Kenneth Russell for valuable comments and to Kevin Burns for his support in setting up the calculational schemes.

This report is based on a thesis submitted by the first author as part of the requirements for the M.S. degree in Nuclear Engineering at M.I.T.

TABLE OF CONTENTS

TABLE OF CONTENTS

(continued)

TABLE OF CONTENTS
(continued)

LIST OF FIGURES

LIST OF FIGURES
(continued)

LIST OF FIGURES
(continued)

LIST OF TABLES

LIST OF TABLES
(continued)

NOMENCLATURE

A	surface area of:	(cm^2)
	A_{CP} "cold" pipe metal	
	A_{HP} "hot" pipe metal	
	A_{HX} heat exchanger	
	A_m breeder tube metal	
A_f	flow area	(cm^2)
C	average tritium concentration in:	(Ci/cm^3)
	C_b breeding material	
	C_c primary coolant	
	C'_c primary coolant (corrected for oxygen addition)	
	C_{CP} "cold" pipe metal	
	C_{HP} "hot" pipe metal	
	C_{HX} heat exchanger	
	C_m breeder tube metal	
	C_p breeder pellet	
	C_{pg} purge gas	
	C_{sol} breeder pellet surface (from solubility considerations)	
	C_∞ environment/building atmosphere	
C_p	specific heat	($J/gm\text{-}^oK$)
d	equivalent diameter of:	(cm)
	d_B primary coolant tube in blanket	
	d_{HX} primary coolant (shell side) in heat exchanger	
	d_p primary coolant in pipe	

d_{pg} purge gas channel

D tritium diffusivity in: (cm^2/sec)

- D_b breeder material
- D_{CP} "cold" pipe metal
- D_G helium gas
- D_{HP} "hot" pipe metal
- D_{HX} heat exchanger
- D_m breeder tube metal

D^o tritium diffusion coefficient at infinite temperature (cm^2/sec)

f fractional release (ref. Equation (2.2))

f_c coolant clean-up flow rate (coolant inventories/day)

G_{He} mass flux of helium (gm/cm^2-sec)

h mass transfer coefficient in: (cm/sec)

- h_B primary coolant in blanket
- h_{CP} primary coolant in "cold" leg
- h_{HP} primary coolant in "hot" leg
- h_{HX} primary coolant in heat exchanger
- h_{pg} purge gas

HX heat exchanger

I tritium inventory in: (Ci)

- I_b breeder material
- I_c primary coolant
- I'_c primary coolant (corrected for oxygen addition)

	I_{pg}	purge gas
J	tritium flow rate	(Ci/sec)
	J_b	total tritium leakage rate from breeder into purge gas
	J_{CL}	tritium loss rate from primary coolant to environment/ building atmosphere
	J_{CPL}	tritium loss rate from primary coolant through "cold" pipe
	J_{film}	tritium transport through fluid film
	J_{fluid}	tritium transport rate through fluid ($\equiv J_F$)
	J_{HPL}	tritium loss rate from primary coolant through "hot" pipe
	J_{HXL}	tritium loss rate from primary coolant through heat exchanger
	$J_{HXL,max}$	maximum allowable tritium loss rate through heat exchanger
	J_{metal}	tritium permeation rate through metals ($\equiv J_M$)
k	thermal conductivity	($W/m-^oK$)
k_{ads}	number of T_2 molecules striking the metal surface per unit area (ref. Equation (4.2))	
K_H	Henry's Law Constant	(cm^3-T_2/cm^3 torr)
K_{H_2O}	equilibrium constant	(ref. Equation (D.4))
K_p	permeability	($cm^3-T_2/cm-sec-torr^{\frac{1}{2}}$)
K_p^o	permeability at infinite temperature	($cm^3-T_2/cm-sec-torr^{\frac{1}{2}}$)
K_s	Sieverts' Constant (solubility)	($cm^3-T_2/cm^3-torr^{\frac{1}{2}}$)
K_s^o	Sieverts' Constant at infinite temperature	($cm^3-T_2/cm^3-torr^{\frac{1}{2}}$)

K_{T_2O} equilibrium constant (ref. Equation (2.77))

L length of the: (cm)

- L_{CP} "cold" pipe segment
- L_{HP} "hot" pipe segment
- L_{HX} heat exchanger

L_p volumetric tritium leakage rate from one pellet ($Ci/sec\text{-}cm^3$)

m_b total mass of breeder material (gm)

M oxide film quality factor

M_1, M_2 molecular weight (ref. Equation (C.5))

n number of moles of:

- n_{pg} tritium gas in purge gas
- n_{T_2} tritium gas in primary coolant
- n'_{T_2} tritium gas in primary coolant (corrected for oxygen addition)
- n_{T_2O} T_2O gas in primary coolant

N number of:

- N_c primary coolant tubes in blanket
- N_p breeder pellets in blanket
- N_{pg} purge gas channels in blanket
- N_t tubes in heat exchanger

Nu Nusselt Number (ref. Equation (2.51))

P^* transition tritium partial pressure (ref. Figure 2-14)

P^{**} transition tritium partial pressure (ref. Figure 2-14)

P_{He} helium pressure (torr)

P_{pg} partial pressure of tritium gas in purge gas (torr)

P_T transition pressure from fluid- to metal- limited permeation (ref. Equation (4-10))

P_{T_2} partial pressure of tritium gas

P_w wetted perimeter (cm)

Q volumetric flow rate of: (cm^3/sec)

- Q_B primary coolant in blanket
- Q_{CP} primary coolant in "cold" leg
- Q_{HP} primary coolant in "hot" leg
- Q_{HX} primary coolant in heat exchanger
- Q_{pg} purge gas

Q energy (cal)

- Q_d activation energy for diffusion
- Q_p activation evergy for the permeation process
- Q_s heat of solution

r radial dimension (cm)

- r_g grain radius
- r_p pellet radius

R resistance to tritium permeation offered by: (sec/cm^3)

- R_{CL} "hot" leg, heat exchanger, "cold" leg fluid and metal (in parallel)
- R_{CPL} "cold" leg coolant fluid and "cold" pipe metal (in series)
- R_{film} fluid film next to metal wall ($\equiv R_F$)

R_{HPL} "hot" leg coolant film and "hot" pipe metal (in series)

R_{HXL} heat exchanger coolant film and metal (in series)

R_m breeder tube metal

R_{mc} blanket coolant film

R_{metal} metal wall ($\equiv R_M$)

R_{pgc} purge gas film, breeder tube metal, blanket coolant film (in series)

R_{pgm} purge gas film

Re Reynolds Number of: (ref. Equation (2.50))

Re_B primary coolant in blanket

Re_{CP} primary coolant in "cold" leg

Re_{HP} primary coolant in "hot" leg

Re_{HX} primary coolant in heat exchanger

Re_{pg} purge gas

S total tritium generation rate (Ci/sec)

S_b volumetric tritium generation rate (Ci/cm^3-sec)

Sc Schmidt Number of: (ref. Equation (2.51))

Sc_B primary coolant in blanket

Sc_{CP} primary coolant in "cold" leg

Sc_{HP} primary coolant in "hot" leg

Sc_{HX} primary coolant in heat exchanger

Sc_{pg} purge gas

Sh Sherwood Number

SOL amount of tritium dissolved in a metal (Ci/cm^3)

T temperature of: (^{o}C)

- T_b breeder pellet (average)
- T_c primary coolant
- T_{edge} pellet surface
- T_{pg} purge gas

T tritium atom

T_2 tritium gas molecule

u flow velocity of: (cm/sec)

- u_B primary coolant in blanket
- u_{CP} primary coolant in "cold" leg
- u_{HP} primary coolant in "hot" leg
- u_{HX} primary coolant in heat exchanger
- u_{pg} purge gas

v diffusion volume (ref. Equation (C.5))

V volume of: (cm^3)

- V_b breeder material
- V_c primary coolant in:
  - V_{c_B} blanket
  - $V_{c_{CP}}$ "cold" leg
  - $V_{c_{HP}}$ "hot" leg
  - $V_{c_{HX}}$ heat exchanger
- V_{pg} purge gas

w mass flow rate of: (gm/sec)

- w_B primary coolant in blanket

w_{CP} primary coolant in "cold" leg

w_{HP} primary coolant in "hot" leg

w_{HX} primary coolant in heat exchanger

w_{pg} purge gas

w_F primary coolant clean-up mass flow rate (from fluid-limited transport considerations) (gm/sec)

w_M primary coolant clean-up mass flow rate (from metal-limited transport considerations) (gm/sec)

x thickness of: (cm)

x_{CP} "cold" pipe metal

x_{HP} "hot" pipe metal

x_{HX} heat exchanger metal

x_m breeder tube metal

X_T atom fraction of tritium in solid

Greek Symbols

α	thermal diffusivity	(cm^2/sec)
α_-^-	sensitivity coefficient	(ref. Appendix E)
μ	absolute viscosity	($gm/cm\text{-}sec$)
ν	kinematic viscosity	(cm^2/sec)
ρ	mass density	(gm/cm^3)
τ	extraction time (ref. Equation (2.2)) (sec)	
τ_c	time constant for primary coolant system dynamics (sec)	
$\tau_{<C>}$	time constant for diffusive pellet concentration dynamics (sec)	
$\tau_{<C_p>}$	time constant for average pellet concentration dynamics (sec)	
τ_{J_b}	time constant for breeding zone leakage rate dynamics (sec)	
τ_{pg}	time constant for purge gas system dynamics (sec)	
τ_{sol}	time constant for solubility pellet concentration dynamics (sec)	

CHAPTER 1 INTRODUCTION

Recent advances in the confinement of thermonuclear plasmas have stimulated worldwide interest in the development and operation of prototypic fusion reactor power plants. As a result of these advances, technological and engineering aspects of controlled thermonuclear plants have become increasingly important. In a number of preliminary studies[1-3], attempts have been made to evaluate the major problem areas confronting the designers of fusion reactor facilities. One such problem area addressed in this thesis will be that of tritium transport within a fusion power plant, and possible tritium permeation from the containment and into the environment.

As the only significant mobile radionuclide existing in proposed deuterium/tritium (D-T)-burning fusion devices, tritium is the focus of considerable attention in evaluation of the overall safety and environmental impact of these devices. From practical considerations, tritium has to be bred at a rate equal to, or greater than, the rate at which it is being consumed, due to its negligible natural abundance and high cost of external breeding. A review of the plant designs proposed thus far indicates that during operation, an appreciable quantity of tritium will be present in the plasma fuel, exhaust system, breeder blanket and the extraction systems. With total tritium inventories in the range 10-50 kg for a 5000 MW_t plant, it is inevitable that some tritium releases to the environment will occur. The need to minimize these releases will necessarily influence any reactor design and operation.

Tritium losses to the environment must be strictly controlled because of its radiological activity and capability of assimilation into living tissues if breathed in. Therefore, based on anticipated standards, tritium releases in excess of 3000 Ci/year/1000 MW_t may begin to constitute an objectionable radiologic hazard to the environment[4]. Although fission plants are required to operate under similar emission ceilings, fusion power plants will be much more difficult to master than fission plants with respect to tritium. Inventories will be much higher and the tritium will be continuously cycled through the

fuel system at very high rates. Dismissing isotopic correction factors, tritium will diffuse through most metals at the same high rate that hydrogen does. It is this inherent property of low mass elements like tritium, of having a high permeability in most metals, that makes it difficult to contain, and hence is the root cause of most of the tritium released to the environment.

Reliable estimates of the magnitude of anticipated steady-state releases of tritium from fusion plants have been difficult to derive because they depend in large part on having detailed knowledge of the tritium inventory size and disposition, and the design features and operating characteristics of all the tritium-intensive subsystems. Although all the tritium loss mechanisms from fusion plants under accident and non-accident conditions cannot be completely defined until actual operating experience with experimental-scale reactors has been acquired, it is possible to outline a few loss mechanisms that are plausible. As currently envisioned the principal tritium loss mechanisms under non-accident conditions are[5]:

1 - leakage through fabrication imperfections and fluid system connections: shaft seals, pinhole ruptures, valves, pumps, etc.

2 - releases incurred during maintenance operations (routine and otherwise)

3 - losses resulting from waste disposal operations and during the course of waste interrment

4 - permeation through elevated temperature surfaces (particularly coolant pipes and heat exchangers) in the primary containment.

The nature of these loss mechanisms in the context of fusion plants has been adequately described elsewhere[6]. Tritium releases during normal operations which occur as a result of Number 4 were the major focus of this study. Tritium releases as a result of accidents were not within the scope of this study and losses numbered 1 through 3 above were not studied because of lack of design detail.

In order to calculate the permeation losses of tritium from the coolant loop (piping runs and steam generators), as it reaches (maximum) steady-state value, it is necessary to model the build-up of the tritium partial pressure in the coolant which is the driving force behind the permeation. Similarly, the time evolution of tritium in the coolant system, starting from system start-up, is dependent on the kinetics of the tritium source, which for the purposes of this study, is taken to be the breeder blanket. Because of the numerous system components separating the rather large tritium inventory in the breeder from the loss points--in the coolant system--and the total resistance (in series) to tritium flow that they represent, it has been speculated[7] that the fusion plant may never reach its steady-state permeation loss from the coolant system, or that it takes such a long time after start-up to be of little immediate concern. This study was initiated in order to evaluate the distribution and leakage profiles for tritium in a typical commercial tokamak reactor as they evolve from system start-up. These profiles are determined by the technical features of the reactor design. It is then possible to establish critical system parameters with regard to tritium transport, and also approximate values for tritium inventories, which can be expected to have an important bearing on the operational characteristics of the modelled design.

The purpose of the proposed transient tritium permeation model for a conceptual fusion reactor design is to provide an analytical method for calculation of the time-varying concentration of the tritium in various reactor subsystems during the transient condition associated with normal start-up procedures. This involves specification of the major reactor components: breeder blanket, tritium recovery system, and primary coolant system. The results of this model based on tritium behavior within the aforementioned reactor components, will provide a description of the total (time-dependent) tritium inventory of the plant excluding the fueling and storage systems, and the corresponding temporal rise in tritium leakage to the environment until it reaches its steady - state value.

The characteristic times for these points of interest to reach steady-state are of considerable importance. They affect both the internal and the external (interfacing with the environment) operations of a fusion

power plant. A breeder that does not diffuse tritium into a processing stream fast enough, or does not attain a steady-state inventory for a long time (the designed-for tritium source) may then adversely affect the economics of refueling the reactor. The need to keep on hand extra supplies of tritium in addition to the initial start-up inventory is very costly, not to mention potentially hazardous in its handling and storage.

At the final step in the tritium pathway to the environment--the heat exchanger which interfaces the primary coolant with the secondary (usually water/steam)--is a potential window to tritium permeation. Although considerable attention has been given to decrease the vulnerability of the heat exchanger to tritium losses, there is no way to preclude all tritium from leaking out. The numerous permeation barriers that have been proposed in light of this problem are not the major consideration here, rather the time it takes to build up a significant tritium partial pressure in the coolant causing tritium permeation through, and escape from, the heat exchangers. It might indeed be possible to show that this does not occur until a relatively long time from reactor start-up. But to conclude that steady-state losses will not be incurred within the reactor lifetime as does Mintz et al.[7], is questionable. Most reference designs have used a steady-state analysis for limiting tritium emissions from the plant. Granted, this is the most conservative approach, but to prove that steady-state losses do not ever occur until much later in the reactor cycle, could have significant impact on designing critical system components. A possible scheme for increasing the coolant loop's resistance to permeation losses as a means of adjustment to a very slow build-up in tritium partial pressure may be warranted.

The transient permeation model that is developed in this study can only be used in modelling tritium behavior within the reactor subsystems for times after start-up (assumes all initial tritium concentrations to be zero), until steady-state is achieved. Although this in itself produces useful results as was explained earlier, a natural extension of this model would be to include transients from the steady-state condition: overpower transients where the blanket temperature is well above average, and loss of pumping power in the tritium extraction system. Both might lead to consid-

erable tritium inventories in the blanket--where this tritium migrates to, and how fast, are questions important to fusion reactor safety. Although this area of concern is out of the scope of the present study, some insight can be gained from the description of the kinetics of tritium transport used in the present model, and applied to the aforementioned transients. One such case will be briefly treated in the Conclusions section of this report.

The format of this study on tritium permeation evolves in a straightforward manner, beginning with model development and methodology, leading to its application to a documented fusion power reactor design, some additional thoughts concerning the principle of resistance to permeation developed earlier, and finally, discussion of the results and merits of the model.

Chapter 2 encompasses the whole of the transient permeation model that was used in the remainder of the study. Perhaps most importantly the assumptions about tritium behavior--both dissolution and diffusion--are largely enumerated upon in this chapter, as well as what was neglected in the representation of the specific reactor subsystems. Given the simplified (yet adequate) tritium behavior characteristics and the outline for the representative fusion reactor, the formulation of the equations for the transient permeation model easily followed.

Chapter 3 describes the direct application of the permeation model developed in Chapter 2. The STARFIRE-Interim design[8] was chosen as the case study for reasons given in the chapter introduction. A separate appendix (Appendix F) was used to present a detailed description of how the system parameters for STARFIRE-Interim were determined. The Conclusion section of the case study includes the predictions for tritium inventories in different parts of the plant, the losses to the environment and characteristic time constants, based on the model equations. Of course, proper choice of the STARFIRE-Interim system parameters as input to the permeation model is crucial to the outcome, as the comparison with the actual design report's figures will demonstrate.

Chapter 4 discusses the relative importance of including the resistance to tritium migration offered by a fluid (or gas) and a metal in series. The characterization of this effect follows closely the method developed

by Zarchy and Axtmann[9] in their attempt to define coolant-limited and metal-limited regimes for tritium permeation. The work is expanded from their results with UWMAK-II[10] parameters, to original studies on GA Field-Reversed Mirror Fusion Reactor[11] (FRM) and STARFIRE-Interim parameters.

Chapter 5 concludes the work done on transient permeation modelling and the results obtained by its application to the STARFIRE-Interim design. In the process of making the run, several vital bits of information were estimated, and thus suggestions are made as to what is needed in an expanded data base. Pertinent information to the specific model plus other data needed to improve tritium technology in general are identified. Suggestions for areas of model improvement other than in the data base (breeder and metal properties) are included with special attention given to the inclusion of off-normal transients mentioned earlier.

The transient permeation model developed herein is only a first step in describing tritium behavior throughout a fusion reactor's major components even before steady-state is achieved. However, the simplifications employed in the design itself, and the assumptions concerning tritium behavior, are not without merit. The results from this model can be used as good indicators of the effect solubility, purge gas flow rate and tritium diffusivities in metals have on tritium inventories in, and losses from, fusion power plants. Once such problems are recognized, those areas can be investigated more thoroughly and described in greater detail and more accurately than the present model permits. But with the understanding that this is a first attempt at modelling the transport of tritium for an entire system design before steady-state is achieved, the results can significantly impact on the choice for critical system parameters in future reference designs.

CHAPTER 2 TRANSIENT MODEL FOR TRITIUM PERMEATION

2.1 Introduction

Questions raised relative to the impact of potential radioactive emissions of a fusion reactor have led to a critical examination of tritium behavior within the plant. Tritium-related engineering problems can be divided into three broad categories: containment, recovery and recycling. Containment includes all the steps undertaken to minimize the release of tritium into the environment. Primary containment refers to the barrier to tritium loss imposed by the boundary of any system that can be expected to carry any tritium, e.g., vessel and piping walls. Secondary containment consists of the immediate reactor building volume which is capable of trapping the tritium that escapes the reactor components enclosed within it. Both primary and secondary containment systems are designed to operate as high integrity barriers so that the tritium released to the environment will be kept to a minimum. Figure 2-1 shows the most general sequence of tritium flows in a fusion power plant; the secondary containment is dashed in to demonstrate the reactor sub-systems included within it.

The second tritium-intensive process is recovery of the bred tritium in the blanket and subsequent transport to a processing system somewhere outside the reactor vessel's walls. This is accomplished in one of two ways, or some combination of the two. Tritium bred in the blanket is swept into a purge gas stream and recovery of tritium easily follows upon processing of this gas. The second method is to let the tritium diffuse from the blanket into the primary coolant, where tritium is extracted from a small bypass flow. Both methods are represented in the drawing; the tritium extraction from the heat transfer circuit is only dashed in because it is not the preferred choice for this model.

The reactor design must include in addition to the recovery systems for bred tritium, the handling of tritium in the plasma fueling and exhaust system. This includes recycling the tritium from what is being bred by pumping it from the processing and/or storage units to the injection system, and the processing of the plasma exhaust in order to sep-

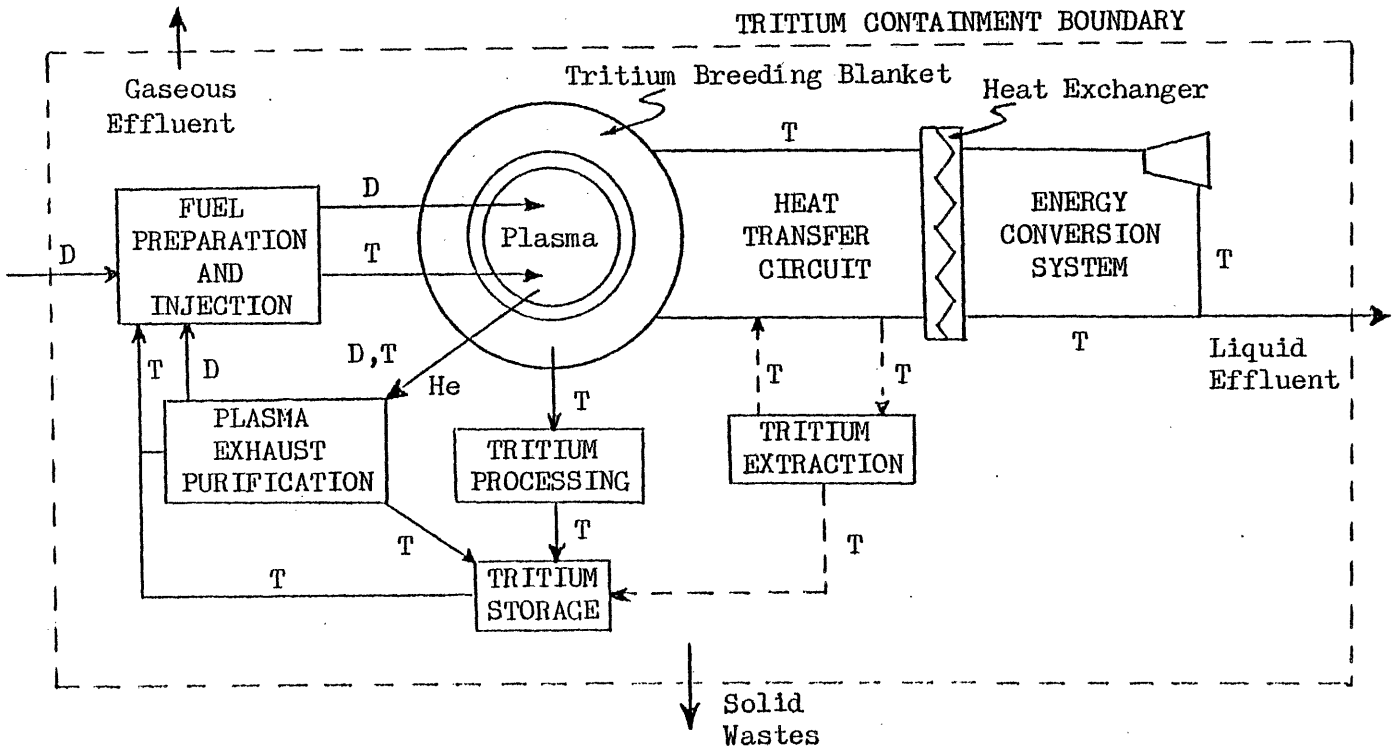

Figure 2-1

Tritium Flows in a Fusion Power Plant

arate the hydrogen isotopes from helium and other heavier, plasma impurities. All the recycling and injection equipment are surrounded by the secondary containment as shown in Figure 2-1.

In order to give due consideration to the practical aspects of those design features which have the greatest influence on tritium inventories and leakage rates, it is necessary to identify the critical tritium release path. The migration pathway that is likely to make the greatest single contribution to the total tritium release from fusion plants and one of the more difficult pathways to deal with, is the continual permeation of tritium from the blanket region into the primary coolant and on from there through the sequence of heat exchangers and working fluids (namely water). The problem arises not so much be-because the tritium partial pressure is likely to reach significant levels in the blanket and interconnecting regions, but because the heat transfer interfaces (which, in this instance, are mass transfer interfaces) which couple the blanket, coolant and working fluids are large in surface area, relatively thin and of necessity, at elevated temperatures. Thus, the principal tritium leakage pathway to the environment for currently conceived D-T fueled fusion power plants appears to be the heat transfer circuit. In Figure 2-1 this is represented by the presence of tritium in the energy conversion loop where water is assumed to be the working fluid.

Once tritium diffuses into the steam system it is isotopically diluted to such an extent that separation and recovery of this tritium would be prohibitively expensive. Since the tritium that enters the steam circuit is immediately transformed into water, it is emitted to the environment as a liquid effluent. Effective water containment could be useful to prevent major tritium releases in the event that a sudden major equipment failure occurs, but it cannot serve as a routine method for tritium control. The piping and the internal heat transfer surfaces of the heat exchanger (or equivalently, the steam gnerator) are the one portion of the fusion power plant which cannot be protected by a further containment system.

The secondary containment system covers the rest of the coolant piping and reactor vessel. The volume enclosed is continuously flushed and processed to remove the tritium leaking from the blanket or coolant piping. A high-integrity containment boundary prevents any further leakage of this tritium that has been oxidized while in the containment building atmosphere, to the environment. PPPL[2] was one of the first designers to propose double-walled piping and vessels as an extension of the primary containment concept, in order to further reduce tritium leakage into the plant atmosphere. Specification of such "double - jacketing" is tempting, but could prove to be very expensive and difficult to engineer on large diameter pipe runs (as anticipated for the heat transfer circuit), particularly if periodic pipe and equipment inspection is required, as it is now for fission power plants.

As in most recent conceptual designs of fusion power reactor systems including those from ORNL[12], PPPL[2] and Wisconsin[10], a controlling parameter has always been the allowable loss to the environment. From the previous discussion it has been shown that the single most important contributor to tritium release to the environment is the tritium migration pathway represented by the coolant/HX/steam systems. Tritium that makes its way into the secondary containment is assumed to be greater than 90 % recoverable[6], and hence is not considered important in calculating releases to the environment.

It is now possible to focus attention on the unintentional transport of tritium from its point of origin -- assumed to be only the breeder blanket -- through the primary coolant, to its point of departure -- the heat exchanger -- and into the steam system where it is assumed to be effectively lost to the environment. The primary coolant is the sole medium through which the tritium migrates from the blanket to the heat exchanger and hence, the permeation model will concentrate on this loop, as well as the breeder processing stream which necessarily affects the amount of tritium diffusing into the coolant. The recycling and injection loops are not modelled, nor the tritium processing and storage units. They are all vital for tritium handling considerations, but are not assumed to be of consequence for tritium release control. It is the expressed purpose of this model to present a systematic method of tracking

tritium diffusion in the breeder and subsequent permeation paths to the environment via the heat exchanger and power conversion cycle (operating directly with water).

It is also the purpose of this permeation model to be general enough in its reactor description so as to be applicable for several designs currently being proposed. A few of the more important aspects of this model that could limit its applicability to all fusion reactor designs are its use of a solid lithium compound as the breeding agent, a helium purge gas running through the breeder which acts as the sole tritium extraction system, and a high-pressure helium gas as the primary coolant. The reasons for making each of these major design choices are briefly discussed below.

Minimization of the chemical energy that may be released during accidents in fusion blankets has been the main impetus behind the study of solid lithium compounds, and the reason why solid breeders are chosen for this model. The use of solid lithium compounds and alloys as components of the tritium breeding zone was first proposed by J.R. Powell et al.[13] in 1973. Since then, additional physical and chemical data on candidate solid breeders have substantiated the advantages of using solid lithium breeders from the standpoint of plant reliability and safety. The objective of this study is not to specify an optimum lithium compound, nor to describe in detail the methods of fabricating it and incorporating it into blanket modules, but rather to describe the long-term behavior of the breeder, initially at reactor start-up, until the steady-state operating condition is achieved.

The tritium in the blanket migrates to the solid surface where it is removed in a stream of moderately-flowing low-pressure helium. This purge gas, as it is called, has as its sole purpose the extraction of tritium from the solid breeder. It can therefore be expected to attain a rather sizable tritium concentration which is carried away out of the blanket and into the processing unit. Ideally, a low-pressure helium purge gas acts as a sink for most of the tritium being bred in the blanket, and would also help to prevent tritium from diffusing into the blanket coolant by offering its own "resistance" to tritium diffusion. Helium, as an inert noble gas, should not affect appreciably the blanket

neutronics as it passes through the numerous purge gas channels in the breeder blanket.

Considerable technology related to the use of helium as a heat transfer medium has already been developed in gas-cooled fission reactor (HTGR) programs. Consequently, the application of helium to a fusion power plant as the primary coolant seems relatively straightforward. It has already been mentioned that helium has insignificant neutronic interactions when it is being pumped through the blanket and thus, can be assumed not to perturb the blanket neutronics. As a gas, helium has to be kept at 50 - 70 atmospheres in order to maintain adequate heat transfer capabilities. Although this means large manifolds and ducts to carry the helium, the flow designs can be kept much simpler since there are no MHD effects for helium to guard against, as it passes across magnetic field lines.

The aforementioned limitations of this model will not hinder its effectiveness in predicting tritium distributions in, and leakage out of, several proposed reactors whose characteristics fit the model. An important result of this systems model would be in its use for comparative analyses among various designs. For example, JAERI[14] has proposed a helium cooled lithium oxide (Li_2O) blanket and INTOR[15] has recently chosen a Li_2SiO_2 breeder and a high pressure helium coolant. The specific application conducted herein, uses the STARFIRE-Interim Design Study[8] system parameters as the specified input.

With this introduction to that part of a fusion power plant which will be included in the transient modelling of the disposition and leakage of tritium, it is now possible to continue with a more detailed analysis of the system components and those parameters which characterize them.

2.2 Overview of Model

Transient tritium behavior associated with reactor start-up until an operational steady-state is achieved, is the basis of this permeation model. Since permeation loss through the heat exchangers is the principal contributor to the total tritium released to the environment, this tritium pathway will of necessity be modelled for this study. Using the same tritium concentration in the helium coolant, it is also possible to calculate permeation losses from the coolant piping into the containment atmosphere. Although not as critical as the tritium emissions into the steam system which make their way to the outside atmosphere, tritium leaks into the reactor building are of importance in sizing the emergency air detritiation systems which are sued to accomodate any accidental tritium spills.

A schematic of the simplified reactor system to be considered is given in Figure 2-2. The components of the design that were determined to be the major influences on tritium transport are clearly represented in Figure 2-2 as:

1 - Blanket - comprised of solid breeder (pellets), helium purge gas system, breeder tube structural metal, and helium coolant

2 - Helium Piping System - both the "hot" leg leading to the heat exchanger(HX), and the "cold" leg leading from the HX back to the blanket

3 - Heat Exchanger - interfaces the primary coolant system (helium loop) with the energy conversion system (steam cycle).

Although it can be anticipated that more than one coolant loop may exist for a given design, these loops running in parallel may be simulated by one, whose parameters are properly chosen to represent the total heat transport system.

The arrows in Figure 2-2 represent the flow of tritium as it is bred in the breeder, diffuses to the surface of the solid pellets, and is then swept away by the purge gas system. Although it is not shown in the diagram, the purge gas stream leads out of the blanket to the pro-

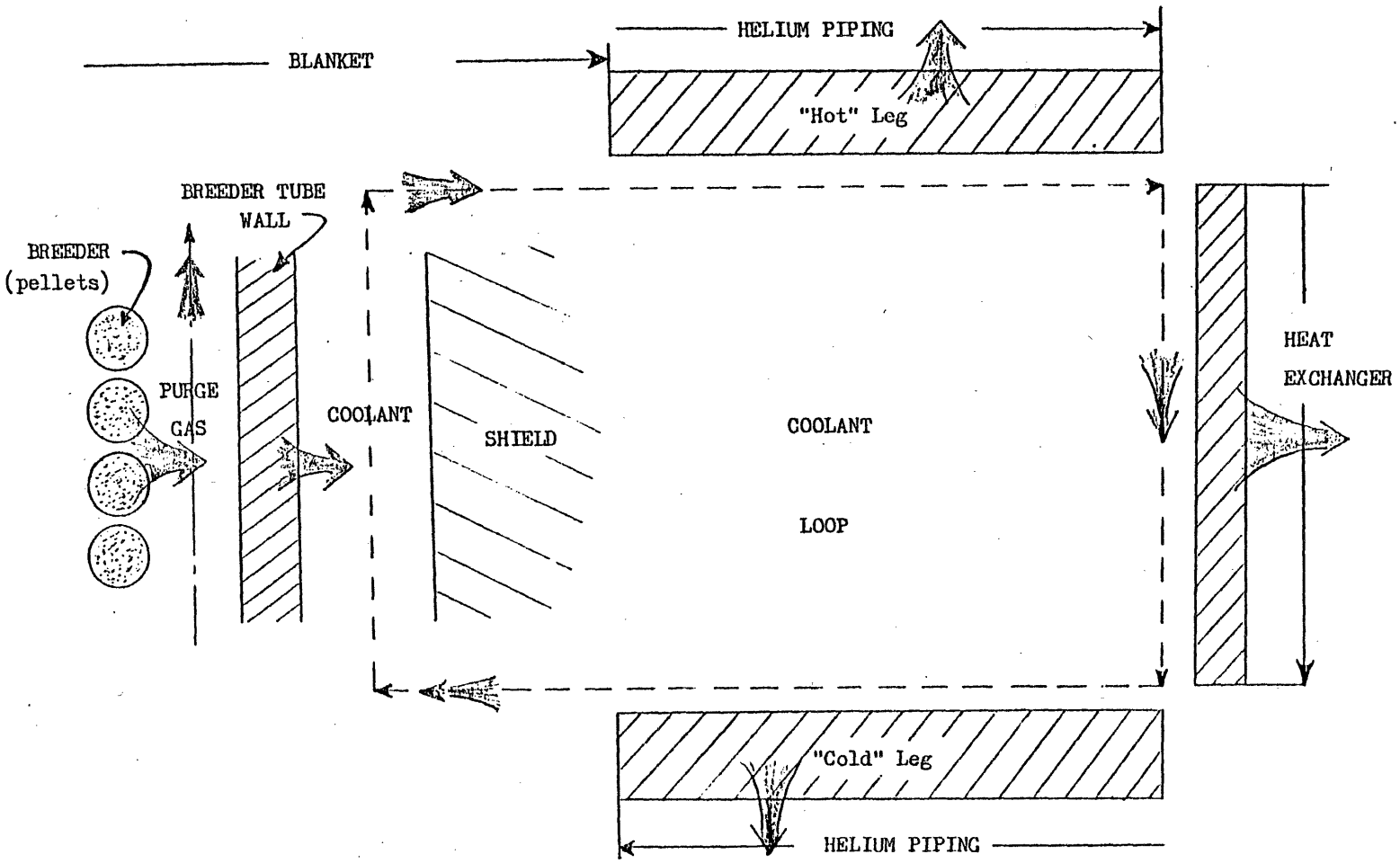

Figure 2-2

Tritium Transport in a Simplified Fusion Reactor Design and Leakage from the Primary Containment
(Note: Not Drawn to Scale)

cessing unit. A brief discussion about possible tritium extraction methods is given in Section 2.3.2. A relatively high tritium concentration in the purge gas is the driving force behind the permeation into the helium coolant. Once in the coolant loop, the tritium is capable of permeating through the piping walls into the secondary containment or through the heat exchanger walls into the steam cycle.

Since the tritium concentrations throughout the plant will necessarily be of interest for both the tracking of tritium transport, and the accumulated tritium inventory, it is convenient to identify these points. A map of tritium concentrations (C) is given in Figure 2-3, where the subscripts to the concentration markers are as defined in the nomenclature at the beginning of this thesis. This map will be a useful reference for the equations describing the diffusion behavior of tritium to be derived in Section 2.4.

The sole tritium source in this model is that which is bred in the blanket. Assuming that the plasma operates in a continuous burn mode, then the tritium source can be assumed to be constant in time also. If the tritium generation is not explicitly given, it can be calculated from the plasma thermal power rating (its nominal value), energy released per fusion -- 20 Mev -- and the (average) breeding ratio of the blanket. The transient build-up of tritium in the breeding zone will necessarily be many orders of magnitude faster than in any other area of the design, due to the source term. This preempts any usage of a simultaneous solution to all the concentrations represented in Figure 2-3. In mathematical terms, such a hierarchy of equations would be a "stiff" problem -- at one end (breeding zone), there are fast dynamics, and at the other end (coolant metal pipes and heat exchanger) there are very slow dynamics since it takes a long time for any appreciable concentrations to appear.

It is therefore appropriate to develop a quasi-steady-state model of the transient build-up of tritium in the various reactor components. This means dividing the total system into sections where the losses to the next section down-line can be neglected over a suitable time period - on the order of characteristic time determined for the first section. The approximations used to describe the equations for the time evolution of various concentrations will be elaborated upon in Section 2.3.

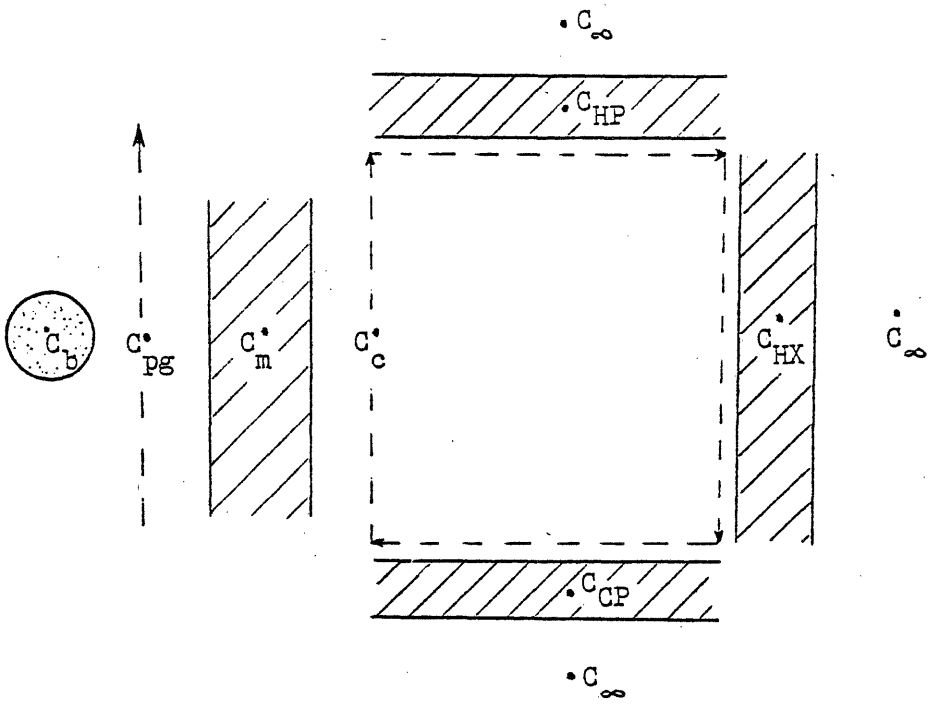

Figure 2-3

Tritium Concentration Map for a Simplified Fusion Reactor Design

(Note: Not Drawn to Scale)

2.3 Considerations for Tritium Transport in the Various Components

The mathematical model development is divided into two major sections. This Section 2.3 includes a detailed description and discussion of each of the major system components: the assumptions as to tritium behavior in each and the design features which are neglected in the present model. The following Section 2.4 presents the time-dependent equations for tritium concentration at various points of interest in the simplified fusion reactor design, in accordance with the approximations made in Section 2.3 for each component.

2.3.1 Breeder

It has already been established that only solid breeding agents will be considered for this model. There are a number of such solids which have good neutronic properties and do not acquire long-lived induced radioactivity under operating conditions --- an important consideration for blankets whose modules have to be replaced from time to time. Handling of solids poses less corrosion problems than for liquid lithium, for example.

Of necessity the solid breeder must be a lithium compound to take advantage of the Li(n,p)T reaction, and the relative abundance of the element lithium. Although some conceptual reactor designs have included the use of beryllium as a small contributor to a breeding ratio greater than unity, the tritium bred in this auxiliary reaction will not be included here.

Among the large number of stable lithium bearing materials, two types of lithium solid compounds appear to offer the best promise for use in a fusion reactor blanket:

1 - Intermetallics:
   LiAl - lithium-aluminum alloy
   Li_7Pb_2 - lithium-lead alloy
2 - Ceramics:
   Li_2O - lithium oxide

$LiAlO_2$ - lithium aluminate
Li_2SiO_3 - lithium metasilicate
Li_4SiO_4 - lithium orthosilicate

Other compounds have been proposed, but these are the favored compounds of each type[16]. The available thermodynamic data for these potentially viable solid breeder materials were tabulated in Appendix A in an effort to help predict their behavior in a fusion reactor environment. Although the thermophysical, chemical and neutronic properties of these candidate materials are continually being reevaluated, the values given in Table A-1 for some of these properties are considered best estimates.

The tritium is bred in situ in a loosely packed bed of solid lithium alloys or lithium ceramics. The physical form of the breeder (pellet radius, grain size) as well as other design parameters, are determined by the requirement that the tritium release rate is sufficiently rapid to minimize the blanket inventory and to allow attainment of tritium self-sufficiency within a reasonable time. To aid in resolving these parameters or more specifically, to analyze those parameters already chosen, a one-dimensional time-dependent tritium transport model is presented in Section 2.4.

The tritium transport model is based on the assumption of spherical pellets with an average radius, r_p. Although each pellet is theoretically composed of uniformly-distributed grains (of characteristic radius, r_g) as depicted in Figure 2-4. The characteristic "step" in the random walk process for tritium diffusion is take to be on the order of the pellet radius. Some studies[17,18] have used the grain dimension as the diffusion path length, and thus assuming that any tritium that has migrated to the grain boundary can easily move along that boundary and leave the breeder pellet. In an analogy with fission gas release in uranium oxide (UO_2), the grain boundaries act as efficient "traps" for gases[19]. Gas molecules collect and coalesce at the grain boundary site until interlinkage causes a direct pathway to some open porosity and hence to the outside (in this case, purge gas). Therefore it is assumed that the tritium gas (T_2) must diffuse through the whole of the pellet and hence, r_p should be the more accurate representation of the

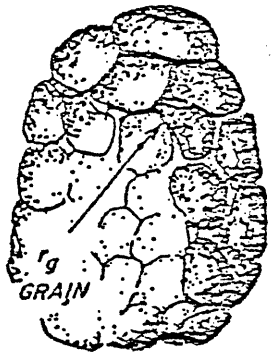

Figure 2-4

Ideallized Breeder Pellet Uniformly Composed of many grains of radius r_g

(Figure taken from Ref. (17))

true diffusion path length. Pellet dimensions are usually in the range 10 - 1000 μ , of sufficient size to allow free passage of the helium purge gas, yet small enough to permit adequate diffusion rates.

No allowance is made for inherent fabrication porosity or intentional porosity designed to enhance tritium removal or heat transfer. If it is not otherwise specified from a particular design, the solid lithium compounds are assumed to be 100 % dense material. Also, the intense radiation that the blanket undergoes while in service, both neutrons and gamma, is assumed not to seriously affect the lithium solids' thermodynamic and neutronic properties when trapping of tritium occurs. Thus the property values for the breeder which will be discussed shortly, are not seriously degraded over time due to irradiation effects.

The integrity of the solid must be preserved under conditions of intense neutron irradiation in which helium gas is being generated along with tritium, and lithium is being consumed.

The temperature of the breeder pellets is an important system parameter that determines several thermochemical properties known to affect the release of tritium from the pellets (namely, diffusivity and solubility). Although all the tritium concentrations throughout the plant are taken to be zero at the time of reactor start-up and then proceed to increase thereafter, the breeder temperature is assumed to be at its operating temperature right from time equals zero. (One pellet with all average property values represents the entire breeding zone.) The pellets reach their steady-state temperature profiles much faster than their concentration profiles even though both source terms, heat generation per unit volume per unit time and tritium generation per unit volume per unit time, are constant in time. This is due to the fact that the thermal diffusivity α, is much greater than the tritium (mass) diffusivity D_b, as is shown in Appendix A.

The tritium generated in the breeder solid is assumed to be of the form of atomic T in the solid, and molecular T_2 in the helium gas. There is considerable evidence[20] that, especially for the ceramic breeders (Li_2O, $LiAlO_2$, Li_2SiO_3) the majority of the tritium comes off as T_2O and HTO. Since there is no other basis of similarity for all the lithium compounds (including the intermetallics) except to use the "pure" form for the tritium bred in the blanket, it will simplify matters to use atomic T in the solids and molecular T_2 in the gas phase when modelling the tritium behavior.

For any lithium compound selected, a steady-state will be approached in which the rate of tritium release equals the rate at which it is formed. Consequently, the factors that affect this steady-state condition are of importance. But it is also important to release the tritium at a rate sufficiently high so that the tritium inventory in the breeder is not excessive. Therefore the kinetic processes involved in tritium removal from solid breeders must be reviewed.

Several important aspects of tritium release have been identified and categorized[17]. Among these, tritium diffusivity and solubility within the breeder solid deserve special note and will be treated in more detail later. Grain boundary migration has been mentioned earlier, where it was shown that it is the diffusion through the bulk of the pellet that is of consequence. Desorption kinetics, whereby the atomic tritium diffusing from the interior of the pellet must combine with another tritium atom at the surface in order to leave the pellet as a diatomic gas molecule T_2, may contribute to the surface effects' role as the rate-limiting mechanism for tritium release. Surface effects were not explicitly addressed by the model because it was assumed that anything happening to the tritium as it reached the surface of the pellet would be necessarily included in the experimentally-determined (from tritium release curves) diffusion coefficients. However, there are several points to be made from the experiments which ran with some protium in the helium sweep gas, and at various flow rates that show how surface effects can affect the extraction rate, and hence the diffusion coefficient which is calculated from it (ref. Equations (2.1), (2.2)).

Figure 2-5 is Wiswall and Wirsing's [21,22] results for tritium extraction from the lithium alloys Li_7Pb_2 and LiAl with some hydrogen added as a scavenging agent. As the atomic tritium makes its way to the surface, it has the opportunity to combine with some hydrogen intentionally left in the helium sweep gas and then enter the purge gas as a HT molecule. Thus, a few parts hydrogen in the helium greatly increases the desorption kinetics.

Similarly, increasing the sweep gas flow rate (ref. Figure 2-6) keeps the tritium concentration in the sweep gas low. For LiAl and Li_7Pb_2 shown in the figure, this means the flow of tritium into the purge stream is not retarded, so tritium readily escapes from the pellet surface.

Percolation of tritium through an assumed porosity in the particle packed bed is another aspect of the kinetics of tritium removal. Since it is not yet at a stage of being well-understood or quantifiable, percolation effects are not included in the modelling of tritium behavior in the breeder. Convective mass transport of the tritium in the purge

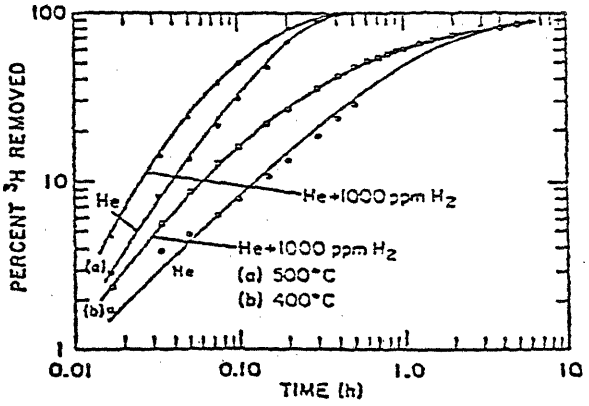

(a) Li_7Pb_2

Tritium Extraction

@ 400, 500 °C

(Figure taken from Ref. (21))

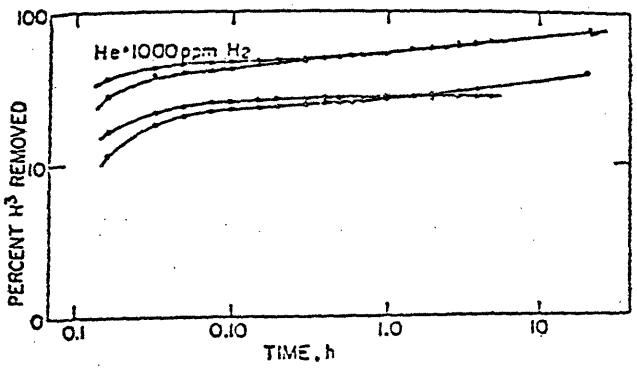

(b) LiAl

Tritium Extraction

@ 400 °C , 10 - 20 mesh

(Figure taken from Ref. (22))

Figure 2-5

Effect of Adding Hydrogen in Helium Sweep Gas on the Removal of Tritium From Irradiated Solid Lithium Compounds

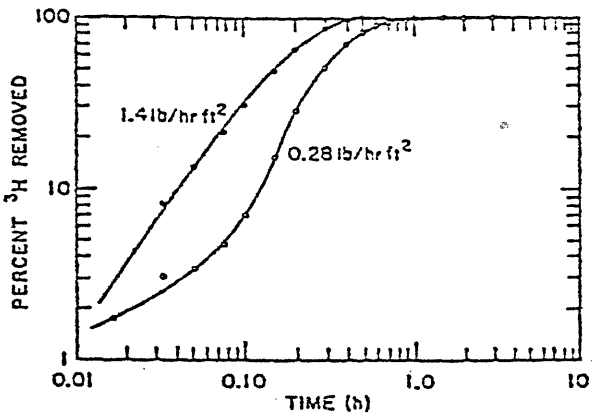

(a) Li_7Pb_2

Tritium Extraction

@ 500 °C

(Figure taken from Ref. (21))

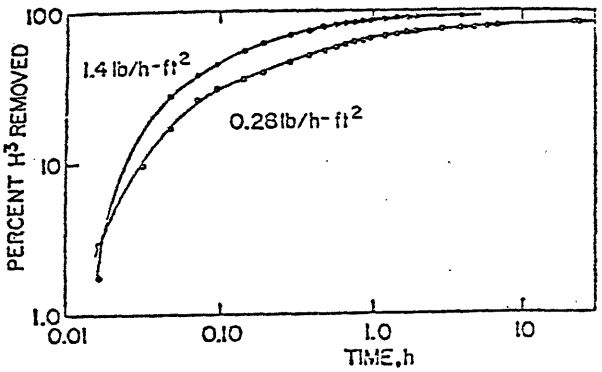

(b) LiAl

Tritium Extraction

@ 500 °C , 10 - 20 mesh

(Figure taken from Ref. (23))

Figure 2-6

Effect of Helium Flow Rate on the Removal of Tritium from Irradiated Solid Lithium Compounds

gas is a crucial element to the transport model because the primary tritium extraction method is the processing of the tritium carried away by the purge gas.

The chief uncertainty for solid breeders is whether the bred tritium could be removed promptly; the tritium inventory in the breeder blanket must be kept low for reasons of both radioactive hazard and nuclear economy. The modelling of tritium escape from solid lithium breeders presented in this study recognizes the relative importance of thermodynamic equilibrium between the pellets and the purge gas and the bulk diffusion of tritium within the solid in the overall process. Other studies [24,25] have concluded that the tritium inventory in the solid breeder will be determined by both diffusion and thermodynamic constraints.

In view of the observed strong dependence of tritium release rate on temperature (ref. figures in Appendix A.2) and the fact that the inventory is extremely sensitive to diffusion path length, it is not surprising that most analyses of tritium removal from the breeder have concentrated on the bulk diffusion-limited aspects of tritium release. The latter observation is a result of extraction experiments done on a lithium compound (see Figure 2-7); each run consisted of uniform particle size (sieved if need to be, to obtain approximately all the same diameter) which were decreased to witness the effect of decreasing the diffusion path length.

Even with essentially no tritium concentration at equilibrium, there would still be a lower limit to the tritium concentration corresponding to the characteristic diffusion time for tritium to escape from the solid lithium alloy or compound. This will depend on the particle size and temperature of the solid which necessarily affects the diffusion coefficient. Even though there is considerable uncertainty in the measurement of diffusion coefficients for various lithium compounds[26], a synopsis of the available data on tritium release rates that have been used to calculate tritium diffusion coefficients for lithium solids is presented in Appendix A.2. A quick observation of the diffusion coefficients plotted in Figure A-1 shows that slow diffusion rates are predicted, implying the lithium compounds must be fabricated as very small pellets indeed.

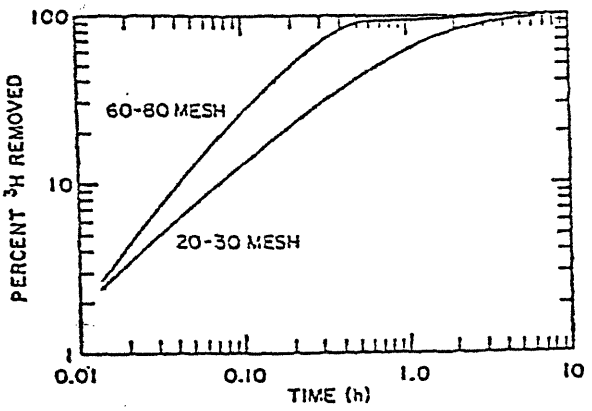

(a) Li_7Pb_2

Tritium Extraction

@ 450 °C

(Figure taken from Ref. (21))

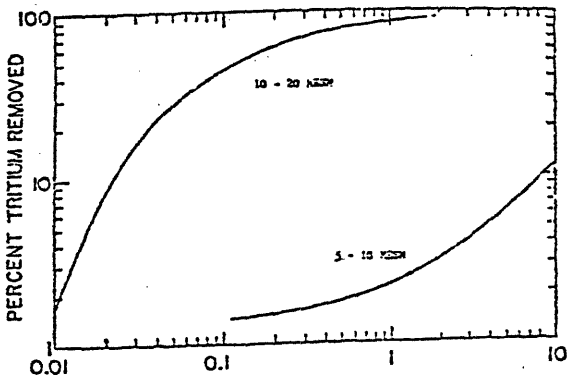

(b) LiAl

Tritium Extraction

@ 500 °C

(Figure taken from Ref. (23))

Figure 2-7

Effect of Particle Size on the Removal of Tritium From Irradiated Solid Lithium Compounds

There are several errors that can be identified when calculating the extraction diffusion coefficient D_b, the magnitude of which must be kept in mind when these diffusion values are used in the model. First, errors of 10 - 100 between the extraction diffusion coefficient and the true diffusion coefficient are easily possible[27] if the analytical techniques assumed a uniform initial concentration of gas in the solid, when in actuality the initial distribution was non-uniform. This will tend to underestimate the true diffusion coefficient. Secondly, less important yet still significant errors of 1.2 to 5 will occur if it is assumed that all particles are identical in size when in fact there is a spread in particle size. The diffusion coefficient will be overestimated because the concentration gradient at the surface is larger than in the case of a uniform particle distribution. The qualitative difference between the results for collections of different size particles can be understood in terms of the trade-off between quick release from smaller particles (shorter diffusion paths) and the greater amount of gas in the larger particles. From the figures in Appendix A.2, it is evident that the rapid early release from the small particles (which leads to an overestimate of D_b) cannot be sustained due to their relatively small volume. The release from the larger particles becomes dominant, so that at longer times the extracted diffusion coefficient will be underestimated compared to the true diffusion coefficient.

If, as it has been used in relating extraction times to diffusion coefficients in the Appendix A.2, the diffusion coefficient for spheres of radius r_p can be conservatively estimated by:

$$D = \frac{r_p^2}{15 \cdot \tau} \qquad (2.1)$$

and the fractional release from irradiated solid lithium compounds is approximated by[23]:

$$f \cong \frac{6}{r_p \sqrt{\pi}} \sqrt{D\tau} \qquad (2.2)$$

then the extraction time is defined as being the time for 87.4 % of the initial tritium in the lithium samples to be released to the sweep gas.

(This assumes continuous generation and extraction.) This representation of diffusion-limited tritium release has been well-cocumented for the extraction work done by Wiswall and Wirsing on solid lithium compounds. Thus, the general approach of taking a straight percentage of the amount of released tritium as the basis for calculating the extraction diffusion coefficient whould mitigate the errors caused by not having a true uniform particle size, because that fraction (0.874) seems to be beyond the limit of the small particle rapid release kinetics.

One final word about tritium diffusion in lithium solids is in order. It has been previously feared that there was a distinct possibility of massive sintering or crystal formation of the solid breeder particles under intense irradiation. In an extreme case in which all the breeder pellets fuse into one massive lump, the retained tritium inventory could rise as much as three orders of magnitude[28]. Of course, particle sintering has been of concern to the breeder operating temperature (ref. Table F-1 in Appendix F) since rapid sintering of especially the metallic alloys occurs at approximately 0.6 times the absolute melting temperature. But prolonged pretreatment of Li_7Pb_2 and $LiAlO_2$ at temperatures higher than the operating temperature did not reduce the extraction rates. In fact, increased extraction rates were observed[21] for sintered samples of Li_7Pb_2 and $LiAlO_2$ (ref. Figure 2-8). Enhanced diffusion for these compounds in particular was attributed to a phase transformation for $LiAlO_2$ at 900 ^{o}C and a phase segregation process for Li_7Pb_2 which more than offset the consequences of a reduced specific area brought on during most pellet sinterings[26].

In addition to the diffusion related component of the tritium inventory (the amount required to maintain sufficient concentration gradients to allow the tritium to diffuse out as rapidly as possible) the solubility related component must also be considered. The solubility of tritium in the compound is determined by the thermodynamic equilibrium constant (i.e., the Sieverts' Constant) and the tritium partial pressure in the extraction system (in the model -- the purge gas stream). In some cases the amount of tritium in the solid held in solution by the equilibrium partial pressure in the purge gas over it, may exceed the diffusive holdup. The lower the lithium chemical activity for a given breeder, the higher

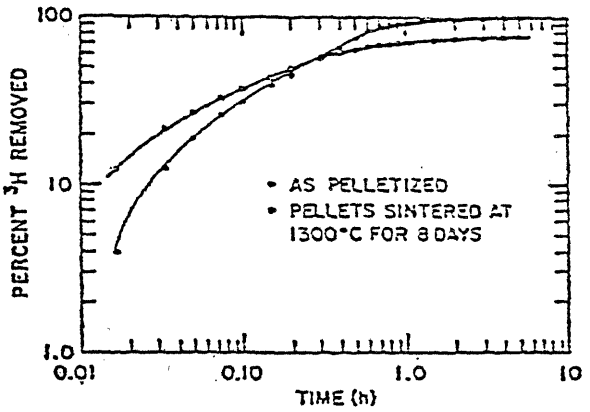

(a) $LiAlO_2$

Tritium Extraction

@ 650 °C

(Both figures taken from Ref. (21))

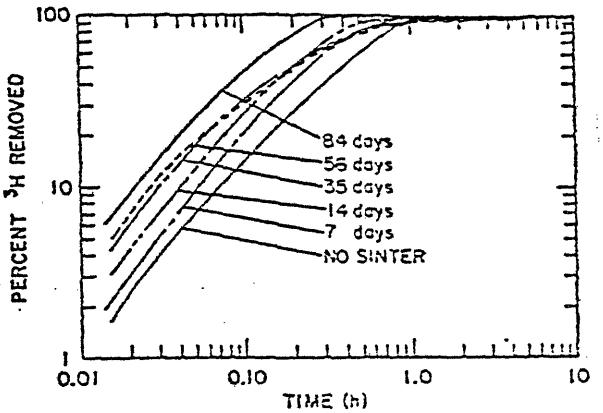

(b) Li_7Pb_2

Tritium Extraction

@ 450 °C

Figure 2-8

Effect of Sintering on the Removal of Tritium from Irradiated Solid Lithium Compounds

the corresponding equilibrium tritium pressure, and hence, the less tritium in solution at any given tritium partial pressure in the purge gas. The tritium solubility is also a weak function of the breeder temperature[24,29]. Clearly, additional thermodynamic data are required to more accurately determine the tritium holdup in solid breeders.

The design solution to this dilemma of diffusion vs. solubility controlled tritium inventory is proper control of temperature and particle size once the choice of solid breeder has been made. The tritium holdup is minimized by

1 - keeping the particle size small to allow adequate diffusion of the bred tritium out of the pellet (and thus, keeping the steady-state inventory at a satisfactory level), and
2 - keeping the pellet temperature high to increase both the diffusion coefficient for a given particular diameter and the tritium equilibrium pressure, but not so high so as to cause excessive restructuring and thermal sintering, which could increase the diffusion path length and thereby reduce diffusion rates.

Considerations of both these aspects of tritium behavior in the breeder, solubility and diffusion processes, lead to important consequences for the tritium inventory, tritium recovery and the blanket designs of fusion reactor systems that employ the solid lithium breeders.

Since experimental data on tritium solubility in candidate solid breeder materials are very limited, it is often necessary to utilize relevant information on hydrogen and extrapolate over a large temperature range[27] to obtain the data required for the inclusion of solubility effects in this permeation model. The only work[24] on the complex lithium oxides has been to compare their behavior with that for ZnO, and assume that the solubility of hydrogen in ZnO is an upper limit to what can be expected for tritium in the complex lithium oxides. Rough estimates for the Sieverts' Constant of tritium in the intermetallics, LiAl and Li_7Pb_2, are also given in Appendix A.3. Since these are the only existing

results available, they are considered satisfactory for use in this model, in light of all the other assumptions made about tritium behavior in lithium solids.

A brief summary is given in the following subsections concerning recent observations on tritium release characteristics for the candidate (lithium) solid breeders. It is obvious that no general statement on tritium behavior can be made for all of them.

2.3.1.1 $LiAlO_2$, Li_2SiO_3

The compounds $LiAlO_2$ and Li_2SiO_3 generally provide a better combination of high temperature stability and high lithium atom density compared to other complex compounds. Most of the tritium given off irradiated samples of these oxides is in the form of T_2O and to a lesser degree, HTO. $LiAlO_2$ and Li_2SiO_3 have provided data consistent with the diffusion-limited model for tritium release. On a log-log plot of the extraction curves, use of Equation (2.1) for the diffusion coefficient would imply a slope of $\frac{1}{2}$ would indicate diffusion as the rate controlling step in the extraction process. Although the data do not cover a range of particle sizes sufficient to absolutely confirm the proposed simple solid diffusion model, it is a good assumption to make for the compounds $LiAlO_2$ and Li_2SiO_3.

The solubility is much less important than the retention resulting from the slow diffusion of tritium. The T_2O pressure over $LiAlO_2$ and Li_2SiO_3 is relatively high, and hence lower tritium concentrations in these solids may be attainable. The calculated solubility[29] of tritium in $LiAlO_2$ is $\sim$10 wppm at a T_2O pressure of 10^{-1} Pa (8×10^{-4} Torr). Therefore, the compounds $LiAlO_2$ and Li_2SiO_3 are not seen to be controlled by equilibrium constraints, and hence would not benefit from lowering the tritium partial pressure in the purge gas.

2.3.1.2 Li_2O

As for the other more complex oxides, the tritium released by Li_2O is of the form T_2O or HTO. Li_2O is unique because of its high lithium atom density and higher melting temperature compared to such compounds

as Li_2Si and Li_2C_2. The measured tritium release decreases as expected from a diffusion controlled process. Although the removal rate is limited by the slow diffusion of tritium from the interior of the particle to the surface, there is a slow transfer of tritium from the surface to the gas phase which may also play a role[23].

The tritium equilibrium pressure for Li_2O is much less than the corresponding pressures for the other oxides, $LiAlO_2$ and Li_2SiO_3. The calculated solubility[29] of tritium in Li_2O at a T_2O partial pressure of 10^{-1} Pa (8×10^{-4} Torr) in the helium purge gas, is substantially in excess of 100 wppm. Thus it is quite possible the solubility tritium inventory may well exceed that due to diffusive holdup.

2.3.1.3 LiAl, Li_7Pb_2

LiAl is similar to Li_7Pb_2 in many respects, except for the superior breeding capability of the Li_7Pb_2 due to the presence of the lead which acts as a neutron multiplier. Lithium aluminates' operating temperature range is reduced by its relatively low sintering temperature. The tritium is expected to be bred in the form T_2 and HT. Tests of the role surface reactions have in the overall extraction process have been conducted and were used previously (Figures 2-5 and 2-6) to show that they were indeed important. Therefore, a model based on bulk diffusion is inadequate, as demonstrated by the non-negigible effects that gas flow rate, protium addition to the helium sweep gas and the particle size (ref. Figure 2-7) had on release behavior. If the surface reactions become rate-limiting then the escaping tendency of the tritium would be proportional to the square of its concentration on the surface of the solid. The proportionality factor is Sieverts' Constant, which is given in Figures A-16 and A-22 for Li_7Pb_2 and LiAl, respectively.

In general, both LiAl and Li_7Pb_2 are conducive to mixed regime effects where bulk diffusion and solid surface-to-sweep gas mass transfer compete for overall control of the tritium excape.

2.3.2 Purge Gas System

The bred tritium can be recovered in situ either by letting the tritium diffuse from the solid, or by periodically removing the solid from the blanket and processing it. The later approach is very costly and difficult while leaving the solid in the blanket and recovering the bred tritium by diffusion may be quite feasible. The permeation model developed in this study lets the tritium migrate to the solid surface which is bathed in a low-pressure helium gas. The tritium is swept into this purge gas stream and carried outside the reactor vessel to a processing unit.

As the sole means of tritium recovery inside the blanket, the helium purge gas system is a vital component to the tritium pathway to the environment and also a major influence on the breeder inventory. Because the pellets are in thermodynamic equilibrium with the tritium partial pressure in the purge gas, it is necessary to keep the purge gas tritium concentration low enough to sustain an acceptable solubility inventory in the breeder, but not so low as to make the processing of this tritium for refuelling the reactor prohibitively expensive. This usually requires increasing the flow rate (ref. Equation (2.46)). If the blanket is not designed properly, the effect of this gas phase mass transfer would be to make the volumetric flow rate of the purge gas on the same order or higher as that for the coolant. For purposes of this model, the assumption will be made that a purge gas at adequate flow rates can be maintained in a fusion reactor blanket to pick up any emitted tritium. This implies that the gas need only be processed at some later point in the flow to effect a straight-forward recovery procedure.

The actual processing scheme for the tritium in the purge gas stream once it is carried outside the reactor is not relevant to the permeation model, although design optimization of the purge gas processing methods would benefit from its results. The only assumption that is necessary for purposes of the model is that the purge gas enters the blanket "clean", meaning free of tritium. Also, there is no scavenging protium gas added to the helium so as to enhance the tritium extraction charact-

eristics of the flowing sweep gas (ref. Figure 2-5). Since it was previously assumed that all the tritium formed in the breeder is T_2, and given that all the tritium migrates through solids as T atoms and through gases as T_2 molecules, then it is consistent to assume no change in the chemical form of the tritium in the purge gas. Oxidation to T_2O or reduction to HT with added oxygen (HTO), would only unduly complicate the kinetic and equilibrium processes already mentioned.

This discussion of tritium recovery from the blanket by continually flushing the pellets with a low pressure helium gas to remove the released tritium is idealized of course. The lithium compound or alloy used as the breeder is not everywhere the same temperature. Both the temperature and breeding rate will vary with position (radially outward). Since this affects the amount of tritium that is being bred and how fast it is getting out, the purge gas system will not be overly loaded. In fact, if the particles are sintered to a large extent or otherwise fragmented into even finer particles, it is possible for the purge gas channels to be blocked and the flow reduced to parts of the blanket. This is not a normal operational mode for the blanket but it does show how delicately the purge gas stream must be treated.

In the model it is assumed that the breeder can be represented by a single pellet operating under average conditions -- both internally and externally. This short analysis indicates how difficult it may be to define an "average" pellet and "average" purge gas conditions. Yet quite severe conditions are imposed on the tritium recovery scheme in order to maintain the desired inward gradient of the tritium pressure from the outer containment to the blanket coolant and finally, to the blanket itself.

2.3.3 Primary Coolant System

The external surface of the tubes containing the solid breeder material are cooled by the flow of the helium coolant system. The purity of helium gas is difficult to maintain in a pumped, pressurized (on the order of 50 atm) system. Small amounts of oxygen, nitrogen, water, carbon monoxide and dioxide and methane would probably be present[30] due to some air leaking in and making contact with lubricated seals, and tritium could be present due to permeation through the inner (blanket) wall. The dimension map for the simplified fusion reactor design used as the basis for this model is given in Figure 2-9. As can be seen from the figure, only the breeder tube metal thickness separates the relatively high tritium concentration in the purge gas, from the helium coolant. A significant amount of tritium has the potential to diffuse through the large surface area of the pins containing the breeder material and contaminate the helium coolant.

The permeation model can be used to estimate the tritium permeation rate through the blanket metal and into the coolant, and also the time the coolant system takes to reach a (maximum) steady-state value for the tritium concentration. No added precautions have been included in the basic modelling of the various reactor components, other than the tritium extraction system operating with the helium purge gas which is isolated from the main helium coolant. So it can be anticipated that the tritium partial pressure in the coolant might buildup to a point where tritium losses from the heat exchanger are no longer insignificant. In this case the permeation model would have predicted unacceptable tritium releases. The critical system parameters which led to them, can be used to determine which of the permeation barriers that are available would be most suitable: the easiest to use and also the most effective.

The choices for practical permeation barriers are described in the next section on tritium behavior in metals. However, the model was expanded to include an effective approach to controlling tritium leakage from the primary coolant system without changing any of the reactor components' properties, geometries or dimensions: oxidizing the helium coolant loop to convert all the tritium present to the nonpermeating

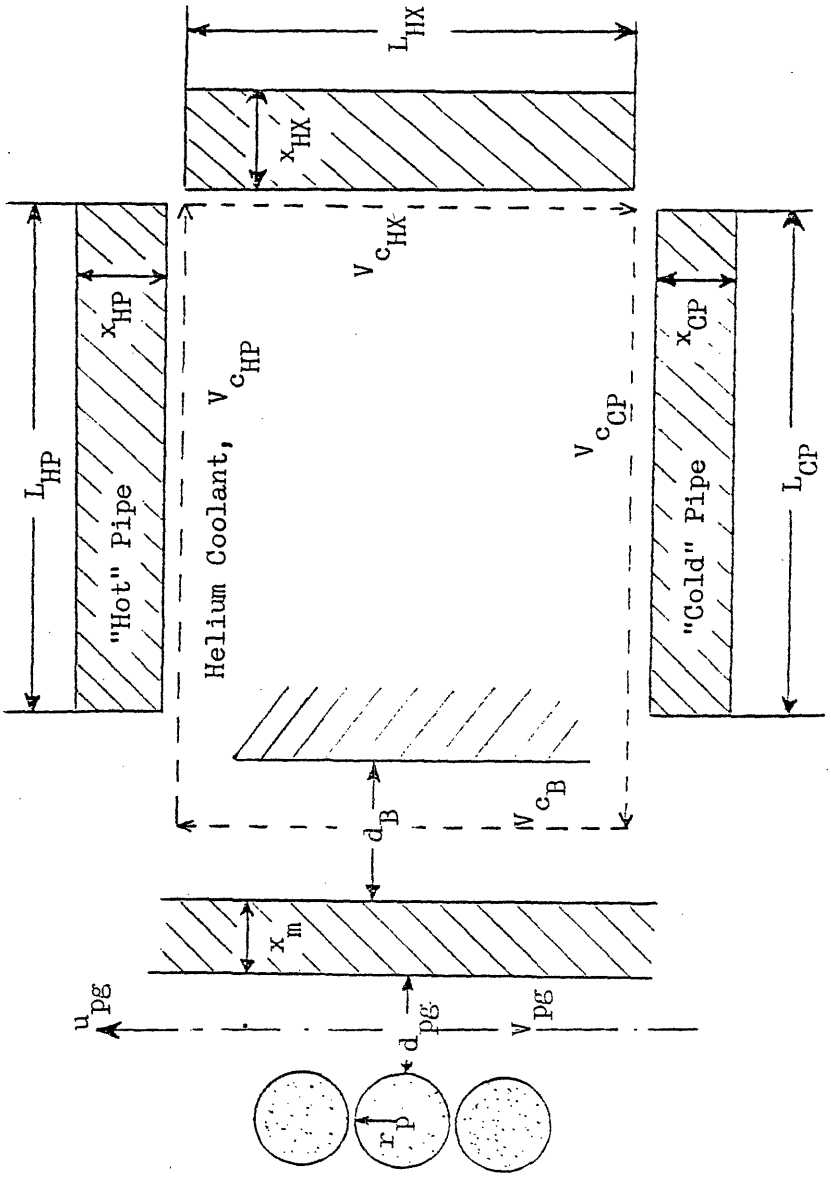

Figure 2-9

Dimension Map for a Simplified Fusion Reactor Design

species T_2O. This scheme is compatible with the presently proposed design and should prevent the large loss of tritium through this pathway.

Initially oxygen (O_2) might be present in the helium at a few ppm, but it would quickly be scavenged by the tritium diffusing into coolant through the blanket wall. A small partial pressure of oxygen is then purposely added to the helium and maintained at a level sufficient to establish the following equilibrium:

$$T_2 + \tfrac{1}{2} O_2 \rightleftharpoons T_2O \qquad (2.3)$$

The kinetics of the formation of the oxidized tritium species can be made more favorable if need be by the use of catalysts[31].

By maintaining a small O_2 pressure in the helium (on the order of 50 ppm)[32] the tritium diffusing into the helium would become tied up as water, thus reducing the T_2 partial pressure so that both permeation loss to the steam system and embrittlement of the vessel walls are avoided. Pumping of even small amounts of oxygen into the helium can be important from the point of view of corrosion. The permeation model assumes all wall materials are resistant to corrosion effects, but it the required oxygen partial pressure becomes substantial, this assumption would no longer be valid. For the immediate problem of a high tritium partial pressure in the coolant, a reduction in this pressure to 10^{-10} torr or less by similar techniques seems beyond the technology available at present[33].

Assuming that a low oxygen partial pressure would not be deleterious to the reactor system, the final aspect of tritium behavior in the coolant is its removal and subsequent recovery. As it was for the helium purge gas, the modelling of the tritium processing system is not necessary for calculating tritium transport within and permeation from, the primary coolant system. Suffice it to say that because the tritium species is now known to be T_2O, the choice of purification techniques is more straight=straight-forward. Several studies have described absorption of the tritiated water on molecular sieve dessicant beds[24,28,31,34] as the most practical technique. In any case, provision must be made for the purification of the coolant in a bypass flow (of the order 1 - 10 %)[20] of the main coolant loop. Such methods are currently being used in the high-

temperature gas-cooled fission reactors [33] (HTGR).

2.3.4 Metals

2.3.4.1 Location

The primary containment consists of the relatively high resistance to tritium permeation offered by the pipe and vessel wall metals. As such, metals are necessarily one of the major system components to be included in the transient permeation model being developed. According to the simplified reactor design depicted in Figure 2-2, the particular metal barriers of interest are those comprising the:

1 - breeder tubes	-	inner (blanket) wall for the coolant system
2 - helium piping	-	both "hot" and "cold" segments
3 - heat exchanger	-	more specifically, the surface metal interfacing the helium and steam loops

All dimensions and properties for each of these four metal surfaces (two for the helium piping: "hot" and "cold" pipes) are characterized by the following subscripts: breeder tube (blanket) metal - m; "hot" pipe - HP; "cold" pipe - CP; and heat exchanger - HX.

Although it has been stated that none of the compounds in the simplified fusion reactor design used in this model are drawn to scale, several comparisons of expected metal thicknesses can be made. The breeder tube wall thickness, x_m, (ref. Figure 2-9) is thought to be relatively thin for purposes of adequate heat conduction from the breeder pellets to the helium coolant. However, from the standpoint of unintentional tritium transport, this will also allow significant tritium permeation to occur from the relatively high tritium concentration in the purge gas to (initially) zero tritium concentration in the coolant. A thin wall, combined with the high operating structural temperatures anticipated for fusion blankets, are not conducive to a high metal resistance as will be shown later in this section. The heat transfer surface

metal separating the two working fluids in the heat exchanger has the same problem as the breeder metal wall -- that of being thin and operating at high temperatures. Without seriously affecting the power conversion efficiency of fusion power plants, it is doubtful whether the factors contributing to the relatively low metal resistances offered by the two previously mentioned reactor components can be altered in order to reduce tritium permeation rates.

With consideration given to the high pressure (50 atm) helium it contains, the primary coolant runs will, of necessity, be relatively thick. The maximum temperature for the "hot" piping metal would be on the order of the "hot" coolant temperature leaving the blanket, and similarly, the maximum operating temperature for the "cold" piping metal would be the "cold" coolant temperature entering the blanket. These two features should result in the highest metal resistance in the model's simplified reactor design. The simple geometry employed by the model does not allow assessment of more detailed diffusion release paths than these, that might exist in a constructed reactor.

2.3.4.2 Tritium Behavior in Metals: Basic Considerations

The important properties of tritium that will determine its distribution and leakage characteristics in currently conceived fusion reactors are its solubility in the materials with which it comes in contact (only the metals are considered here), and its diffusion rate through the structural components. First it is important to review the formalisms that will later permit these properties to be expressed in terms of the parameters that can be expected to be controlled.

For the relatively dilute (unsaturated) solution environments that most structural materials are expected to encounter in fusion reactor applications, the formalism used to relate the amount of tritium dissolved in a metal, SOL, with the tritium pressure P_{T_2} is given by:

$$SOL = K_S P_{T_2}^{\frac{1}{2}} \qquad (2.4)$$

where the proportionality factor is called the Sieverts" Constant for tritium in that metal. K_s can be expressed in terms of the Sieverts' Constant at infinite temperature, K_s^o , and a heat of solution Q_s :

$$K_s = K_s^o \exp - (Q_s/RT) \qquad (2.5)$$

where T is the absolute temperature (^oK) of the metal. Equilibrium must exist between the gas and the metal at the interface in order for Sieverts' Law (Equation (2.4)) to hold[35]. Values of the solubility in various metals of interest are given in Figure 2-10.

It is fundamental to know the permeation properties of many kinds of metals under realistic operating conditions, in order to complete the dynamic analysis of the tritium flow in this part of the model. The first to consider is the diffusivity. The diffusion coefficient for tritium diffusing through a metal is given by the relationship:

$$D = D^o \exp - (Q_d/RT) \qquad (2.6)$$

where D^o is the diffusion coefficient at infinite temperature, Q_d is the activation energy for diffusion and T is the absolute temperature (^oK) of the metal. When the dissolution (tritium molecules dissolving as atoms at the metal surface) and diffusion processes are not grossly affected by surface and bulk impurity interactions or microstructural irregularities[36], meaning the rate of migration is limited by true bulk diffusion, the tritium permeability K_p, can be determined as the direct product of the tritium concentration gradient and the bulk diffusion coefficient. Thus, K_p is well estimated by:

$$K_p = D \; K_s \qquad (2.7)$$

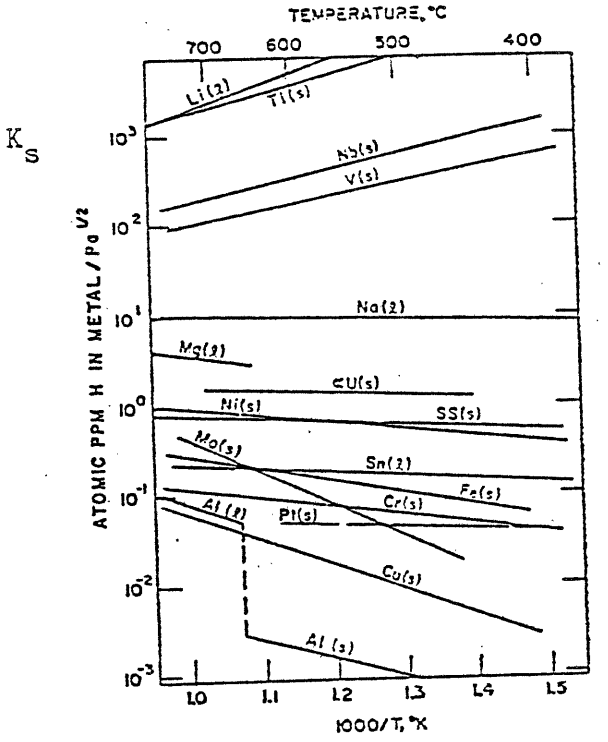

K_S

Metal Temperature

Figure 2-10

Sieverts' Constant for Hydrogen as a Function of Temperature for Selected Metals and Alloys

(Figure taken from Ref. (36))

Attributing Arrhenius temperature dependence* to the permeability, i.e.,

$$K_p = K_p^o \exp - (Q_p/RT) \qquad (2.8)$$

then the following values can be equated:

$$K_p^o = D^o K_s^o \qquad (2.9A)$$

$$Q_p = Q_d + Q_s \qquad (2.9B)$$

Values of the permeability in various metals of interest are given in Figure 2-11.

The metals molybdenum[36], niobium[36] and iron[37] are examples of materials for which this tri-partite relationship between dissolution (K_s), diffusion (D), and permeation (K_p) has been verified. However, with metals that are more sensitive to impurity and microstructural effects (e.g., vanadium[36]) this relationship tends to break down.

Because virtually all materials are permeable to hydrogen and its isotopes, it is important to understand the permeation process and its possible effect on the tritium migration in fusion reactors. Throughout the remaining discussion on tritium behavior in metals, it is allowable to use hydrogen data for the particular properties of interest because the isotopic effect at the relatively high temperatures encountered in fusion reactor application is likely to be small[36]. Therefore, calculations based on protium rather than tritium would probably not be greater than the factor of $(1/3)^{\frac{1}{2}}$ predicted from diffusion theory, which is insignificant for this model. (Grahm's Law[38] states: Relative rates of diffusion of gases under the same conditions are inversely proportional to the square roots of the densities of those gases.)

*Note: In the absence of significant impurity element or microstructural perturbations, dissolution (K_s), diffusion (D), and permeation (K_p) all show an Arrhenius type (exponential) dependence on temperature.[37]

K_p

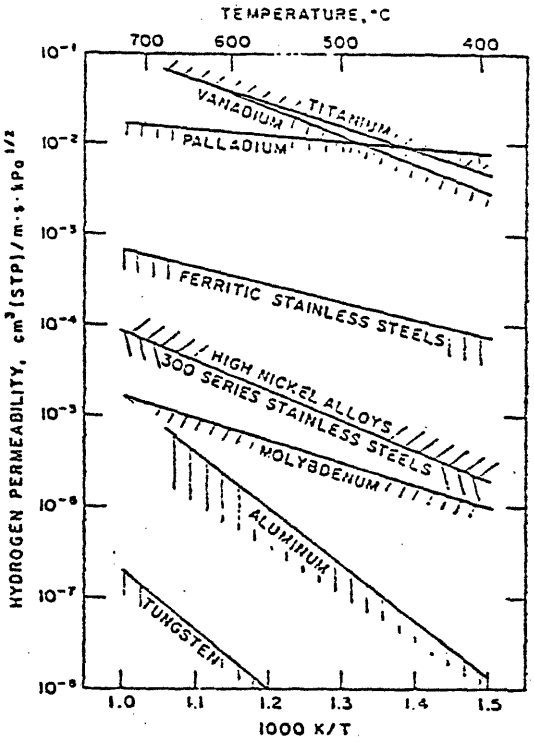

Metal Temperature

Figure 2-11

Hydrogen Permeability as a Function of Temperature for Selected Metals and Alloys

(Figure taken from Ref. (37))

Richardson[39] derived a theoretical relation predicting the rate of permeation J_{metal}, of a molecular gas through a metal or alloy as a function of the gas phase pressure P_{T_2}, system temperature T, and system dimensions: area (A) and thickness (x) of metal wall. Richardson's Equation assumes that bulk diffusion of the atomic species is the rate-limiting process, thus:

$$J_{metal} = \frac{A}{x} K_p(T) \Delta(P_{T_2})^{\frac{1}{2}} \qquad (2.10)$$

where $K_p(T)$ is given by Equation (2.8) and $\Delta(P_{T_2})^{\frac{1}{2}}$ is the driving pressure differential across the wall ($\equiv P^{\frac{1}{2}}_{T_2,high} - P^{\frac{1}{2}}_{T_2,low}$). Implicit in the assumption of diffusion limited permeation is thermodynamic equilibrium between the gas phase and the bulk metal close to the surface as expressed in Equation (2.4). Richardson's Equation thus predicts an inverse dependence on the metal thickness and a square root dependence on the pressure, which is characteristic of umimpeded bulk diffusion as the rate-controlling step in the permeation process.

The expected operating conditions for fusion reactors include cases[40] where the tritium pressure is extremely low, falling considerably below the range of existing permeation data. In these cases, it is normally assumed that the permeation rate may be estimated by extrapolating the experimental data obtained at higher pressures. The common extrapolation based on the relation $J \propto P^{\frac{1}{2}}_{T_2}$ is not valid at very low pressures because there are various gas phase and surface processes that become increasingly important at decreasing pressure.

On the atomic scale, it is evident[41] that the tritium gas molecule T_2, must first dissociatively chemisorb and pass through a normally heterogeneous surface to reach the bulk metal. It undergoes the opposite rate process after diffusing through the bulk metal to reach the downstream gas phase. Although this describes the overall permeation scheme, at each surface both dissociative chemisorption ($T_2 \rightarrow 2T$) and recombinative desorption ($2T \rightarrow T_2$) must occur. When both these rates are fast compared to the diffusion rate, then thermodynamic equilibrium and bulk diffusion-limited permeation are good assumptions and Equation

(2.10) naturally follows. However, if the surface reaction rate is slow or of the same magnitude compared to the diffusion rate, as it is at very low tritium partial pressures, then it cannot be expected that the functional dependence of the permation rate on the system variables would be that predicted by Richardson's Equation.

Recent experiments[31] indicate that at low tritium pressures ($\sim$ 1 torr) the pressure dependence of the permeation rate is close to first order. These results seem to prove that inefficient surface desorption is the rate limiting step in the permeation. Without any other surface impurity layers to complicate the model, the "clean" model of tritium permeation through metals is shown in Figure 2-12 as a function of pressure. If the surfaces are indeed kept clean and a mechanism is provided for the removal of tritium from the downstream surface (as it is in the heat exchanger) then the square root dependence of the permeation is probably the best model to use. If these conditions cannot be met for all the metal barriers in the simplified fusion reactor design, then the square root dependency represents a "worst case" (i.e., most conservative) analysis. For this model, the square root pressure dependency of the permeation rate has been consistently used.

However, it should be made clear what the consequences are of neglecting a possible transition to linear pressure dependency at low driving pressures. The inherent error in blindly using the $P_{T_2}^{\frac{1}{2}}$ rule in extrapolating data to very low pressures is that Richardson's Equation would give permeation rates that are orders of magnitude higher[41] than what would otherwise be the case. It could then be concluded that the control of permeation losses of tritium to the steam cycle is unlikely to be as critical an item for fusion power plants as has been visualized heretofore.

Two major effects of using a linear pressure dependency of the permeation rate are immediately obvious. First, it would be possible to operate fusion platns at a much higher tritium concentration in the coolant. As a consequence, the driving potential for any tritium extraction system operating in the coolant loop would be greater thus making tritium recovery easier. Secondly, major tritium releases to the environment would be more likely to arise from leaks through cracks in structures at

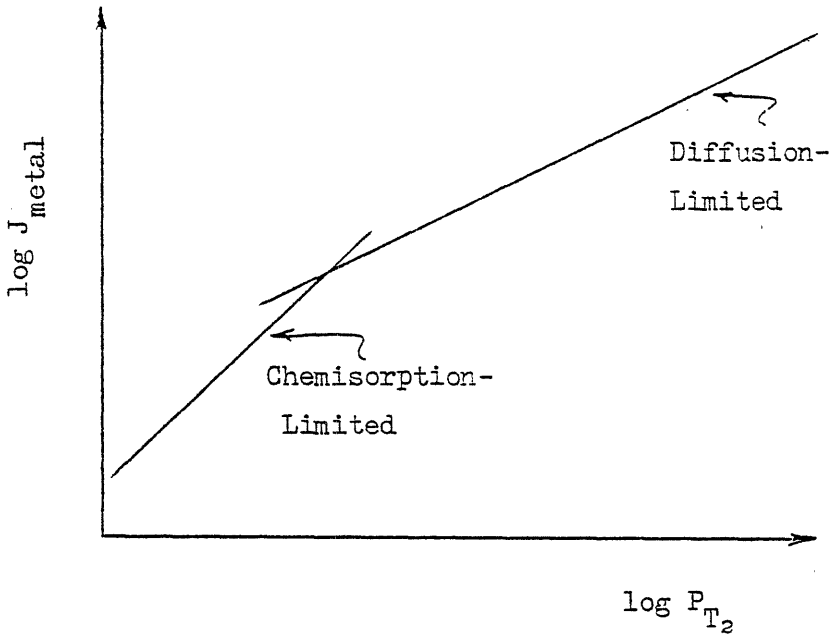

Figure 2-12

Pressure Dependence of Permeation Rate
for the "Clean Surface" Model

seals, and from unavoidable releases during maintenance shutdowns, rather than permeation losses. Perhaps a helpful feature of the fusion reactor design with respect to controlling tritium release to the environment is that the steam pressures under normal operating conditions are much higher than that for the helium (1800 psig vs. 750 psig)[8]. This difference in pressure would tend to mitigate the transport losses to the environment since cracks in the walls of the heat exchanger would result in the leakage of steam into the helium coolant rather than the reverse.

2.3.4.3 Tritium Behavior in Metals: Special Considerations

There are several other important aspects of tritium behavior in metals that because they were not explicitly included in the model, deserve an explanation. Grain boundary diffusion is one of them; it predicts a much faster diffusion rate than that calculated from a bulk diffusion-controlled permeation model. Grain boundaries have been observed[42] to be deficient in tritium and therefore are presumably rapid transport paths for tritium. Although grain boundary diffusion effects at high tritium concentrations have not been observed[42], it is possible that grain boundary transport may be important in fusion reactors where the tritium concentrations in metals are apt to be low.

The temperature of the metal may play a deciding role in deciding whether to use a grain boundary or a bulk diffusion coefficient. At the high operating temperatures expected for the fusion reactor heat transfer system, the diffusion coefficient may indeed be determined by the bulk metal properties. Results[42] above 500 °C have given tritium release rates consistent with bulk diffusion coefficients, while diffusivity results at lower temperatures were anomalous. Thus if the values of D° and Q_d in Equation (2.6) are properly averaged for a wide range of metal temperatures and tritium concentrations, there should be no adverse effects of not explicitly calculating grain boundary diffusion coefficients. Grain boundary effects should already have been included in the diffusivity values tabulated in Appendix B.

Radiation effects on tritium behavior in metals could exacerbate the problem of controlling tritium migration in the metal barriers of fusion devices. The effects of irradiation on tritium permeation rates have not been well studied and are, therefore, difficult to assess[5]. However, a few words about what has been observed is in order. Increased surface and bulk trapping of tritium due to internal defects generated by neutron damage[37] can be expected to compound problems associated with tritium control and reactor maintenance. (Excessive tritium heldup in the metal walls would be a radiological hazard to maintenance men working on them.) In general, neutron irradiation of metal (especially for the breeder tube metal wall which is subject to an unhindered plasma neutron fluence) results in the enhancement[37] of: 1) surface dissociation rates for molecular tritium, T_2 and 2) bulk diffusion rates, both of which translate into an increased tritium flow into the helium coolant. However, for purposes of this model, no allowance was made for neutron-induced enhancement of metal diffusivities over time.

The effects of bulk and surface impurities and microstructural defects on dissolution, diffusion and permeation of tritium in metals have been studied elsewhere[37]. Surface impurities have been found to be instrumental in altering the boundary processes by which tritium absorbs on and diffuses into metals. Dislocations, interstitial vacancy clusters, grain boundary effects, voids and gas bubbles have all been shown to impact on tritium migration profiles in metals. Internal trapping sites[37] can in some instances promote, and in others, retard dissolution and diffusion in metals. In general then, tritium tends to concentrate at defects within the alloy, which could produce tritium concentrations well above the average, as calculated from a bulk diffusion model.

Since it is possible to have such a wide range of effects concerning tritium behavior in metals most of which cannot be quantified, including linear pressure dependency at low pressures, grain boundary diffusion, radiation and impurity effects, it is understandable why a "clean surface" model exhibiting bulk diffusion characteristics has been chosen for the metals represented in the simplified fusion reactor design. Inclusion of these effects, if possible, would only complicate the description of the metal properties without changing the basic concepts of

dissolution, diffusion and permeation in any definitive way.

2.3.4.4 Tritium Permeation Barriers

Although the tritium transport model developed in this report utilizes only "clean" metal components, it is possible to expand the model to include certain additional permeation barriers other than that offered by the metals and the presence of oxygen in the coolant. Three types of permeation barriers are currently recognized as being particularly useful in fusion reactor related tritium control problems. They are, and by no means implying their order of effectiveness:

1 - ceramic surface layer
2 - bonded-metal composite layers
3 - oxide film layer

Each of these will be treated in some detail later.

The use of permeation barriers to assist in reducing the transport of tritium from one reactor component to another in no way precludes the work already done by the model in predicting the tritium concentration build-up in the coolant and elsewhere, and its corresponding permeation leakage out of the containment. These results have already been shown to be useful when estimating how much oxygen should be added to the helium coolant for example, if the permeation losses had been found to be unacceptably high. In the same way, the permeation model can be used to size the necessary permeation barriers if oxidation of the coolant proves undesirable. The effectiveness of each type of barrier is discussed qualitatively in the next few pages, but the use of auxiliary permeation barriers could be accomodated by the model in some later study.

The first such permeation barrier to be discussed is the ceramic surface coating applied to some metals. The utility of ceramics as permeation barriers particularly in and around secondary containment systems (i.e., reactor building walls) is well recognized[37]. Both Al_2O_3 and SiC can be useful as coatings on metal to limit tritium permeation. High-density, sintered Al_2O_3 exhibits[43] no accelerated diffusion due

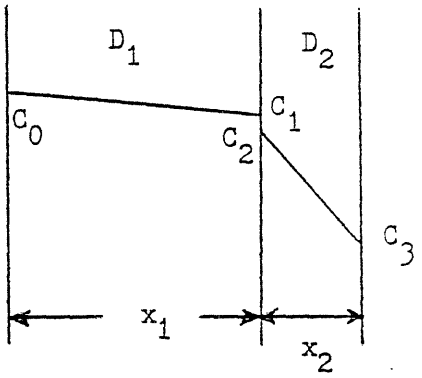

Figure 2-13
Elleman et al. Permeation Model With Surface Coating Intact

(Figure taken from Ref. (45))

microstructural defects, and little increased permeation resulting from tritium transport along grain boundaries. In fact, the permeability of Al_2O_3 was consistent with the values predicted from diffusivity and solubility results (Equation (2.7)) which suggests that grain boundaries, voids and other potential rapid transport paths did not lead to increased permeability[44].

The effectiveness of these special ceramic coatings was examined in detail by Elleman et al.[45]. The effectiveness of various surface coatings was deduced from their experimental work based on the simple model reproduced above in Figure 2-13. Using their assumptions of $C_1 = C_2$ and $C_3 = 0$, the system is said to be at equilibrium. Defining the effectiveness of the coating in preventing the permeation of tritium through it, as

$$\frac{R'}{R} = \frac{\text{equilibrium release rate -- coating}}{\text{equilibrium release rate -- no coating}} \qquad (2.11)$$

the value for $\frac{R'}{R}$ in terms of the system dimensions is given by:

$$\frac{R'}{R} = \frac{\frac{x_1}{D_1}}{\frac{x_2}{D_2} + \frac{x_1}{D_1}} \qquad (2.12)$$

The effectiveness of various surface coatings were determined for several candidate structural materials, at typical operating conditions for the heat exchanger ($T = 600\ ^{o}C$, $x_1 = 0.2$ cm, $x_2 = 0.01$ cm). Their results are repeated here in Table 2-1; the coatings seem to reduce the permeation rate by several orders of magnitude. It is obvious that some incentive exists for developing coatings, paints, or other surface preparations that would resist tritium absorption and permeation.

The concept of a surface coating permeation barrier can be extended to include those strong oxide-forming elements (like aluminum, previously) which also show some promise[37] in yielding permeation-resistant coatings. However, Van Deventer[46] concluded that the presence of aluminum in the bulk alloy is preferable to aluminum coating methods from the standpoint of developing high permeation reduction factors and assuring permeation barrier resiliency. It is conceivable that as a coating, aluminum oxide could crack and/or chip off leaving a part of the bulk metal exposed. For this reason better surface barrier "healing rates" are achieved when aluminum is part of the bulk alloy.

The second type of permeation barrier quoted earlier, is the bonded-metal composites. They are particularly useful for reducing tritium permeation rates through thermally hot structures like the heat exchanger in fusion power reactors. ANL[47] has completed experimental work on three such composites: 316-SS/Cu/316-SS, 304-SS/Nb and 304-SS/Cu/Nb and have concluded that they may have some practical application as tritium permeation barriers. In later tests[48] ANL obtained a reduction factor of 30 for the following two metallurgically bonded aluminum bronze multiplexes: 304-SS/Al bronze sample and a 304-SS/Al bronze/304-SS sample. This was increased to more than 50 by using stainless steel-clad composites containing an intermediate layer of a selected copper

Table 2-1

Evaluation of Ceramic Tritium Barriers
Based Upon Diffusion Coefficients[45]

$-\log \frac{R'}{R}$

Surface Coatings	Tungsten	Molybdenum	Niobium	Austenitic Stainless Steel
Al_2O_3	6 - 8	6 - 7	7 - 8	6 - 7
BeO	7 - 9	7 - 9	8 - 10	7 - 9
Y_2O_3	4	4	5	4
SiC	6 - 10	6 - 9	7 - 10	6 - 9
LUCALOX	3	2	3	2
YTTRALOX	3	3	4	3
SCB GLASS	5	5	6	5
PyC (LAM.)	16	16	17	16

alloy. These are particularly desirable because they combine the corrosion-resistant properties of stainless steel with the tritium permeation-resistant properties of aluminum or copper. In conclusion, the concept of using a laminated permeation barrier is a valuable one, especially in such applications as the interface between the helium coolant and water (steam) loops.

The third, and probably most thoroughly studied, auxiliary permeation barrier is that of an oxide film layer on the metal surface. Oxide films could play a significant role in controlling tritium flow and inventories if conditions favored their formation. Oxygen potentials high enough to sustain these films may be possible with the use of a helium coolant[7]. Even under conditions where the oxidation potential is very low, the addition of strong oxide-forming elements (like aluminum) as surface coatings or to the bulk alloys has already been shown to exhibit increased permeation resistance.

Perhaps the most economical barrier to tritium permeation through metals would be to allow layers of oxides to form in situ on the steam side of the steam generator at, or near, operating conditions. Johnson[49] and Watson[50] have considered ways of using the intentional oxidation of tritium gas in the helium coolant to advantage in creating barriers to tritium migration. Hopefully these intact oxide layers inside the steam generator would not reduce its heat transfer properties.

It is known that ceramic materials are much less permeable than metals; a relatively thin film of metal oxide is considerably more resistive to permeation than is metal. The reason[51] for the relatively high resistance of ceramics is that the tritium gas molecules (T_2) in the helium coolant do not dissociate on the surface and thus cannot dissolve as atoms in the bulk of the ceramic. Permeation through ceramic materials therefore involves molecular species and is much slower than permeation of atoms. In fact, most permeation of a ceramic will occur through defects in the material[51].

The presence of an oxide layer on the metal surface necessarily affects the diffusive behavior of the permeating species. The pressure dependency of permeation through a scrupulously clean metal as shown in Figure 2-12 is altered by the existence of an oxide layer. The overall

permeation behavior through a metal with an oxide surface film is shown qualitatively in Figure 2-14. The results for a clean metal are repeated in Figure 2-14 for comparison.

In the high pressure limit, the permeation rate J_{metal}, is given by Richardson's Equation. Here, diffusion through the bulk metal is rate-limiting. At reduced pressure, the diffusion of molecules through the intact oxide layer takes over because of its linear pressure dependency. Here, transport through the film is the rate-limiting step. At still lower pressures, defects in the oxide film become more important. Permeation through these defects is inherently proportional to the square root of the pressure and it occurs in parallel with diffusion through the intact oxide layer. Thus in this pressure range, transport through the cracks and pores of the oxide film is rate-limiting[41]. Finally, at the ultimate low pressure limit, dissociative chemisorption once again takes over as it did in the clean metal case, because of its linear pressure dependency. All these pressure ranges and their corresponding permeation behavior characteristics, are shown in Figure 2-14 for both the presence and the absence of an oxide film.

The thickness of the oxide layer determines P^*, which marks the onset of the film limitation[52]. It may be difficult[42] to characterize the film by a specific film thickness, however. The film quality factor M, is defined as the fraction of uncoated metal (typically $M \ll 1$)[52]. This governs the pressure at which the transition back to one-half power occurs (P^{**} in Figure 2-14).

The effects of the in situ formed oxide coatings to impede tritium permeation are dependent on the chemical and physical compositions of the oxides. These, in turn, are influenced by several factors:[53,54]

1 - rate of corrosion of the parent metal
2 - aging of the oxide itself
3 - temperature-time history of the film
4 - oxidation potential of the medium
5 - composition of the alloy
6 - annealing and surface treatments of the alloy

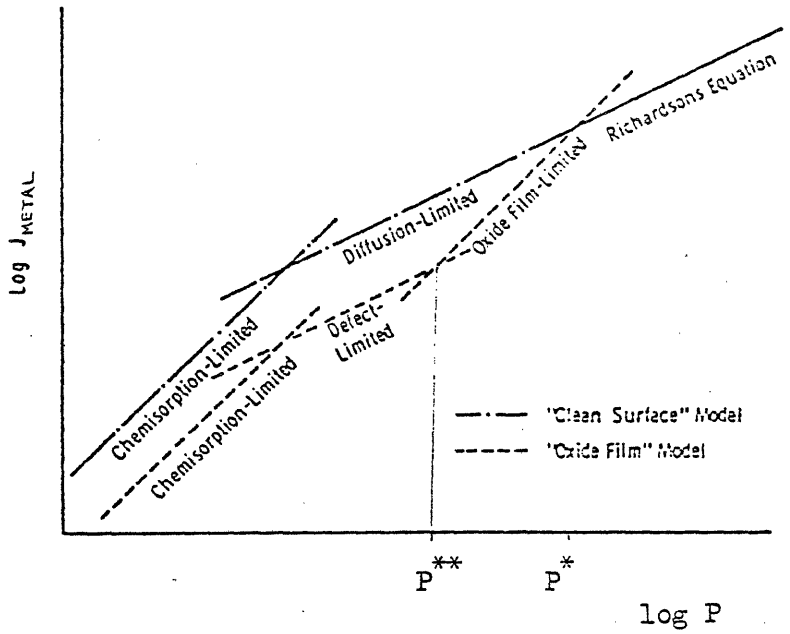

Figure 2-14

Pressure Dependence of Permeation Rate

(Figure taken from Ref. (41))

There is no significant difference[51] in the effects on permeation through in situ formed oxides by an increase in steam pressure from 0.3 to 0.7 atm. The results for Incoloy 800 being exposed to steam at a pressure of 0.7 atm are given in Figure 2-15. A decrease in the rate of permeation (proportional to the permeability plotted in Figure 2-15) from a very high value initially to an equilibrium value several orders of magnitude lower is accomplished by oxidation at the metal surface.

It is possible that defects in the oxide layer inside the steam generator (where this oxidation is assumed to take place) caused by thermal stresses during normal operation could seriously thwart the effort to control tritium permeation in this manner. In order to have an effective permeation barrier an oxide must be used that exhibits "self-healing" characteristics. It has been shown[37] that continued steam oxidation of defected oxide layers on some metals "healed" them with the result that the original barrier effectiveness was restored.

Laboratory experiments[37] have indicated that permeation rates through most austenitic-, nickel-, and refractory metal-base alloys can be reduced by factors of up to 10^5 depending on the extent of oxidation of the surface and the continuity of the oxide layer. More definitive results from experiments under conditions that simulate steam generator environments have shown[37] that steam oxidation of some nickel- and iron-base alloys produces oxide layers that reduce tritium permeation rates by factors of 200 to 600. The few reports[56-59] of hydrogen permeation rates through alloys that were measured while the alloy oxidized, have concluded that the in situ surface oxidation of construction alloys (those candidate steam generator materials) can also produce oxide barriers that reduce tritium permeation rates by significant factors (up to 10^3). A reduction in the surface diffusion coefficient relative to the bulk diffusion coefficient was realized by Elleman and Verghese[60] in their work on oxide formation on stainless steels (two orders of magnitude difference) and niobium and Zircaloy-2 (8-10 orders of magnitude difference). These results were obtained over a temperature range of interest for fusion-related applications. Even

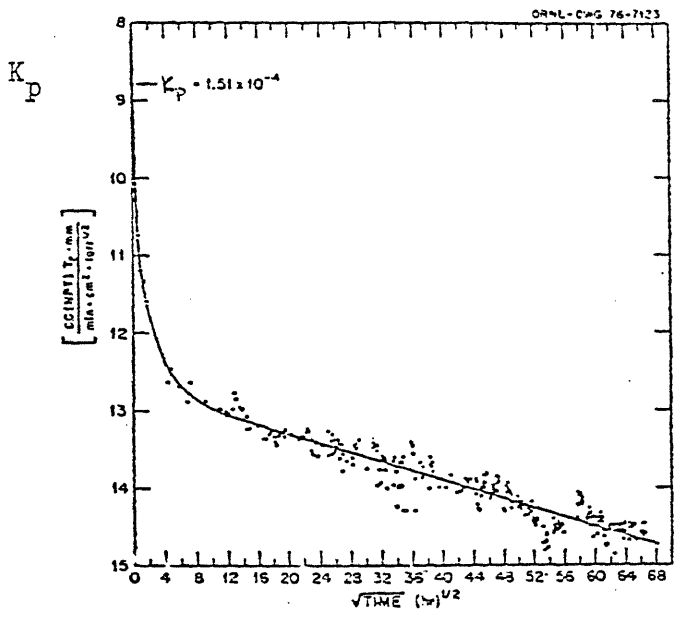

Figure 2-15

Permeability of Tritium Through Incoloy 800 Exposed to Steam at a Pressure of 0.7 atm and a Temperature of 600 °C

(Figure taken from Ref. (55))

the effects of air oxidation on the exterior surfaces of the Haynes* alloys have been found[48] to lead to increased permeation resistances. This might be of some use for controlling tritium leakage through the helium piping, if stable oxide layers can be made to persist. A brief summary of some experimental results in reducing permation through several metals and alloys by the formation of oxide layers is given in Table 2-2.

However, there are no tritium permeation measurements that can be extrapolated to fusion reactor conditions[53] and as a consequence, all the previously-mentioned experimental results can only be used as an indication of what could happen in a fusion reactor steam generator. The presence and effectiveness of oxide layers can only be satisfactorily resolved by measurements on a system in which the mechanisms of formation, chemical composition and stability of oxide layers are representative of those occurring in a fusion power system.

To summarize this section on tritium behavior in metals, it is appropriate to reiterate the two major uncertainities in the chemical and physical behavior of tritium which would significantly impact on the calculation of tritium permeation through metals for the fusion design used in this model. First, the lack of data on tritium permeation in low pressure regimes where extrapolation indicates that some fusion systems may operate has not allowed the verification of the linear pressure law. The use of Richardson's Equation for all metal permeation calculations throughout the model assumes that permeation is bulk diffusion-controlled everywhere. Secondly, the effect of oxide film barriers being formed in situ inside the steam generator could reduce the tritium loss rate to the environment by a factor of 100 or more. This may be enough to preempt the need to include additional permeation barriers in the basic tritium permeation model.

*Note: Haynes is a series of vanadium-base alloys.

Table 2-2

Reduction in Tritium Permeability for Several Metals and Alloys Due to a Surface Oxide Film

	Temperature	Reduction Factor	Reference
347 - SS	- - - -	400	(61)
406 - SS	- - - -	≥ 100	(54)
Croloy T9	- - - -	100	(54)
Croloy T22	- - - -	≥ 100	(54)
Fe-Cr-Al Alloy	1111 °C	1000	(61)
Incoloy 800	525, 660, 720 °C	30 - 700	(61)
Vanadium	- - - -	≥ 100	(62)

2.4 Mathematical Formulation of Model

The series of equations which comprise the transient permeation model will be presented in this section. Following the logic developed in the last section as to the choice of fusion reactor components used in this model, the tritium transport will be followed in a systematic way starting in the breeding zone. Some of the more important assumptions concerning the model will be repeated where it is necessary in the formulation of the equations.

2.4.1 Tritium Behavior in the Breeder

The tritium concentration profile within a breeder pellet, $C_p(r,t)$, is governed by Fick's Law of Diffusion which, in spherical coordinates, becomes:

$$\frac{\partial}{\partial t} C_p(r,t) = {}^{D_b}/_{r^2} \frac{\partial}{\partial r}\left[r^2 \frac{\partial}{\partial r} C_p(r,t)\right] + S_b \qquad (2.13)$$

Both the tritium generation rate and the diffusion coefficient for tritium in a pellet are assumed to be constant in time, and uniform throughout a pellet. For the tritium generation rate to be constant in time, the plasma must theoretically be at its nominal thermal power level at time equal to zero, and the blanket must be operating at its specified breeding ratio. For S_b to be uniform throughout a pellet, one must assume that the neutron fluence emanating from the plasma strikes the pellets uniformly, causing random n + Li reactions. These in turn, would produce a random (and uniform) generation of tritium (T atoms) which are free to diffuse through the pellets. In order for the value of the diffsuion coefficient to be uniform throughout a pellet, one must be able to define an average pellet temperature from which D_b is calculated. Constant D_b with time requires that average temperature to be constant in time also. Fortunately, the temperature profile reaches steady-state much faster than the concentration profile. This is easily proven by comparing the values of the thermal diffusivity for the candidate solid breeders with typical tritium diffusivity values. From Table A-1 of

Appendix A, values of the thermal diffusivity α, are in the range 10^{-3} to 10^{-2} cm^2/sec, while the diffusion coefficient rarely gets above 10^{-7} cm^2/sec (ref. Figure A-1). Thus the assumption will be made that the breeder pellet operates at its steady-state temperature from time equals zero onwards, and the diffusion coefficient will be evaluated based on that temperature. The temperature dependence of the tritium diffusion coefficent for the solid lithium compounds is typically of the Arrhenius form: $D(T) = D^o \exp - (Q_d/RT)$. If the values for the constant D^o (cm^2/sec), or the activation energy for diffusion, Q_d (kcal/mole) are not given then usually a value for D at a particular temperature is quoted (see Appendix A.2 for details).

Equation (2.13) can be solved analytically for the pellet concentration as a function of time and position with a zero surface concentration as a boundary condition:(63)

$$C(r,t) = \frac{S_b}{6D_b}\left[r_p^2 - r^2\right] + \frac{2S_b}{D_b}\frac{r_p^3}{\pi^3 r}\sum_{n=1}^{\infty}\frac{(-1)^n}{n^3}\sin\left(\frac{n\pi}{r_p}\right)\exp - \left[D_b t\left(\frac{n\pi}{r_p}\right)^2\right] \quad (2.14)$$

for, Boundary Condition $C(r_p,t) = 0$
Initial Condition $C(r,0) = 0$

The shape of this function is given in Figure 2-16. This is not considered to be an adequate representation of the breeder pellet because of the zero surface concentration assumption. There will be tritium diffusion from the pellet giving rise to a significant purge gas concentration. The pellet surface concentration is in thermodynamic equilibrium with the surrounding tritium partial pressure in the purge gas, and thus, is necessarily non-zero. Assuming $C(r_p,t) = 0$ at all times and thereby using the expression in Equation (2.14) as the total tritium pellet concentration will seriously misrepresent the magnitude of the concentration. The steady-state limit to Equation (2.13) is considered first, because it gives some insight into the development of the concentration profile.

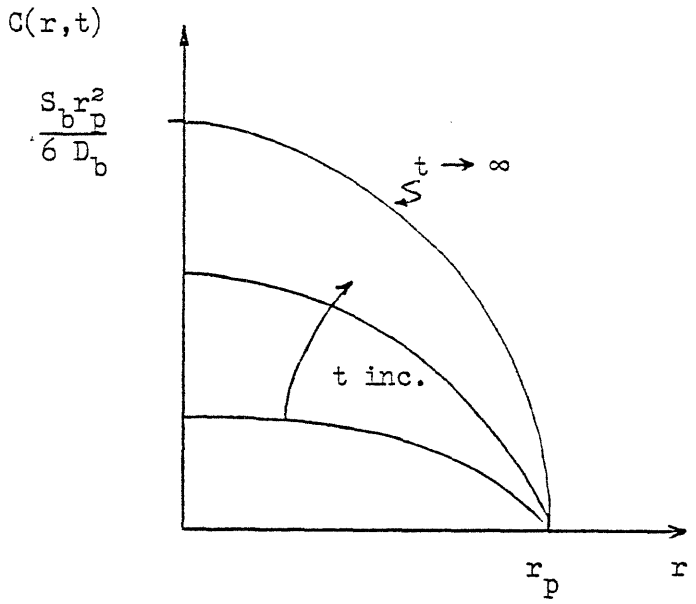

Figure 2-16

C(r,t) Solution to Fick's Diffusion Equation with the Conditions:

$$C(r,0) = 0$$
$$C(r_p,t) = 0$$

For $t \rightarrow \infty$, Equation (2.13) becomes

$$\frac{D_b}{r^2} \frac{\partial}{\partial r} \left[r^2 \frac{\partial}{\partial r} C_p(r,t) \right] + S_b = 0 \qquad (2.15)$$

The following boundary conditions must be satisfied:

$$1 - \quad \frac{\partial}{\partial r} C_p(r,t) \Big|_{r=0} = 0 \qquad (2.16A)$$

and

$$2 - \quad C_p(r_p,t) = C_{sol}(t) \qquad (2.16B)$$

Boundary condition #2 simply restates what was mentioned above: the surface concentration is determined by solubility considerations. Therefore, the surface concentration would be a function of the purge gas concentration:

$$C_{sol}(t) = fn \left(C_{pg}(t) \right) \qquad (2.17)$$

Without specifying this functional reletionship yet, it is possible to solve Equation (2.13) in the limit $t \rightarrow \infty$:

$$C_p(r,SS) = \frac{S_b}{6D_b} \left[r_p^2 - r^2 \right] + C_{sol}(SS) \qquad (2.18)$$

Because $C_{sol}(SS)$ is just the surface concentration calculated from solubility effects, then $C(r_p)$ and C_{sol} are interchangeable. The steady-state tritium concentration in a pellet is given by:

$$C_p(r,SS) = \frac{S_b}{6D_b} \left[r_p^2 - r^2 \right] + C_{sol}(SS) \qquad (2.19)$$

The first two terms on the right-hand side of Equation (2.19) are just the steady-state terms in $C(r,t)$ of Equation (2.14), which, is the solution to the Fick's Law with a zero surface concentration. Therefore the solution to the general Fick's diffusion equation with the actual boundary conditions (2.16A) and (2.16B) can be separated into two terms, one of the form of Equation (2.14) and the other (2.16B) to recover the

non-zero surface concentration. A finite surface concentration must exist in order for a concentration gradient to exist at the surface and thereby provide the driving force for gas phase mass transfer to the purge gas. The following equation for the pellet concentration distribution will now be used:

$$C_p(r,t) = C(r,t) + C(r_p,t) \tag{2.20}$$

where

$$C(r,t) = \frac{S_b}{6D_b}\left[r_p^2 - r^2\right] + \frac{2S_b}{D_b}\frac{r_p^3}{\pi^3 r}\sum_{n=1}^{\infty}\frac{(-1)^n}{n^3}\sin\left(\frac{n\pi}{r_p}\right)\exp - \left[D_b t\left(\frac{n\pi}{r_p}\right)^2\right] \tag{2.21A}$$

and

$$C(r_p,t) = C_{sol}(t) = fn\ (\ C_{pg}(t)\ ) \tag{2.21B}$$

The concentration profile is simply displaced upward by the amount in solution at the surface. The proper concentration profile will now be as depicted in Figure 2-17.

A volume-averaged property is defined in the following way:

$$\langle A(r,t)\rangle \equiv \frac{\int_0^{r_p} 4\pi\, r'^2\, A(r',t)\, dr'}{\int_0^{r_p} 4\,\pi\, r'^2\, dr'}$$

$$= \frac{4\pi \int_0^{r_p} r'^2\, A(r',t)\, dr'}{4/3\,\pi\, r_p^3} \tag{2.22}$$

Taking the volume average of both sides of Equation (2.20) gives

$$\langle C_p(r,t)\rangle = \langle C(r,t)\rangle + \langle C(r_p,t)\rangle \tag{2.23}$$

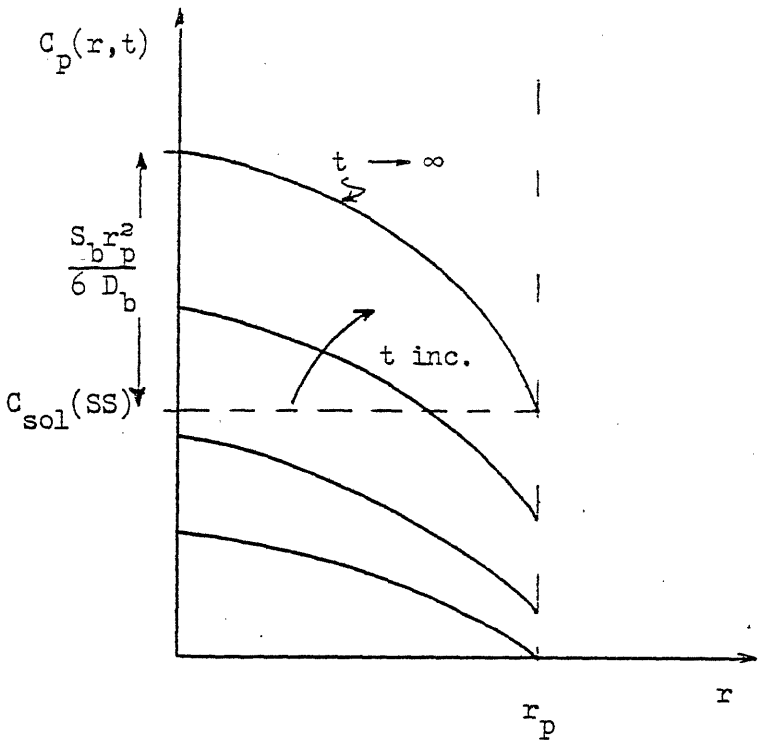

Figure 2-17

$C_p(r,t)$ Solution to Fick's Diffusion Equation with the Conditions:

$$C_p(r,0) = 0$$

$$C_p(r_p,t) = C_{sol}(t)$$

where

$$\langle C(r,t)\rangle = \frac{S_b}{D_b}\frac{r_p^2}{15}\left[1 - \frac{90}{\pi^4}\sum_{n=1}^{\infty}\frac{1}{n^4}\exp -\left[D_b t\left(\frac{n\pi}{r_p}\right)^2\right]\right] \qquad (2.24A)$$

$$\langle C(r_p,t)\rangle = C(r_p,t) = C_{sol}(t) \qquad (2.24B)$$

Conservation of tritium requires the difference in the tritium generation and leakage rates for a given pellet, to be equal to the change in the average pellet concentration. Thus,

$$\frac{\partial}{\partial t}\langle C_p(r,t)\rangle = S_b - L_p(t) \qquad (2.25)$$

where $L_p(t)$ is the leakage from one pellet (Ci/sec cm^3).

The total leakage rate from all the breeder pellets into the purge gas system (Ci/sec) is denoted by $J_b(t)$ and is related to the pellet leakage rate by:

$$J_b(t) = V_b\ L_p(t) \qquad (2.26)$$

Substitution of Equations (2.23) and (2.26) into Equation (2.25) gives

$$\frac{\partial}{\partial t}\langle C(r,t)\rangle + \frac{\partial}{\partial t}C_{sol}(t) = S_b - \frac{J_b(t)}{V_b} \qquad (2.27)$$

or equivalently,

$$\frac{\partial}{\partial t}C_{sol}(t) = S_b - \frac{J_b(t)}{V_b} - \frac{\partial}{\partial t}\langle C(r,t)\rangle \qquad (2.28)$$

where the time derivative of Equation (2.24A) is

$$\frac{\partial}{\partial t}\langle C(r,t)\rangle = S_b\ \frac{6}{\pi^2}\sum_{n=1}^{\infty}\frac{1}{n^2}\ \exp -\left[D_b t\left(\frac{n\pi}{r_p}\right)^2\right] \qquad (2.29)$$

2.4.2 Tritium Behavior in the Purge Gas

The leakage rate from the breeding zone ($J_b(t)$) can easily be related to the total purge gas concentration. A quasi-steady-state model for the purge gas system ignores the (small) permeation losses of tritium from the purge gas through the blanket metal. A mass balance on the purge gas system yields

$$V_{pg} \frac{\partial}{\partial t} C_{pg}(t) = J_b(t) - Q_{pg} C_{pg}(t) \tag{2.30}$$

where

$Q_{pg} C_{pg}(t)$ = rate of tritium being swept away by purge gas

In the form

$$\frac{\partial}{\partial t} C_{pg}(t) + \frac{Q_{pg}}{V_{pg}} C_{pg}(t) = \frac{J_b(t)}{V_b} \tag{2.31}$$

a time constant τ_{pg} is easily recognizable. For the purge gas system, a time constant is defined as

$$\tau_{pg} = \frac{V_{pg}}{Q_{pg}} \tag{2.32}$$

For typical fusion reactor parameters (ref. Appendix F), the time constant τ_{pg} is expected to be very small (on the order of a few seconds). If this is true, then the purge gas responds almost instantaneously to the tritium entering from the pellets. The time evolution of $C_{pg}(t)$ would "track" $J_b(t)$ and the following equality is true for τ_{pg} small ($\leq$ 1 hour):

$$C_{pg}(t) \cong \frac{J_b(t)}{Q_{pg}} \tag{2.33}$$

Substitution of (2.33) into (2.28) gives

$$\frac{\partial}{\partial t} C_{sol}(t) = S_b - \frac{Q_{pg}}{V_b} C_{pg}(t) - \frac{\partial}{\partial t} \langle C(r,t) \rangle \qquad (2.34)$$

$C_{pg}(t)$ can be related to the surface concentration $C_{sol}(t)$, by using Sieverts' Law. For a tritium surface concentration in solution with a tritium partial pressure in the purge gas:

$$C_{sol}(t) = K_{s_{T_2}} P^{\frac{1}{2}}_{T_2,pg}(t) \qquad (2.35)$$

where $K_{s_{T_2}}$ = Sieverts' Constant for tritium in a solid

$P_{T_2,pg}$ = tritium partial pressure in the purge gas

Assuming that the tritium in the purge stream acts as an ideal gas, then

$$P_{T_2,pg} = \frac{n_{pg}(t)\, RT_{pg}}{V_{pg}} \qquad (2.36)$$

where $n_{pg}(t)$ = number of gm-moles of T_2 = $1/6 \times 10^{-4} C_{pg}(t) V_{pg}$ (2.37)

Equations (2.36) and (2.37) are then substituted into Equation (2.35):

$$C_{sol}(t) = K_{s_{T_2}} \left[\frac{RT_{pg}\, C_{pg}(t)}{6 \times 10^4} \right]^{\frac{1}{2}} \qquad (2.38A)$$

Solving for the purge gas concentration as a function of the pellet surface concentration:

$$C_{pg}(t) = \frac{6 \times 10^4\, C^2_{sol}(t)}{R\, T_{pg}\, K^2_{s_{T_2}}} \qquad (2.38B)$$

Substitution of Equations (2.29) and (2.37) into (2.34) gives the general differential equation for the pellet surface concentration:

$$\frac{\partial}{\partial t} C_{sol}(t) + \frac{6 \times 10^4 \, Q_{pg}}{V_b \, K_{s_T}^2 \, RT_{pg}} \, C_{sol}^2(t) = S_b \left[1 - \frac{6}{\pi^2} \sum_{n=1}^{\infty} \frac{1}{n^2} \exp - \left[D_b t \left(\frac{n\pi}{r_p} \right)^2 \right] \right] \qquad (2.39)$$

with the initial condition, $C_{sol}(0) = 0$.

The steady-state surface concentration due to solubility effects, would therefore be

$$C_{sol}(SS) = K_{s_{T_2}} \left[\frac{S \, R \, T_{pg}}{6 \times 10^4 \, Q_{pg}} \right]^{\frac{1}{2}} \qquad (2.40)$$

Equation (2.39) can be solved numberically for $C_{sol}(t)$, by using a programmable hand calculator, and thus it wasn't necessary to formulate a computer solution. The solution to (2.39) combined with the value for $\langle C(r,t) \rangle$ calculated from Equation (2.24A), will give the desired result, $\langle C_p(r,t) \rangle$, according to Equation (2.23). Once the value for $\langle C_p(r,t) \rangle$ is known, then the total tritium breeder inventory is calculated from

$$I_b(t) = V_b \langle C_p(r,t) \rangle \qquad (2.41)$$

The steady-state pellet concentration is given by

$$C_p(r,SS) = \langle C(r,SS) \rangle + C_{sol}(SS) \qquad (2.42)$$

which is just

$$C_p(r,SS) = \frac{S_b}{D_b} \frac{r_p^2}{15} + K_{s_{T_2}} \left[\frac{S \, R \, T_{pg}}{6 \times 10^4 \, Q_{pg}} \right]^{\frac{1}{2}} \qquad (2.43)$$

The steady-state breeder inventory would therefore be:

$$I_b(SS) = V_b \langle C_p(r,SS) \rangle \qquad (2.44)$$

From Equation (2.27) as $t \longrightarrow \infty$, one obtains for the steady-state leakage from the pellets

$$J_b(SS) = S_b V_b = S \tag{2.45}$$

According to Equation (2.33) the steady-state purge gas concentration would be

$$C_{pg}(SS) = \frac{J_b(SS)}{Q_{pg}} = \frac{S}{Q_{pg}} \tag{2.46}$$

The time constants for reaching the steady-state values in Equations (2.40) through (2.46) can be of great interest when analyzing a specific reactor design. The form of the differential equation for $C_{sol}(t)$ (Equation (2.39)) is not conducive for defining its time constant, τ_{sol}. Since τ_{sol} cannot be determined analytically, a value has to be found from numerically integrating the differential equation and examining how long it takes to reach steady-state. The expression for $\langle C(r,t) \rangle$ is a complicated function, involving an infinite series over time, and again, a time constant $\tau_{\langle C \rangle}$ cannot be analytically determined. The same procedure of calculating $\langle C(r,t) \rangle$ as a function of time in order to find the time to reach steady-state is used for this concentration expression also. The time constant for the average pellet concentration, $\langle C_p(r,t) \rangle$, would therefore be equal to the larger of the two values for the time constants, τ_{sol} and $\tau_{\langle C \rangle}$.

The breeding zone leakage rate reaches steady-state at the same time that the average pellet concentration does ($\tau_{J_b} = \tau_{\langle C_p \rangle}$). Since the purge gas concentration responds quickly to $J_b(t)$, one expects the effective time constant for the purge gas, τ'_{pg} to be equal to that for the breeder leakage rate. In summary then, the time constants are expected to follow the ordering:

$$\tau_{pg} \ll \tau_{\langle C \rangle} < \tau_{sol} \approx \tau_{C_p} = \tau_{J_b} = \tau'_{pg} \tag{2.47}$$

2.4.3 Tritium Diffusion in Gases and Through Metals

A gas flowing within a closed channel has a stagnant boundary layer next to the walls. The resistance to diffusion of a trace element, in this case tritium gas (T_2) diffusing through helium gas, offered by this "film" is characterized by a mass transfer coefficient for that gas, h. The rate of tritium diffusion through the film is given by

$$J_{film} \ (Ci/sec) = A\ h\ \Delta C \qquad (2.48)$$

where A = surface area of the channel wall

ΔC = tritium concentration drop across the film = $C_{gas} - C_{\substack{metal \\ surface}}$

A film resistance to tritium diffusion is therefore defined as being

$$R_{film} = \frac{1}{A\ h} \qquad (2.49)$$

The value for the mass transfer coefficient depends on the flow regime for the helium gas (either laminar or turbulent) and the helium gas properties which by themselves are a function of temperature and pressure. The Reynolds Number for the helium determines which flow regime the system is operating in:

$$Re \equiv \frac{u\ d}{\nu} < 2300 \Rightarrow \text{LAMINAR} \qquad (2.50)$$

$$" > 2300 \Rightarrow \text{TURBULENT}$$

Coorelations[64] for the Nusselt Number (Nu) are used to solve for a value of the mass transfer coefficient.

$$\text{LAMINAR} \longrightarrow Nu \equiv \frac{h\ d}{D_G} = 3.66 \qquad (2.51A)$$

$$\text{TURBULENT} \longrightarrow Nu \equiv \frac{h\ d}{D_G} = 0.023\ Re^{0.83} Sc^{0.44} \qquad (2.51B)$$

where the Schmidt Number is defined as $Sc \equiv \frac{\nu}{D_G}$.

The coorelation for the laminar flow Nusselt Number assumes a uniform surface concentration on the pellet. Since the entire breeder is represented by a single, average pellet with an angular-independent surface concentration, this assumption is valid. The values of D_G (tritium diffusivity in the helium gas), ρ_{He} and ν_{He} which are required to solve for the mass transfer coefficients, are all given as functions of temperature and pressure in Appendix C.

Tritium permeation through the metal is assumed to be governed by Richardson's Equation:

$$J_{metal} = \frac{A\, K_p(T)}{x} \left[P_{high}^{\frac{1}{2}} - P_{low}^{\frac{1}{2}} \right] \qquad (2.52)$$

where

$K_p(T)$ = tritium permeability for that metal, as a function of temperature

P_{high}, P_{low} = tritium partial pressures on either side of the metal thickness (x)

Although there is evidence that at low tritium partial pressures, the pressure dependency becomes linear[52,54,65], the form of Equation (2.52) will be used to represent tritium flux behavior through metals in this model. The concentration of tritium in a metal is related to the partial pressure of tritium in the cover gas by a solubility factor (Sieverts' Constant) according to Sieverts' Law for metals:

$$C_{metal} = K_s(T)\ P^{\frac{1}{2}} \qquad (2.53)$$

Both the Sieverts' Constant and permeability are of the Arrhenius form:

$$K_s(T) = K_s^o \exp - (Q_s/RT) \qquad (2.54A)$$

$$K_p(T) = K_p^o \exp - (Q_p/RT) \qquad (2.54B)$$

where K_s^o and K_p^o are constants, and Q_s and Q_p are activation energies.

Since the diffusivity is equal to the permeability divided by the solubility:

$$D(T) = \frac{K_p(T)}{K_s(T)} = \frac{K_p^o}{K_s^o} \exp - \left[\frac{Q_p - Q_s}{RT}\right] \qquad (2.55)$$

the following relationships may be useful if the values for D^o and Q_d are not explicitly given:

$$D(T) = D^o \exp - (Q_d/RT) \qquad (2.56)$$

such that

$$D^o = K_p^o / K_s^o \qquad (2.57A)$$

$$Q_d = Q_p - Q_s \qquad (2.57B)$$

Appendix B includes the tritium diffusivity information needed for many different types of metals frequently encountered as candidate structural materials.

Substitution of Equations (2.53) and (2.55) into Richardson's Equation yields:

$$J_{metal} = \frac{A\ D(T)}{x}\ \Delta C \qquad (2.58)$$

where

ΔC = tritium concentration drop across the metal

The corresponding resistance to diffusion offered by the metal is given by

$$R_{metal} = \frac{x}{A\ D(T)} \qquad (2.59)$$

which is only a function of the metal temperature and system dimensions.

In summary then, the tritium flux behavior is related to concentration and system parameters by:

$$J_{film} = R_{film}^{-1}\ \Delta C \qquad (2.60A)$$

$$J_{metal} = R_{metal}^{-1}\ \Delta C \qquad (2.60B)$$

where the resistances are as defined in Equations (2.49) and (2.59).

2.4.4 Tritium Behavior in the Coolant

If one assumes that the coolant concentration is approximately the same around the coolant loop (blanket → "hot" leg → heat exchanger → "cold" leg → blanket) then the time rate of change in the coolant concentration would be equal to the difference between the rate of tritium entering the coolant from the breeding zone ($J_{pgc}(t)$) and the rate of tritium leaving the coolant system through the piping and heat exchanger ($J_{CL}(t)$). This mass balance for the tritium in the coolant can be written:

$$V_c \frac{\partial}{\partial t} C_c(t) = J_{pgc}(t) - J_{CL}(t) \tag{2.61}$$

The transport terms J(t) are defined below:

$$J_{pgc}(t) = R_{pgc}^{-1} \left[C_{pg}(t) - C_c(t) \right] \tag{2.62}$$

$$J_{CL}(t) = R_{CL}^{-1} \left[C_c(t) - C_\infty \right] \tag{2.63}$$

where the purge gas concentration is given by Equation (2.33) and the concentration C_∞ in the "environment" (containment atmosphere and/or steam system) is assumed to be zero. The resistances R_{pgc} and R_{CL} are defined below:

$$R_{pgc} = R_{pgm} + R_m + R_{mc} \tag{2.64}$$

$$\frac{1}{R_{CL}} = \frac{1}{R_{HPL}} + \frac{1}{R_{HXL}} + \frac{1}{R_{CPL}} \tag{2.65}$$

These resistances to tritium flow can be represented by a circuit diagram (ref. Figure 2-18) where the "current" is the flow of tritium induced by the concentration gradients. The resistances on the right-hand side of Equations (2.64) and (2.65) are all functions of the system parameters. Therefore, the values for the system parameters for the system resistances

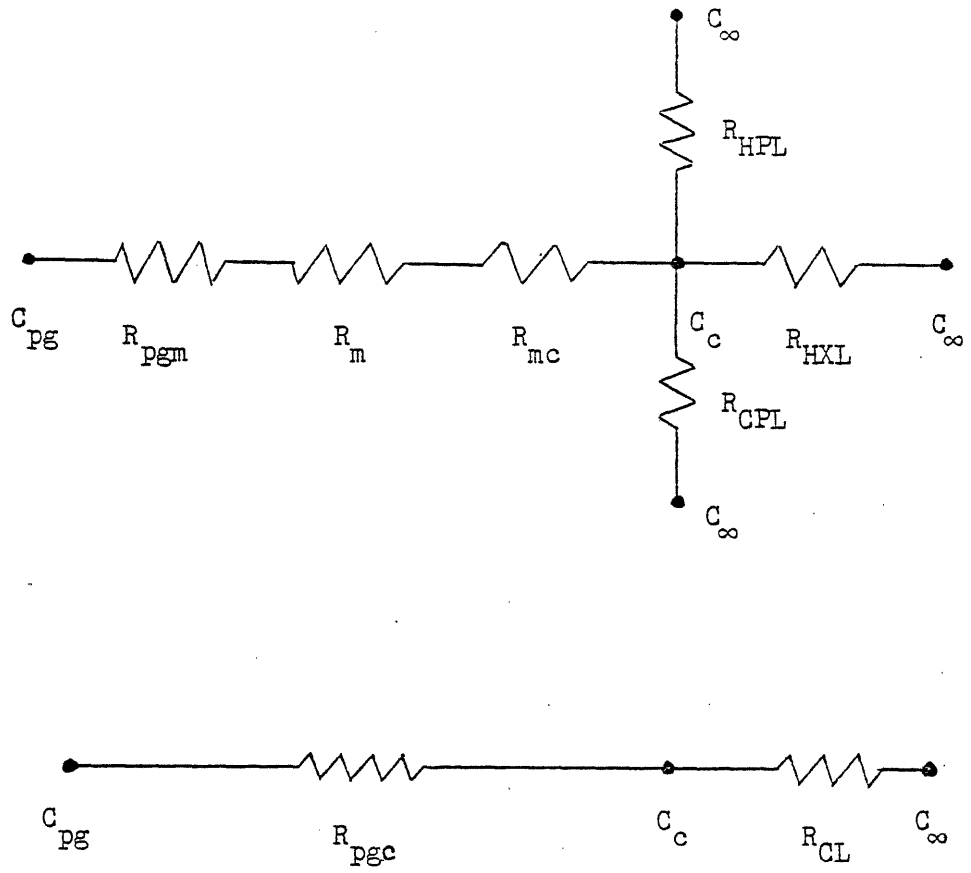

Figure 2-18

Circuit Diagram for Tritium Flow in a Simplified Fusion Reactor System Design

are explicitly written here for future use:

Purge Gas to Coolant: R_{pgc}

$$R_{pgm} = \frac{1}{A_m h_{pg}} \tag{2.66A}$$

$$R_m = \frac{x_m}{A_m D_m} \tag{2.66B}$$

$$R_{mc} = \frac{1}{A_m h_B} \tag{2.66C}$$

Coolant to Environment: R_{CL}

$$R_{HPL} = \frac{1}{A_{HP} h_{HP}} + \frac{x_{HP}}{A_{HP} D_{HP}} \tag{2.67A}$$

$$R_{HXL} = \frac{1}{A_{HX} h_{HX}} + \frac{x_{HX}}{A_{HX} D_{HX}} \tag{2.67B}$$

$$R_{CPL} = \frac{1}{A_{CP} h_{CP}} + \frac{x_{CP}}{A_{CP} D_{CP}} \tag{2.67C}$$

The general differential equation for the coolant concentration makes use of Equations (2.62) and (2.63) combined with the original form, Equation (2.64) and (2.65). Thus, the equation

$$\frac{\partial}{\partial t} C_c(t) + \frac{1}{V_c}\left[\frac{1}{R_{pgc}} + \frac{1}{R_{CL}}\right] C_c(t) = \frac{1}{V_c R_{pgc}} C_{pg}(t) \tag{2.68}$$

yields the time constant for the response of the coolant system to a non-zero purge gas concentration:

$$\tau_c = \frac{V_c}{\frac{1}{R_{pgc}} + \frac{1}{R_{CL}}} \tag{2.69}$$

If τ_c is much greater than the time for the purge gas to reach steady-state (τ'_{pg}, Equation (2.47)), then it is possible to treat the purge gas concentration as constant in time, and equal to its steady-state value, $C_{pg}(SS)$. With this simplication, there is an analytical solution to Equation (2.68):

$$C_c(t) \cong \frac{\tau_c}{V_c R_{pgc}} C_{pg}(SS) \left[1 - \exp -(t/\tau_c) \right] \quad (2.70)$$

where

$$C_{pg}(SS) = \frac{S}{Q_{pg}}$$

The steady-state concentration in the coolant would therefore be:

$$C_c(SS) \cong \frac{\tau_c}{V_c R_{pgc}} C_{pg}(SS) \quad (2.71)$$

and the corresponding steady-state coolant inventory is just:

$$I_c(SS) = V_c C_c(SS) \quad (2.72)$$

2.4.5 Tritium Loss Terms

A description of this permeation model has already stated that only tritium leakages from the coolant piping system and the heat exhanger would be considered. Tritium lost from the "hot" leg and "cold" leg segments of the piping system ($J_{HPL}(t)$ and $J_{CPL}(t)$ respectively) enters the containment building atmosphere. A continuously operating air detritiation system recovers approximately 90 % of this tritium. However, tritium lost through the heat exchanger ($J_{HXL}(t)$) enters the steam cycle and is assumed lost to the environment. Therefore, it is important to state the dependence of these loss terms on the coolant tritium concentration function, developed in the preceding section.

Tritium losses are calculated from the following equations:

$$J_{HPL}(t) = R_{HPL}^{-1} C_c(t) \qquad (2.73A)$$

$$J_{CPL}(t) = R_{CPL}^{-1} C_c(t) \qquad (2.73B)$$

and,

$$J_{HXL}(t) = R_{HXL}^{-1} C_c(t) \qquad (2.73C)$$

The resistances are as defined in Equations (2.67) and the coolant concentration is given in Equation (2.70). The steady-state tritium losses from the helium coolant are therefore:

$$J_{HPL}(SS) = R_{HPL}^{-1} C_c(SS) \qquad (2.74A)$$

$$J_{CPL}(SS) = R_{CPL}^{-1} C_c(SS) \qquad (2.74B)$$

$$J_{HXL}(SS) = R_{HXL}^{-1} C_c(SS) \qquad (2.74C)$$

The maximum tritium leakage from this reactor plant will be its steady-state value, which occurs in a time approximately equal to $\tau'_{pg} + \tau_c$.

2.4.6 Addition of Oxygen to Coolant

It is anticipated that the value for the coolant concentration may give unacceptably large values for the tritium loss terms, even before steady-state is reached. A method to combat this problem, without changing any of the system dimensions or operating temperatures, is to introduce some oxygen gas into the helium coolant. This will effectively reduce the tritium gas partial pressure in the coolant which is the driving force behind the tritium permeating out of the system. The tritium gas present in the coolant will react with the oxygen to form tritiated water:

$$T_2 + \tfrac{1}{2} O_2 \rightleftharpoons T_2O \tag{2.75}$$

At equilibrium, this reaction has the equilibrium constant defined by:

$$K_{T_2O}(T) = \frac{P(T_2O)}{P(T_2)\, P^{\frac{1}{2}}(O_2)} \tag{2.76}$$

The equilibrium constant K_{T_2O} is a strong function of the coolant temperature; a method for evaluating K_{T_2O} is presented in Appendix D.

The largest coolant concentration occurs in steady-state, so that value is the one which must be dealt with during the oxygen addition calculations. The number of grams of T_2 gas in the coolant in steady-state (as yet, uncorrected by oxygen addition) is given by $I_c(SS) \times 10^{-4}$. The number of moles of T_2 gas in the coolant is therefore

$$n_{T_2} = 1/6 \times 10^{-4} \; I_c(SS) \tag{2.77A}$$

When oxygen is added to the helium system, so that at equilibrium, the number of moles of T_2O gas equals the number of moles of T_2 gas already there, then

$$n_{T_2O} = 1/6 \times 10^{-4} \; I_c(SS) \tag{2.77B}$$

Assuming the T_2O gas behaves as an ideal gas, then the resulting partial pressure of T_2O would be

$$P_{T_2O} = \frac{n_{T_2O} \; R \; T_c}{V_c} \tag{2.78}$$

where T_c is the temperature of the coolant.

Since guidelines on the maximum allowable tritium release rate to the environment set a maximum value on the loss rate through the heat exchanger ($J_{HXL,max}$), this then, is the most stringent condition for the maximum coolant concentration. This can be quantified in the following way. First set $J_{HXL}(SS)$ in Equation (2.74C) equal to the specified value

$J_{HXL,max}$. The "corrected" tritium concentration in the coolant has to be kept below

$$C_c'(SS) = R_{HXL}\, J_{HXL,max} \qquad (2.79)$$

in order to keep within the allowable release rate of $J_{HXL,max}$. The maximum coolant inventory is therefore

$$I_c'(SS) = V_c\, C_c'(SS) \qquad (2.80)$$

The number of moles of T_2 gas in the coolant system, corresponding to the release rate $J_{HXL,max}$ is then

$$n_{T_2}' = 1/6 \times 10^{-4}\, I_c'(SS) \qquad (2.81)$$

Assuming the T_2 gas exhibits ideal gas behavior, then the corrected tritium partial pressure in the coolant is given by:

$$P_{T_2}' = \frac{n_{T_2}'\ R\ T_c}{V_c} \qquad (2.82)$$

The necessary oxygen partial pressure in the helium coolant to maintain tritium leakage rate from the heat exchanger of $J_{HXL,max}$ is found by substituting Equations (2.78) and (2.82) into (2.76) and solving for $P(O_2)$:

$$P(O_2) = \left[\frac{I_c(SS)}{I_c'(SS)}\ \frac{1}{K_{T_2O}(T)}\right]^2 \qquad (2.83)$$

Once the value for the equilibrium constant is evaluated from the information in Appendix D, Equation (2.83) will give the correct oxygen partial pressure which should be introduced into the helium coolant system in order to maintain the acceptable tritium loss of $J_{HXL,max}$.

CHAPTER 3 CASE STUDY: STARFIRE (INTERIM DESIGN)

3.1 Description of STARFIRE Design

The STARFIRE Reference Design was chosen as the case study for application of the transient permeation model developed in the previous chapter. There are several reasons for making this choice. First, STARFIRE is of the the size thought to be characteristic of first-generation fusion reactors: 3 - 4 GW_{th} (STARFIRE-Interim is designed to produce 3.8 GW of thermal power.). The Interim Design Report for STARFIRE[8] also has specified features which are needed in the application of the aforementioned permeation model. The major criteria were: a solid breeding material, a helium purge gas stream running through the blanket, and a helium coolant which acts as the sole means of transport of tritium from the blanket and through the steam generator to the environment.

Although the STARFIRE Final Design Report[17] was published before this investigation was completed, it was not considered for use as a case study because a major design change had been implemented. The Final STARFIRE Design involves a water-cooled blanket, as well as a different solid lithium compound breeder. For these reasons, the system parameters as specified in the STARFIRE-Interim Design were used as input to the permeation model. Those parameters needed for input, but not given in the Interim Design, were, if possible, taken from the Final Design, or another "best" value was chosen. (See Applendix F for a detailed account of how all the necessary system parameters were determined.)

The STARFIRE-Interim tokamak reactor is designed to operate with a continuous plasma burn and develops $\sim$ 3800 MW of thermal power. The blanket consists of a tritium breeding medium of solid Li_2O pellets encased in a ferritic steel structure with numerous coolant tubes passing through it. A high pressure helium coolant is used to cool the blanket, and a separate low pressure helium stream acts as a purge mechanism for tritium diffusing out of the breeder pellets. This purge gas system is then processed for eventual tritium refuelling of the reactor. There are six primary coolant loops attached to the blanket. Each one carriers 50 atm of hot (500 ^{o}C) helium gas at 317 kg/sec to a steam generator, where press-

urized water is heated to steam at 427 °C. The helium coolant is then returned to the blanket, with an average inlet temperature of 300 °C. There are no intermediate heat exhangers or coolants in this design, so that any tritium that permeates through the first steam generator into the water cycle is assumed lost to the environment. Appendix F describes in greater detail the points of interest in the STARFIRE-Interim Design.

3.2 Application of Transient Permeation Model to STARFIRE

Once the STARFIRE system parameters were determined (as given in Appendix F), values for the necessary coolant and metal resistances could be calculated. The definitions of these resistances are consistent with those used in Chapter 2. The values for the resistances are given in Table 3-1. An important observation to make is that the major contributor to the resistance to tritium flow is that of the metal, x/AD, and not the fluid film resistance. Only by using real design values for these parameters has this effect become obvious.

3.2.1 Response Times

The purge gas system was assumed to respond very quickly to the leakage of tritium from the breeder pellets, which allowed us to write

$$C_{pg}(t) \cong \frac{J_b(t)}{Q_{pg}} \tag{3.1}$$

Although it was an assumption during the formulation of the model equations, it can now be shown that this is indeed the case. The response time for the purge gas system was given in Chapter 2, Equation (2.32):

$$\tau_{pg} \equiv \frac{V_{pg}}{Q_{pg}} \tag{3.2}$$

Substituting the STARFIRE-Interim Design values for the purge gas volume and volumetric flow rate, the response time for the purge gas is just 5.6

Table 3-1

STARFIRE - Interim Resistances to Tritium Permeation

Resistance	Definition	System Values
Of the Breeder Tube Wall		
R_{pgc}	$= R_{pgm} + R_m + R_{mc}$	
	$= \frac{1}{A_m h_{pg}} + \frac{x_m}{A_m D_m} + \frac{1}{A_m h_B}$	$= 1.130 \times 10^{-9} + 5.453 \times 10^{-3} + 8.135 \times 10^{-10}$
		$= 5.453 \times 10^{-3}$ (sec/cm³)
Of the Hot Pipe		
R_{HPL}	$= \frac{1}{A_{HP} h_{HP}} + \frac{x_{HP}}{A_{HP} D_{HP}}$	$= 3.888 \times 10^{-9} + 4.930 \times 10^{-1}$
		$= 4.930 \times 10^{-1}$ (sec/cm³)
Of the HX		
R_{HXL}	$= \frac{1}{A_{HX} h_{HX}} + \frac{x_{HX}}{A_{HX} D_{HX}}$	$= 2.198 \times 10^{-9} + 3.501 \times 10^{-4}$
		$= 3.501 \times 10^{-4}$ (sec/cm³)
Of the Cold Pipe		
R_{CPL}	$= \frac{1}{A_{CP} h_{CP}} + \frac{x_{CP}}{A_{CP} D_{CP}}$	$= 4.291 \times 10^{-9} + 1.192 \times 10^{+1}$
		$= 1.192 \times 10^{+1}$ (sec/cm³)
Of the Coolant Loop		
R_{CL}		$\cong 1.241 \times 10^{+1}$ (sec/cm³)

sec. The time for it to reach steady-state is another matter, because that time constant will depend on the leakage from the pellets, which means the time to reach steady-state in the purge gas depends on how long it takes the breeder to reach its final tritium concentration. The time to reach steady-state tritium concentration in the breeder, and hence steady-state purge gas concentration, will be addressed in Section 3.2.3.

The response time for tritium build-up in the helium coolant loop was thought to be very long so that one could assume that the helium coolant is effectvely driven by the steady-state purge gas concentration. This assumption is valid if the time constant for the coolant, τ_c, is much longer than that for the purge gas to reach steady-state. Again, for the latter time, the value will be determined in Section 3.2.3. The time constant for the coolant system is, as defined in Chapter 2, Equation (2.69).

$$\tau_c \equiv \frac{V_c}{\frac{1}{R_{pgc}} + \frac{1}{R_{CL}}} \qquad (3.3)$$

STARFIRE-Interim values for these parameters give a time constant for the coolant equal to 1.016×10^7 sec (118 days). As long as this time is greater than the time to reach a steady-state purge gas concentration, then using the following equation for the coolant concentration

$$C_c(t) = \frac{\tau_c}{V_c R_{pgc}} \; C_{pg}(SS) \left[1 - e^{-t/\tau_c} \right] \qquad (3.4)$$

will only be slightly overestimating the coolant concentration, until itself reaches its steady-state value.

3.2.2 Time Evolution of Breeder Concentration

The general form of the differential equation for the surface concentration due to solubility effects is taken from Equation (2.34) and repeated here for convenience:

$$\dot{C}_{sol}(t) = S_b - \frac{Q_{pg}}{V_b} C_{pg}(t) - \frac{\partial}{\partial t} \langle C(r,t) \rangle \qquad (3.5)$$

where

$$C(r,t) = S_b \frac{6}{\pi^2} \sum_{n=1}^{\infty} \frac{1}{n^2} \exp -\left[D_b t \left(\frac{n\pi}{r_p}\right)^2\right]$$

The relationship between the surface concentration of tritium in the breeder pellet, and the tritium partial pressure in the sweep gas (deduced from C_{pg}) is usually given by a Sieverts relationship of the form

$$C_{sol} = K_s P_{pg}^{\frac{1}{2}} \qquad (3.6)$$

Since the Sieverts' Constant for tritium (or hydrogen) in solid Li_2O, the breeding material used in STARFIRE-Interim, was unavailable, the vapor pressure data given in Appendix F for Li_2O is used instead. Substitution of Equation (F.2) of Appendix F into Equation (3.5) above, and after some rearrangement, yields:

$$\dot{C}_{sol}(t) + 6 \times 10^4 \frac{Q_{pg}}{V_b R T_{pg}} 10^{\left[\frac{C_{sol}(t)}{299/5 \times 10^{-2} \rho_b} - 8.017\right]} = S_b \left[1 - \frac{6}{\pi^2} \sum_{n=1}^{\infty} \frac{1}{n^2} \exp -\left[D_b t \left(\frac{n\pi}{r_p}\right)^2\right]\right] \qquad (3.7)$$

The steady-state surface concentration would therefore be:

$$C_{sol}(SS) = 299/5 \times 10^{-2} \rho_b \left[8.017 + \log \frac{S}{6 \times 10^4} \frac{RT_{pg}}{Q_{pg}}\right] \qquad (3.8)$$

Equation (3.7) was solved numerically for the STARFIRE-Interim system parameters listed in Tables F-2 and F-3, using a fourth-order Runge-Kutta integration scheme on a programmable hand calculator. The time evolution of $C_{sol}(t)$ is plotted in Figure 3-1. The surface concentration reaches its steady-state value of 9.060 Ci/cm^3 in approximately 1.3×10^6 sec

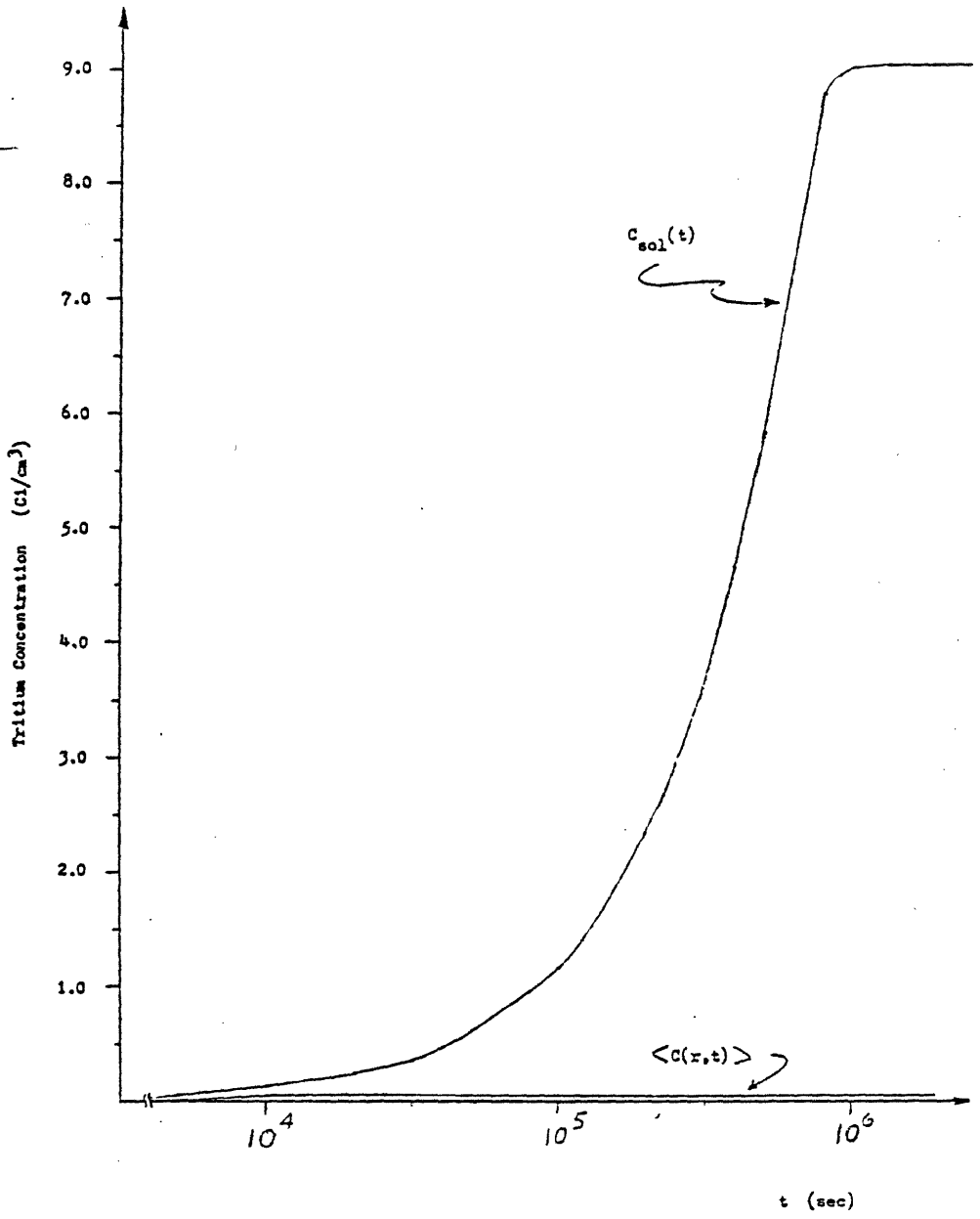

Figure 3-1

Time Evolution of the Tritium Concentration in a Li_2O Breeder Pellet

(for the STARFIRE-Interim Design)

($\sim$ 15 days).

The average radial concentration $\langle C(r,t)\rangle$ as defined in Chapter 2, Equation (2.23), exhibits the following time dependence:

$$\langle C(r,t)\rangle = \frac{S_b}{D_b}\frac{r_p^2}{15}\left[1 - \frac{90}{\pi^4}\sum_{n=1}\frac{1}{n^4}\exp -\left[D_b t\left(\frac{n\pi}{r_p}\right)^2\right]\right] \qquad (3.9)$$

Its steady-state value is just

$$\langle C(r,SS)\rangle = \frac{S_b}{D_b}\frac{r_p^2}{15} \qquad (3.10)$$

The concentration $\langle C(r,t)\rangle$ was determined as a function of time, using a programmable hand calculator, for the STARFIRE-Interim system parameters listed in Table F-2. The results are plotted on the same Figure 3-1 as for $C_{sol}(t)$, showing the great difference in their values. Because $\langle C(r,t)\rangle$ would be the pellet average concentration in the absence of solubility, it is clear that solubility has an enormous impact on the pellet concentration. $\langle C(r,t)\rangle$ reaches its steady-state value of 1.556×10^{-2} Ci/cm^3 in approximately 2.5×10^4 sec ($\sim$ 6.9 hrs), a much shorter time than that for the surface concentration.

The total tritium concentration in the breeder pellets as a function of time, is:

$$\langle C_p(r,t)\rangle = \langle C(r,t)\rangle + C_{sol}(t) \qquad (3.11)$$

The sum of the two concentrations, done visually from Figure 3-1, is basically the top curve for $C_{sol}(t)$. The steady-state pellet concentration is therefore 9.076 Ci/cm^3. The time constant for the breeder would be the longer of those for the two contributors to $\langle C_p(r,t)\rangle$, i.e., $\tau_{\langle C_p\rangle} \sim 1.3 \times 10^6$ sec.

The total breeder tritium inventory $I_b(t)$, which is just $V_b \cdot \langle C_p(r,t)\rangle$ is plotted in Figure 3-2. A steady-state breeder inventory of 4.48 kg, calculated using solubility effects, is much larger than the breeder inventory when solubility is not accounted for ($\sim$ 7.7 gm). Of course it

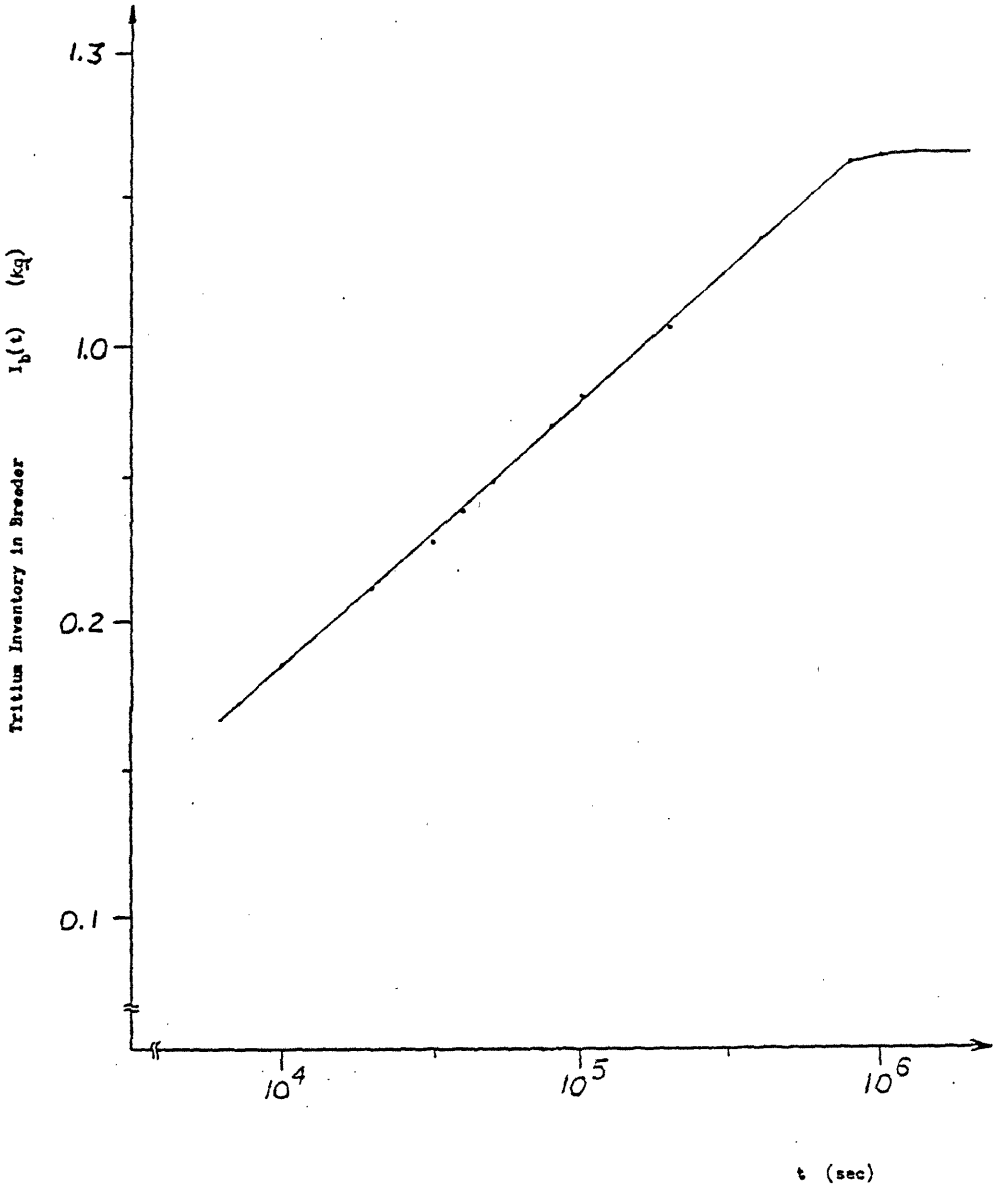

Figure 3-2

Time Evolution of the Breeder Tritium Inventory

(for the STARFIRE-Interim Design)

takes a much longer time to reach the higher steady-state inventory --- on the order of 15 days. When the no-solubility-effects case has reached steady-state of 7.7 gm at 6.9 hrs, the solubility-included case (the one presented here) has an inventory of ~ 130 gm. Thus, it is obvious that solubility effects must not be neglected when calculating the tritium concentration of breeder pellets.

Since the breeder inventory is so sensitive to the solubility effects the purge gas concentration has on the surface concentration, it is thought that a second look at that relationship for this case of Li_2O would be beneficial. A value for the Sieverts' Constant (K_s) for other solid lithium oxides is given in Appendix A. An analogy was made between ZnO, and $LiAlO_2$ and Li_2SiO_3 , from which it was deduced that the value for K_s for tritium in ZnO would be an upper-limit for the value of K_s in the lithium oxides. Therefore, an approximate value of K_{s,T_2} in Li_2O can be determined from Equation (A.2). At an average edge temperature of 800 ^{o}K, the Sieverts' Constant for Li_2O is approximately:

$$K_{s,\ Li_2O} \approx 1.97 \times 10^{-4} \quad \frac{cm^3\text{-}T_2}{cm^3\ atm^{\frac{1}{2}}}$$

Substitution of this value and other STARFIRE-Interim system parameters into the steady-state equation for the surface concentration due to solubility, Equation (2.40) yields:

$$C'_{sol}(SS) = \left[\frac{S}{Q_{pg}} \frac{R\ T_{pg}}{6 \times 10^4}\right]^{\frac{1}{2}} K_{s,T_2} \qquad (3.12)$$

$$= 4.06 \times 10^{-6} \quad Ci/cm^3$$

Since $C'_{sol}(SS) \ll \langle C(r,SS)\rangle$, the solubility effects in this case are practically negigible. One must wonder how accurately the only other source of data for T_2 vapor pressure over Li_2O, describes the solubility effects. Clearly, a definitive value for the Sieverts' Constant of tritium in Li_2O, preferably as a function of temperature, must be obtained in order to more accurately determine the tritium inventory in breeder

pellets.

3.2.3 Steady-State System Values

It has already been shown that the breeder inventory reaches its steady-state value of 4.48 kg in approximately 1.3×10^6 sec when the following expression was used for the solubility of tritium in Li_2O:

$$C_{sol}(t) = 299/5 \times 10^{-2} \rho_b \left[8.017 + \log P_{pg}(t) \right] \qquad (3.13)$$

The steady-state purge gas concentration is given by:

$$C_{pg}(SS) = \frac{S}{\alpha_{pg}} \qquad (3.14)$$

which translates into 4.46×10^{-4} Ci/cm^3 for the STARFIRE-Interim Design parameters, or equivalently, a steady-state tritium partial pressure in the purge gas of 0.323 torr. Multiplying $C_{pg}(SS)$ by the purge gas volume, the steady-state tritium inventory in the purge gas is only 3.22×10^{-2} gm (3.22×10^2 Ci).

The steady-state helium coolant tritium concentration is given by Equation (2.71) taken from Chapter 2:

$$C_c(SS) = \frac{\tau_c}{V_c R_{pgc}} C_{pg}(SS) \qquad (3.15)$$

Substitution of the STARFIRE-Interim parameters into Equation (3.15) gives a steady-state coolant concentration of 4.45×10^{-4} Ci/cm^3, or because of the large coolant volume, an equivalent 3.113×10^3 torr (4.1 atm) of tritium gas partial pressure (at an average temperature of 400 °C). This is very nearly the same number as for the steady-state purge gas concentration. One would expect the coolant concentration to be almost equal to that of the purge gas, because the resistance offered by the breeder tube metal and corresponding film barriers, is so small ($R_{pgc} \sim 5 \times 10^{-3}$ sec/cm^3).

The time constant for the coolant system is on the order of 118 days in response to a significant purge gas concentration. But the purge gas itself does not reach its final concentration value until approximately 18 days (same as the time for the breeder pellets to reach a steady-state concentration). Therefore the coolant does not contain its steady-state inventory of 83 grams until ~ 136 days from start-up of the reactor's full power.

When a steady-state tritium concentration is reached in the coolant, the corresponding steady-state tritium losses from the coolant piping are

$$J_{HPL}(SS) = 78.11 \quad Ci/day$$

from the "hot" leg segment, and

$$J_{CPL}(SS) = 3.23 \quad Ci/day$$

from the "cold" leg segment. These leakages to the building containment are quite large and could be a considerable load on the tritium recovery system not to mention, a hazard for the personnel working near the helium transport system components.

The steady-state tritium leakage from the coolant through the heat exchanger and into the steam system is

$$J_{HXL}(SS) = 1.832 \times 10^{4} \quad Ci/day$$

It has already been stated that any tritium in the steam system will eventually find its way to the environment. Thus, a 10^{4} Ci loss to the environment is quite unacceptable according to most standards. Without changing any STARFIRE-Interim dimensions or compositions (e.g., metal type or thickness) it is possible to reduce this leakage rate by introducing oxygen into the coolant loop. This will effectively limit the (high) tritium partial pressure in the coolant, which is the driving force behind tritium permeation through the heat exchanger. The effects of adding oxygen to the helium coolant are examined in the next section.

3.2.4 Addition of Oxygen to the Helium Coolant

Since by far the leakage through the steam generator constitutes the largest tritium leakage rate from the fusion plant systems, it will be exploited for determining how much oxygen should be introduced into the helium coolant. Assuming the maximum allowable release rate to the environment is set at 0.1 Ci/day*, the corresponding maximum coolant concentration is:

$$C_{c,max} = R_{HXL} \; J_{HXL,max}(SS)$$

$$= 4.05 \times 10^{-10} \quad Ci/cm^3$$

The "corrected" tritium inventory ($I'_c(SS)$) and partial pressure ($P'_c(SS)$) in the coolant would therefore be 7.5×10^{-5} gms and 2.83×10^{-3} torr (3.7×10^{-6} atm)

The equilibrium constant for the reaction $T_2 + \frac{1}{2}O_2 \rightleftharpoons T_2O$ is given as a function of temperature in Appendix D. At the "hot" helium temperature of 500 °C (oxygen would be added in the "hot" leg of the coolant, in front of the heat exchanger) the value for the equilibrium constant is 3×10^{12} torr$^{-\frac{1}{2}}$. Since the equilibrium constant is rather large, inclusion of a catalyst to make the reaction of Equation (2.75) reach equilibrium faster is unnecessary. From Equation (2.8.3) of Chapter 2, the necessary oxygen pressure to keep the tritium partial pressure in the coolant down to an acceptable level, is

$$P_{O_2} = \left[\frac{I_c(SS)}{I'_c(SS)} \; \frac{1}{K_{T_2O}} \right]^2 = 1.3 \times 10^{-13} \text{ torr} \qquad (3.16)$$

* Acceptable operating conditions for a fusion power plant based on tritium release from fission power plants could include a total release rate of $\sim$ 1 Ci/day. Since the permeation rate into the steam system could account for as much as 50 % of the release rate[53], and without calculating other means of tritium release to the environment (solid wastes, etc.), a conservative value for $J_{HXL,max}$ is set at 0.1 Ci/day.

This small amount of oxygen added to the high pressure helium (3.8×10^{4} torr) would keep the tritium release to the environment down to 0.1 Ci/day. The other tritium current terms for leakage from the "hot" and "cold" piping respectively, are reduced to:

$$J'_{HPL}(SS) = 7.1 \times 10^{-5} \quad \text{Ci/day}$$

and

$$J'_{CPL}(SS) = 2.9 \times 10^{-6} \quad \text{Ci/day} \qquad (3.17)$$

The total amount of tritium leaking from the piping system is only 7.4×10^{-5} Ci/day. The tritium recovery system acting within the primary containment boundary is assumed to be able to handle this daily input. Losses of tritium through the reactor shield were thought to be negigible. But, the tritium fuelling and processing piping systems have not been included and could be contributors to tritium leakage to the containment building, on a comparable level with that for the piping system carrying helium coolant.

3.2.5 Sensitivity Analysis

The various system parameters for the STARFIRE-Interim Design were examined as to their effect on the coolant concentration and tritium loss out the heat exchanger. These effects can be quantified by factors called sensitivity coefficients (α) which are indicators of the proportional change in one result due to a percentage change in an input parameter. The value of the coolant concentration, for example, is a function of many different yypes of system parameters (e.g., resistance of the "hot" pipe segment) which, in turn, are dependent on the individual component dimensions and properties. It is possible to represent mathematically, the percentage change in a desired quantity by a dimensionless change in one of its input parameters:

$$\frac{da}{a} = \alpha_x^a \frac{dx}{x} \qquad (3.18)$$

The analytical method for determining these multiplying factors, α (sensitivity coefficients), is given in Appendix E. The evaluation of these coefficients depends on the original value of the system variables, and hence those used in the transient permeation model are again used in this sensitivity analysis.

Following the procedure outlined in Appendix E for the sensitivity analysis of system variables, and using the values for the STARFIRE design presented in Table 3-1, the following values were generated and tabulated in Table 3-2 (patterned after Table E-1) and Table 3-3 (patterned after Table E-2). The results of Tables 3-2 and 3-3 are combined to give the overall sensitivity coefficients for the STARFIRE-Interim Design shown in Table 3-4 (patterned after Table E-3).

For the type of metals and flow parameters chosen for the STARFIRE-Interim design, only a change in the dimensions of the heat exchanger, or its operating temperature (which determines the diffusion coefficient, D_{HX}), will have a significant effect of reducing the tritium losses to the environment. The sensitivity of the heat exchanger components is almost linear; i.e., a 10% increase in the wall thickness will cause a 10% reduction in tritium lost through the heat exchanger. Thus one is apt to conclude that the best way to attack the problem of tritium leakage from the heat exchanger is to adjust the parameters associated with the heat exchanger's resistance, namely A_{HX}, X_{HX}, and D_{HX}. This attempt, coupled with the previous approach of adding oxygen to the coolant to decrease the effective tritium gas partial pressure, should enable an acceptable coolant system to be built within the 0.1 Ci/day tritium release rate guidelines.

It should also be noted from Table 3-4 that the tritium concentration in the coolant and the leakage from the heat exchanger, are both quite insensitive to the helium film resistance - or more specifically - the mass transfer coefficient, in any area of the design. This means that there will be good communication between the tritium carried by the helium gas and the channel walls, such that any changes in the flow regime or fluid parameters will have little effect on the concentration at the surface. This is unfortunate because it means one less area is available for fine-tuning the system for minimizing the tritium permea-

Table 3-2

Resistance Sensitivity Coefficients* for
STARFIRE-Interim

	$C_c(SS)$	$J_{HXL}(SS)$
α_S^-	1	1
$\alpha_{Q_{pg}}^-$	-1	-1
$\alpha_{R_{HPL}}^-$	1.74×10^{-5}	1.74×10^{-5}
$\alpha_{R_{HXL}}^-$	1.24×10^{-8}	-1.0004
$\alpha_{R_{CPL}}^-$	4.22×10^{-4}	4.22×10^{-4}
$\alpha_{R_{pgc}}^-$	-4.39×10^{-4}	-4.39×10^{-4}

*Note: Specific sensitivity coefficients are explicitly defined in Appendix E.

Table 3-3

System Parameter Sensitivity Coefficients for STARFIRE-Interim

	R_{HPL}	R_{HXL}	R_{CPL}	R_{pgc}
α_A^-	-1	-1	-1	-1
α_h^-	~ 0	~ 0	~ 0	N.A.
α_D^-	~ -1	~ -1	~ -1	~ -1
α_x^-	~ 1	~ 1	~ 1	~ 1
$\alpha_{h_{pg}}^-$	N.A.	N.A.	N.A.	~ 0
$\alpha_{h_B}^-$	N.A.	N.A.	N.A.	~ 0

Note: N.A. ≡ Not applicable

Table 3-4

Sensitivity Coefficients of $C_c(SS)$ and $J_{HXL}(SS)$ for the Various System Parameters for the STARFIRE-Interim Design

System Parameter	Total Sensitivity Coefficients for $C_c(SS)$	Total Sensitivity Coefficients for $J_{HXL}(SS)$	
S	1	1	*
Q_{pg}	-1	-1	*
A_m	4.39×10^{-4}	4.39×10^{-4}	
D_m	4.39×10^{-4}	4.39×10^{-4}	
x_m	-4.39×10^{-4}	-4.39×10^{-4}	
h_{pg}	0	0	
h_B	0	0	
A_{HP}	-1.74×10^{-5}	-1.74×10^{-5}	
D_{HP}	-1.74×10^{-5}	-1.74×10^{-5}	
x_{HP}	1.74×10^{-5}	1.74×10^{-5}	
h_{HP}	0	0	
A_{HX}	-1.24×10^{-8}	1.0004	*
D_{HX}	-1.24×10^{-8}	1.0004	*
x_{HX}	1.24×10^{-8}	-1.0004	*
h_{HX}	0	0	
A_{CP}	-4.22×10^{-4}	-4.22×10^{-4}	
D_{CP}	-4.22×10^{-4}	-4.22×10^{-4}	
x_{CP}	4.22×10^{-4}	4.22×10^{-4}	
h_{CP}	0	0	

Note: * System parameters with a significant impact on tritium losses

tion from the blanket into the coolant system and outwards.

One must not neglect the obvious effect that changing the breeding rate and the purge gas volumetric flow rate has on the value for $C_c(SS)$ and $J_{HXL}(SS)$. In the case of generating more tritium per unit time, there will necessarily be more tritium diffusing from the pellets and hence more tritium available for permeation. If the purge gas flow rate is increased, more tritium diffusing out of the pellets will be swept away leaving a smaller steady-state purge gas concentration. Since all the other steady-state values in the system down line from the purge gas will be affected by altering the purge gas concentration, then it is clear how significant a sensitivity of $|1|$, for the $C_c(SS)$ and $J_{HXL}(SS)$ to S and Q_{pg}, is in keeping with the specified design objective of minimizing the tritium inventroy in the coolant.

3.3 Conclusions from the STARFIRE-Interim Case Study

3.3.1 Summary of Results

Based upon the limited information that was available for the solubility of tritium in solid Li_2O, the tritium inventory in all the breeder pellets was calculated to be 4.48 kg. The time for the breeder concentration to reach steady-state, $\tau_{<C_p>}$, which is also the time for the purge gas concentration to reach its final value, is approximately 18 days. The purge gas inventory builds up to 3.22×10^{-2} gm where it levels off due to the continuous extraction of the tritium gas after the purge gas leaves the blanket, and is thus returned "clean" of all T_2. Since the time constant for the coolant system was much longer than that for the purge gas (118 days versus 18 days), the coolant effectively sees the steady-state purge gas concentration. As the coolant concentration itself reaches steady-state, this simplification becomes unimportant.

The "uncorrected" steady-state coolant inventory (meaning no tritium conversion via oxygen addition to the helium coolant) is 83 grams which leads to the unacceptable tritium leakage rates of:

$$J_{HPL}(SS) = 78.11 \text{ Ci/day}$$
$$J_{HXL}(SS) = 1.832 \times 10^{4} \text{ Ci/day (i.e., 1.8 gm/day)}$$
$$J_{CPL}(SS) = 3.23 \text{ Ci/day}$$

from the "hot" pipe, heat exchanger and "cold" pipe, respectively. Since the total tritium leakage from the plant to the environment must be kept below 1 Ci/day by most accounts, a maximum value of 0.1 Ci/day was set for tritium losses from the heat exchanger since it communicates with the atmosphere via the steam cycle. Tritium losses from the helium piping to the containment building are at least 90% recoverable by the continuously-operating air detritiation system.

Without changing the choice of metal or any of the component dimensions, the reduction in the coolant concentration corresponding to a value of 0.1 Ci/day for $J_{HXL}(SS)$ was accomplished by introducing 1.3×10^{-13} torr of oxygen into the high-pressure helium coolant loop (the equivalent of 1.7×10^{2} cc/day). The corrected coolant inventory would therefore be 7.5×10^{-5} gm, and losses from the helium piping system would total 7.4×10^{-5} Ci/day--easily handled by the tritium recovery system. The purge gas concentration and breeder inventory are, of course, left unaffected. This small partial pressure of oxygen is thought not to be of concern for any oxygen-related corrosion problems in the coolant loop, thus would not be deleterious to the reactor system.

3.3.2 Comparison with Results from STARFIRE-Interim Report[8]

The design report cites a total tritium inventory of 2.55 kg on site. This includes 1 kg in the breeder itself, and 250 gm in the tritium recovery system. The rest of the tritium is held in storage or other parts of the plant (for example: vacuum pumps, surge tank and fuel preparation units) which were not included in this model. Therefore the only meaningful comparisons to be made are for the inventories: $I_b(SS)$ and $I_{pg}(SS)$. These are stated below:

	This Study	STARFIRE[8]
$I_b(SS)$	4.48 kg	1 kg
$I_{pg}(SS)$	0.03 gm	250 gm

The large difference in the values for the steady-state breeder inventories can probably be attributed to the solubility effects which were included in this report but not in STARFIRE-Interim. Their value is even higher than the calculated value of $\langle C(r,SS)\rangle$ (7.6 gm) which is considered to be a measure of inventory due to diffusion only. Perhaps the fact that neither the diffusion coefficient for Li_2O nor its pellet radius were specified by STARFIRE[8], both of which were needed to calculate $\langle C(r,SS)\rangle$, would explain this discrepancy.

The value given for the tritium recovery system inventory (250 gm) may be indeed more than that for just the purge gas system alone. STARFIRE stated that the tritium (as T_2O) would be recovered either from the helium purge stream, or the helium coolant. So, this tritium recovery system inventory could be defined as including other systems than just the purge stream.

3.3.3 Implication of Results

The various resistances to tritium permeation as defined in Chapter 3 and applied to STARFIRE-Interim were given in Table 3-1. A quick look at these numbers shows that the resistance offered by the heat exchanger is the smallest, which is expected due to its large surface area and thin walls operating at a relatively high temperature. Next-to-the-smallest resistance is that for the breeder tubes. Perhaps the fact that only a 0.15 cm thickness was used for the canisters would make the resistance so low. X_m has to be kept relatively thin to allow for adequate heat transfer from the breeder pellets inside to the helium coolant flowing past on the outside. Since the sensitivity of the coolant concentration to the resistance of the breeder fuel metal (R_{pgc}) is one of the largest (behind only S and Q_{pg}), it may be worthwhile to investigate the optimum thickness and/or area (A_m) with the tradeoff between heat transfer and tritium permeation considerations being the major factor.

The resistance offered by the "cold" pipe is much greater than that for the "hot" pipe even though the thickness and surface area are the same for both. What makes the difference then is either the value for the mass transfer coefficient (h_{CP},h_{HP}) of tritium within the helium coolant, or the tritium diffusivity (D_{CP},D_{HP}) in the pipe metal. From Table 3-1 it is obvious that only the metal resistances were different, and thus their values of D. One can exploit this fact by using a different type of metal for the "hot" pipe which has a lower diffusivity at the hot operating temperature — 500 ^{o}C, and thus making the pipe resistances almost equal.

In summary then, for the STARFIRE-Interim parameters the magnitudes of the tritium permeation resistances are of the order:

$$R_{HXL} < R_{pgc} \ll R_{HPL} \ll R_{CPL} \tag{3.19}$$

It is important to point out that the fluid- and metal- contributions to the total resistances in Equation (3.19) are far from equal. In fact, the fluid resistances (α 1/Ah) are several orders of magnitude less than the metal resistances (α x/AD). From the numbers given for these total resistance components in Table 3-1, the ratio of fluid resistance to metal resistance ranges from 10^{-10} to 10^{-6}. The fact that the STARFIRE-Interim parameters yield negligible fluid-resistances cannot be overlooked. This means, of course, the surface concentration in the metal walls will be whatever is in equilibrium with the gas concentration. This relationship is given by a Sieverts' Law for the tritium concentration in a metal in solution with a tritium partial pressure above the metal:

$$C_{T \text{ in metal}} = K_s \, P^{\frac{1}{2}}_{T_2 \text{ in gas}} \tag{3.20}$$

One cannot expect the flow regime to assist in keeping the tritium "off the walls".

There are several other results of this case study which deserve to be re-stated and more fully expanded upon than they were in the last section. First, it has been shown that including solubility effects in the calculation for the breeder inventory leads to significantly different results. If data given for T_2O vapor pressure over solid Li_2O pellets is

used to describe the thermodynamic equilibrium, then the steady-state inventory is ~ 4.475 kg. If the value for the Sieverts' constant of T_2 in Li_2O (which is the preferred approach) is approximated by that for T_2 in ZnO, then the inventory determined by solubility effects is only 2×10^{-3} g. Obviously, the solubility-inventory is quite important, and a more accurate value for the Sieverts' constant of T_2 in Li_2O is crucial to determining the true breeder inventory. This has been shown to range from several grams (7.6 gm) to several kilograms (4.48 kg) depending on how the solubility effects are modelled. Although there has been considerable experimental work done for determining diffusion-limited extraction rates (see Appendix A, Figure A-1), and thus in determining tritium diffusion coefficients, there is very little information concerning Sieverts' constants. Values of K_s for T_2 in the lithium-lead, and lithium-aluminum alloys are quoted in Appendix A.3, while the approximation of K_{s,T_2} in ZnO is used for the lithium aluminates and silicates. For purposes of this study, an empirical value for K_s of T_2 in Li_2O would have been most helpful.

A second result of this STARFIRE case study was the surprisingly long time calculated for the breeder to reach its steady-state inventory ($\tau_{<C_p>} \approx 18$ days). Since the tritium generation rate would therefore be equal to the leakage rate to the sweep gas, then the purge gas reaches its steady-state concentration in time $\tau_{<C_p>}$ too. Assuming that processing of the purge gas tritium does not become economically feasible until the steady-state concentration has been reached, then approximately an 18 day supply of tritium must be on hand when the reactor is brought up to full power in addition to the large start-up inventory. After the time $\tau_{<C_p>}$, the breeding ratio of greater than one assures that the tritium in the purge gas (and if need be, a bypass flow of the helium coolant) will be sufficient to refuel the reactor after passing through the processing unit.

Although a maximum breeder tritium inventory of 4.48 kg may be acceptable from the point of view of a potential radiological hazard, the fact that an 18 day supply (e.g., 9 kg) must always be kept on site whenever the plant is to begin start-up operations is not in keeping with the

stated design objective of minimizing tritium storage. Careful examination of the simultaneous effects of solubility- and diffusion- limited inventory is necessary in order to decrease the time constant $\tau_{<C_p>}$ to an acceptable value from fuel reprocessing considerations.

The third and last result of particular interest is that the response time for the coolant system is very long - on the order of 118 days. Together with the time to reach the steady-state concentration for the purge gas, the effective time constant of the coolant system is approximately 136 days. If the scheduled down-time for the fusion reactor is one month every year, then the plant is expected to be operating at its steady-state concentration values for approximately 194 days a year. This implies a minimum tritium leakage to the environment of 19.4 Curies for every year of operation.

Since it takes so long for the coolant to reach steady-state, perhaps the addition of oxygen to the coolant can be delayed until the tritium partial pressure reaches a value corresponding to a leakage from the heat exchanger of 0.1 Ci/day (i.e., 4.05×10^{-10} Ci/cm^3). From Equation (2.70) this time is 9 sec. Obviously, the oxygen must be part of the helium coolant system right from reactor start-up, or soon thereafter, before the purge gas concentration reaches steady-state.

The preceding analyses of the tritium inventory in the breeder, using STARFIRE-Interim system parameters, was expanded to four other lithium solids so as to ascertain the implication of the choice of solid breeder on the amount of tritium in the breeder. Since both the operating temperature and the pellet size are important design specifications when considering an alternative breeding compound, these parameters were varied for all the lithium compounds considered: Li_2O, $LiAlO_2$, Li_2SiO_3, LiAl and Li_7Pb_2 and their effect on the tritium concentration was noted. The results for the effect of temperature on the tritium inventory is given in Table 3-5; the effect of pellet radius in Table 3-6. All STARFIRE system parameters were used in the calculations, except for the changes in property values (D_b and K_s) which are taken from Appendix A.

The results indicate that in general, as the operating temperature increases, the amount of tritium that is diffusively held up decreases, while the amount that is dissolved in the breeder pellets (assuming the

Table 3-5

Effect of Operating Temperature[a] on the Tritium Inventory in Sveral Lithium Solid Breeders

		Li_2O			$LiAlO_2$		
T_{avg}	(°C)	650	550	450	650	550	450
T_{edge}	(°C)	527	427	327	527	427	327
D_b[b]	(cm^2/sec)	5.0×10^{-11}	3.0×10^{-11}	2.0×10^{-11}	6.0×10^{-10}	3.0×10^{-10}	1.2×10^{-10}
K_s	(cm^3-T_2/$cm^3 atm^{\frac{1}{2}}$)	d	------	------	1.94×10^{-4} e	7.29×10^{-6} e	8.98×10^{-8} e
$<C(r,SS)>$	(Ci/cm^3)	1.556×10^{-2}	2.59×10^{-2}	3.89×10^{-2}	1.297×10^{-3}	2.59×10^{-3}	6.48×10^{-3}
τ_{diff}	(sec)	2.5×10^{4}	3.5×10^{4}	5.5×10^{4}	1.8×10^{3}	3.5×10^{3}	8.0×10^{3}
$C_{sol}(SS)$	(Ci/cm^3)	9.06015	------	------	4.064×10^{-6}	1.504×10^{-7}	1.853×10^{-9}
τ_{sol}	(sec)	1.3×10^{6}	------	------	h	------	------
$I_b(SS)$	(cm)	4.48×10^{3}	4.49×10^{3}	4.49×10^{3}	6.41×10^{-1}	1.28×10^{0}	3.20×10^{0}
τ_b	(sec)	1.3×10^{6}	1.3×10^{6}	1.3×10^{6}	1.8×10^{3}	3.5×10^{3}	8.0×10^{3}

NOTE: a - $r_p = 10^{-3}$ cm

b - from Figure A-1

c - extrapolated from Figure A-1

d - equilibrium vapor pressure for T_2 in Li_2O given in Appendix F; ~ same in the temperature range 600 - 1000 °K(29)

e - from Equation (A.2)

f - from Figure A-19

g - from Figure A-16

h - negligible solubility contribution

Table 3-5

(continued)

		Li_2SiO_3			LiAl		
T_{avg}	(°C)	650	550	450	650	550	450
T_{edge}	(°C)	527	427	327	527	427	327
D_b [b]	(cm^2/sec)	1.2×10^{-10}	6.0×10^{-10}	2.5×10^{-10}	4.0×10^{-6} [c]	9.0×10^{-7} [c]	9.0×10^{-8}
K_s	(cm^3-T_2/cm^3-$atm^{\frac{1}{2}}$)	1.97×10^{-4} [e]	7.29×10^{-6} [e]	6.98×10^{-8} [e]	4.01×10^{-1} [f]	2.29×10^{-1} [f]	1.00×10^{-1} [f]
$\langle C(r,SS) \rangle$	(Ci/cm^3)	6.483×10^{-4}	1.30×10^{-3}	3.11×10^{-3}	1.945×10^{-7}	8.64×10^{-7}	8.64×10^{-6}
τ_{diff}	(sec)	8.0×10^{2}	1.8×10^{3}	6.0×10^{3}	3.0×10^{-1}	1.5×10^{0}	1.5×10^{1}
$C_{sol}(SS)$	(Ci/cm^3)	4.064×10^{-6}	1.504×10^{-7}	1.052×10^{-9}	8.272×10^{-3}	4.724×10^{-3}	2.063×10^{-3}
τ_{sol}	(sec)	[h]	- - - - - -	- - - - - -	3.8×10^{3}	2.0×10^{3}	1.0×10^{3}
$I_b(SS)$	(m)	3.22×10^{-1}	6.42×10^{-1}	1.54×10^{0}	4.09×10^{0}	2.33×10^{0}	1.02×10^{0}
τ_b	(sec)	8.0×10^{2}	1.8×10^{3}	6.0×10^{3}	3.8×10^{3}	2.0×10^{3}	1.0×10^{3}

NOTE: a - $r_p = 10^{-3}$ cm

b - from Figure A-1

c - extrapolated from Figure A-1

d - equilibrium vapor pressure for T_2 in Li_2O given in Appendix F; $\sim$ same in the temperature range 600 - 1000 °K(29)

e - from Equation (A.2)

f - from Figure A-19

g - from Figure A-16

h - negligible solubility contribution

Table 3-5

(continued)

		Li_7Pb_2		
T_{avg}	(°C)	650	550	450
T_{edge}	(°C)	527	427	327
D_b [b]	(cm^2/sec)	1.0×10^{-6} c	1.4×10^{-7}	2.0×10^{-8}
K_s	(cm^3-T_2/cm^3 atm$^{\frac{1}{2}}$)	2.29×10^{-4} g	2.23×10^{-3} g	6.35×10^{-3} g
<C(r,SS)>	(Ci/cm^3)	7.78×10^{-7}	5.56×10^{-6}	3.89×10^{-5}
τ_{diff}	(sec)	1.2×10^{0}	9.0×10^{0}	5.5×10^{1}
C_{sol}(SS)	(Ci/cm^3)	4.724×10^{-6}	4.600×10^{-5}	1.311×10^{-4}
τ_{sol}	(sec)	2.0×10^{0}	2.0×10^{1}	6.0×10^{1}
I_b(SS)	(m)	2.72×10^{-3}	2.55×10^{-2}	8.40×10^{-2}
τ_b	(sec)	2.0×10^{0}	2.0×10^{1}	6.0×10^{1}

NOTE: a - $r_p = 10^{-3}$ cm

b - from Figure A-1

c - extrapolated from Figure A-1

d - equilibrium vapor pressure for T_2 in Li_2O given in Appendix F; $\sim$ same in the temperature range 600 - 1000 °K (29)

e - from Equation (A.2)

f - from Figure A-19

g - from Figure A-16

h - negligible solubility contribution

Table 3-6

Effect of Pellet Radius[a] on the Tritium Inventory in Several Lithium Solid Breeders

		Li_2O			$LiAlO_2$			Li_2SiO_3		
r_p	(cm)	1.0×10^{-4}	1.0×10^{-3}	1.0×10^{-2}	1.0×10^{-4}	1.0×10^{-3}	1.0×10^{-2}	1.0×10^{-4}	1.0×10^{-3}	1.0×10^{-2}
$\langle C(r,SS)\rangle$	(Ci/cm^3)	1.556×10^{-4}	1.556×10^{-2}	1.556×10^{0}	1.297×10^{-5}	1.297×10^{-3}	1.297×10^{-1}	6.483×10^{-6}	6.483×10^{-4}	6.483×10^{-2}
τ_{diff}	(sec)	2.5×10^{2}	2.5×10^{4}	2.5×10^{6}	1.8×10^{1}	1.8×10^{3}	1.8×10^{5}	8.0×10^{0}	8.0×10^{2}	8.0×10^{4}
$C_{sol}(SS)$ [b]	(Ci/cm^3)	9.06015	-------	-------	4.064×10^{-6}	-------	-------	4.064×10^{-6}	-------	-------
τ_{sol} [b]	(sec)	1.3×10^{6}	-------	-------	c	-------	-------	c	-------	-------
$I_b(SS)$	(gm)	4.48×10^{3}	4.48×10^{3}	5.24×10^{3}	8.41×10^{-3}	6.43×10^{-1}	6.41×10^{1}	5.21×10^{-3}	3.22×10^{-1}	3.21×10^{1}
τ_b	(sec)	1.3×10^{6}	1.3×10^{6}	2.5×10^{6}	1.8×10^{1}	1.8×10^{3}	1.8×10^{5}	8.0×10^{0}	8.0×10^{2}	8.0×10^{4}

NOTE: a - $T_b = 650\ ^{o}C$; $T_{surface} = 527\ ^{o}C$; D_b, K_s from Table 3-5

b - very weakly dependent on pellet radius

c - negligible

Table 3-6

(continued)

		LiAl			Li_7Pb_2		
r_p	(cm)	1.0×10^{-4}	1.0×10^{-3}	1.0×10^{-2}	1.0×10^{-4}	1.0×10^{-3}	1.0×10^{-2}
$\langle C(r,SS) \rangle$	(Ci/cm^3)	1.945×10^{-9}	1.945×10^{-7}	1.945×10^{-5}	7.78×10^{-9}	7.78×10^{-7}	7.78×10^{-5}
τ_{diff}	(sec)	3.0×10^{-3}	3.0×10^{-1}	3.0×10^{1}	1.2×10^{-2}	1.2×10^{0}	1.2×10^{2}
$C_{sol}(SS)$ [b]	(Ci/cm^3)	8.272×10^{-3}	-------	-------	4.724×10^{-6}	-------	-------
τ_{sol} [b]	(sec)	3.8×10^{3}	-------	-------	2.0×10^{0}	-------	-------
$I_b(SS)$	(gm)	4.09×10^{0}	4.09×10^{0}	4.10×10^{0}	2.34×10^{-3}	2.72×10^{-3}	4.08×10^{-2}
τ_b	(sec)	3.8×10^{3}	3.8×10^{3}	3.8×10^{3}	2.0×10^{0}	2.0×10^{0}	1.2×10^{2}

NOTE: a - $T_b = 650\ ^{o}C$; $T_{surface} = 527\ ^{o}C$; D_b, K_s from Table 3-5

b - very weakly dependent on pellet radius

c - negligible

purge gas characteristics remain the same) increases. A larger pellet radius implies a larger diffusion path-length which translates into a larger diffusion-related inventory, but has no effect on the steady-state solubility concentration. Assuming the source of property data is reasonably accurate, the breeder inventory can decrease as much as thirty-fold (Li_7Pb_2) for a 200 °C rise in operating temperature. However, the pellet radius has an even more dramatic effect on the inventory: increasing the pellet radius from 1 μ to 100 μ can increase the breeder inventory by more than three orders of magnitudes. This brief analysis has shown how critical the choice of operating temperature and pellet radius can be on the final value of the breeder tritium inventory.

Under the same operating conditions, lithium oxide has been shown to exhibit the highest tritium inventory of all the other lithium compounds. Its tritium diffusivity is very low as well as its equilibrium tritium vapor pressure. Both of these contribute to a rather large tritium inventory for Li_2O. Unless the other design considerations (among them, neutronic and heat transfer capabilities) are overwhelmingly in its favor, the use of Li_2O as a breeder is seriously challenged.

A comparison can be made between the results calculated from the permeation model as given in Table 3-5 for $LiAlO_2$ and those for the breeder tritium inventory in the STARFIRE-Final Design[17] which used lithium aluminate as the breeding agent. Without considering any adverse radiation effects on the tritium behavior in the solid blanket, the estimates of the diffusive and solubility inventories were given as 0.14 kg and 8 kg respectively. These are considerably larger than their counterparts in Table 3-5. A brief explanation of these differences is in order since it requires the comparison of the system parameters and assumptions that went into the calculation of these inventories.

The diffusive inventory will be considered first. In the STARFIRE Design[17], it was assumed that the radius of the grain is the characteristic diffusion path length, and thus a value for r in the steady-state diffusion-related component to the "pellet" tritium concentration:

$$\langle C(r,SS)\rangle = \frac{S_b}{D_b}\,\frac{r^2}{15} \qquad (3.21)$$

was set equal to the grain radius ($r_g \sim 1\ \mu$ (10^{-4} cm)). A pellet radius of 10^{-3} cm was used in the calculations of the diffusive concentration in Table 3-5. The tritium source term for STARFIRE-Final is 62.5 Ci/sec; for STARFIRE-Interim, it was 57.64 Ci/sec. STARFIRE-Final also specifies a breeder operating temperature of 500 - 850 °C. A diffusive inventory of 140 gm corresponds to an "average" temperature of 617 °C when their equation for the tritium diffusivity is used:

$$D_b \quad (cm^2/sec) \;=\; 3.26 \exp -\left[\frac{57.2}{RT}\right] \tag{3.22}$$

This relationship for the hydrogen diffusivity in Al_2O_3 was used to represent the tritium diffusivity in $LiAlO_2$. At 617 °C, the diffusivity is only 3×10^{-14} cm^2/sec, which is not surprising since the compound Al_2O_3 has been considered a potential permeation barrier for use as a ceramic coating on metals (see Section 2.3.4.4). An experimentally-determined value of D_b for tritium in $LiAlO_2$ is found in Figure A-1 for particle diameters in the range 0.05 - 0.15 mm.

Since the diffusive inventory is given by

$$I_{diff} \;=\; \frac{S}{D_b}\,\frac{r^2}{15} \tag{3.23}$$

the STARFIRE-Final Design system parameters give:

$$I_{diff}\,(617\ ^\circ C) = \frac{6.25 \times 10^{-3}\,(10^{-4})^2}{3 \times 10^{-14}\quad 15} \quad gm$$

$$= 140 \quad gm \tag{3.24}$$

The permeation model using STARFIRE-Interim system parameters and Figure A-1 property data give for the diffusive inventory:

$$I_{diff}\,(650\ ^\circ C) = \frac{5.764 \times 10^{-3}\,(10^{-3})^2}{6 \times 10^{-10}\quad 15} \quad gm$$

$$= 0.6 \quad gm \tag{3.25}$$

The discrepancy is therefore traced back to the values chosen for the following:

$$\left.\frac{r}{D_b}\right|_{\text{STARFIRE}} = 3.33 \times 10^5 \qquad (3.26A)$$

$$\left.\frac{r}{D_b}\right|_{\text{model}} = 1.67 \times 10^3 \qquad (3.26B)$$

A smaller diffusion path length tends to offset the use of a smaller diffusion coefficient in STARFIRE, but the combined effect is to substantially increase the diffusive inventory over that calculated from the permeation model.

The system parameters that were included in the solubility inventory calculation will be considered next. In the STARFIRE Design it was assumed that the tritium bred in the blanket is of the form T_2O and that a "reasonable value for the average T_2O pressure in the blanket is $\sim$ 130 Pa (1 torr)"[17]. For an ideal solution of LiOT and Al_2O_3 in equilibrium with $LiAlO_2$ and T_2O, the amount of tritium dissolved in the solid $LiAlO_2$ is 13 wppm at a temperature of 1000 $^{\circ}$K (727 $^{\circ}$C). (This is higher than the average breeder temperature used in their diffusive inventory calculations.) For a breeder blanket inventory of 6.26×10^5 kg of $LiAlO_2$, the calculated tritium solubility inventory is 8 kg early in the blanket life.

Following the method described in Section 2.4 for the permeation model's calculation of the solubility inventory, the value of the Sieverts' Constant (from Equation (A.2)) is 2.04×10^{-2} cm^3-T_2/cm^3 $atm^{\frac{1}{2}}$ at a breeder temperature of 1000 $^{\circ}$K. Using the equation for the steady-state solubility concentration, Equation (2.40),

$$C_{sol}(SS) = \left[\frac{S\ R\ T_{pg}}{6 \times 10^4\ Q_{pg}}\right]^{\frac{1}{2}} K_s \qquad (3.27)$$

and STARFIRE-Interim system values: $T_{pg} = 698$ $^{\circ}$K, $Q_{pg} = 1.3 \times 10^5$ cm^2/sec, the corresponding weight fraction of tritium dissolved in $LiAlO_2$ is found to be 0.02 wppm. For a total mass of 6.26×10^5 kg (STARFIRE-Interim

value: $m_b = 10^7$ gm), the solubility inventory would be 13 gm.

The discrepancy in solubility inventory calculations is due to the choice in representation of the solubility effects. In the STARFIRE Design, it was assumed that a rather large T_2O partial pressure in the blanket (1 torr) gave rise to a substantial dissolved tritium fraction (13 wppm) in the breeder by making several estimates concerning the activity coefficient, equilibrium constant and the lithium burn-up rate. Although the calculated steady-state tritium gas (T_2) partial pressure in the purge gas is lower (0.3 torr) for the permeation model, it also makes the approximation of using the hydrogen solubility constant in ZnO as the tritium solubility in $LiAlO_2$. This approximation caused the solubility contribution to the inventory to be quite small (again) in the case of the permeation model.

Specification of the T_2O partial pressure in the blanket as ~ 1 torr (versus $P_{T_2} \sim 0.3$ torr in STARFIRE-Interim) is not consistent with the other specification made in the STARFIRE-Final Design - that being the purge gas volumetric flow rate equal to 1×10^7 cm^3/sec (versus $Q_{pg} \sim 1.3 \times 10^5$ cm^3/sec used in STARFIRE-Interim calculations, corresponding to $u_{pg} = 1$ ft/sec). Since the purge gas channel diameters are the same (2 mm) and if the number of channels were approximately the same, this would imply that the helium velocity in the STARFIRE Design is greater than the 1 ft/sec suggested limit. Such a high flow velocity could lead to significant purge gas pumping requirements.

Although the effect of radiation on the breeder is difficult to quantify, it can be anticipated[17] that the diffusive inventory could be increased as much as three orders of magnitude due to tritium trapping in the pellets. Radiation sintering and the resulting fusion of pellets together could increase the tritium gas pressure over the solid by two orders of magnitude. Since $C_{sol}(SS) \propto P_{T_2}^{\frac{1}{2}}$, this means the solubility concentration would increase one order of magnitude. If the solubility is already a major contributor to the tritium inventory, the inclusion of radiation effects would substantially increase the total breeder inventory.

Irrespective of the potentially large tritium inventory contribution due to radiation-induced trapping (which increases the diffusive hold-up) and radiation-enhanced sintering (which leads to a higher equilibrium tritium vapor pressure, thus increasing the amount of tritium in solution), both of which were taken into account in the STARFIRE-Final Design Report, the inclusion of a temperature gradient in the breeder material perhaps led to the much larger inventory value quoted in the STARFIRE Report, compared with the present model's predictions (ref. Table 3-5). Since the temperature dependency of both the diffusion coefficient D_b, and the solubility constant K_s, are non-linear, it may not be appropriate to calculate the total breeder tritium inventory based on one (average) temperature. For the case of a $LiAlO_2$ breeder in the STARFIRE-Final Design, ". . . about 90% of the tritium inventory (was) located in the coldest 10% of the blanket, i.e., those regions below 550 ^{o}C."[17] It can be anticipated that the representation of the entire breeder zone by a single temperature could seriously underestimate the tritium inventory. In Table 3-5, it was shown that for any particular lithium compound, the breeder inventory increases at lower operating temperatures. A more structured approach to the calculation of the tritium inventory for the range of operating temperatures existing in the blanket is a straightforward extension of the present model and will be further discussed in the Recommendations Section 5.2.1.

CHAPTER 4 EFFECTIVE TRITIUM PERMEATION RESISTANCE OF A COOLANT/METAL COMBINATION

Amid the speculation brought about by tritium transport studies[9,50] involving fluid carriers, one interesting and potentially significant fact concerning tritium behavior in fluids is their ability to act as permeation barriers in conjunction with the metal resistance. The possibility that the fluid resistance dominates that afforded by the metal is worthy of further study because of the implication with regard to fusion reactor heat transfer system design. Studies, such as those undertaken by Johnson[66] and Fraas[67] in which candidate blanket materials and coolants were examined to obtain an optimum combination with respect to several operational design parameters, would have to be expanded to include the tritium transport properties of possible reactor fluids in order to take full advantage of this effect.

In the following two sections the tritium permeation resistance of a coolant and metal in series will be investigated. Section 4.1 describes the mechanics of tritium behavior in both fluids and metals. The method of comparing their resistances to tritium diffusion is given in terms of calculating fluid- and metal- limited (tritium) partial pressure regimes. The analysis presented herein is then applied to the GA FRM design[11] and the ANL STARFIRE-Interim Design[8] based on their specified steady-state operating conditions. The effect of including the coolant (helium gas) resistance to tritium permeation on the amount of the fractional clean-up is examined for the GA FRM design. The results for STARFIRE are compared to the relative importance of fluid resistances in the overall system design already determined from the transient permeation model (ref. Table 3-1).

4.1 Characterization

The major tritium loss pathway to the environment is taken to be the permeation losses from the primary coolant system through the heat exchanger to the steam cycle where, for economic reasons[68], the power conversion system (ref. Figure 2-1) is vented to the open atmosphere. The analysis of

fluid and metal resistance to tritium diffusion as part of this pathway is necessarily focused on tritium behavior inside the heat exchanger (or equivalently, steam generator). The preliminary work done by Zarchy and Axtmann[9] in this area is used as an outline for the extended investigation presented in this chapter.

The permeation rate of tritium through the heat transfer metal thickness inside the heat exchanger is the overall rate of transfer of the permeating species (T_2) from the bulk fluid on the upstream side of the barrier (helium coolant) to the bulk fluid on the downstream side (water/steam). Because this is a multistep process, the overall rate is determined by the slowest step in the series. Since each process is a function of the tritium partial pressure and system temperature, it should be possible to identify certain operating regimes where each process is dominant. The two possible rate limiting processes: metal-limited and fluid-limited tritium transport, are described in the following subsections.

4.1.1 Tritium Permeation Through Metals

The tritium permeation rate through metals is assumed to be governed by Richardson's Equation:

$$J_{metal} = \frac{A}{x} K_p(T_M) \left[P_1^{\frac{1}{2}} - P_2^{\frac{1}{2}} \right] \qquad (4.1)$$

where P_1 = tritium gas (T_2) partial pressure on one side of the metal barrier

P_2 = tritium gas (T_2) partial pressure on the other side of the metal thickness

This assumption has already been challenged in Section 2.3.4 where it was shown that at low tritium partial pressure, the permeation rate is proportional to the linear power of the tritium pressure. This phenomenon occurs regardless of the presence of an oxide film layer because in the ultimate low pressure limit, dissociative chemisorption is the rate limiting process which is inherently first power (ref. Figure 2-14). The possibility of the

metal permeation rate being proportional to the first power of the pressure may be of consequence when comparing it with the fluid-limited permeation at low pressures. However, the proportionality factors used in Richardson's Equation are well documented as opposed to those that might be derived for a linear pressure dependent metal permeation equation.*

Assuming negligible downstream concentration (in the water cycle) then Equation (4.1) becomes

$$J_{metal} = \frac{A}{x} K_p(T_M) \quad P_1^{\frac{1}{2}} \qquad (4.3)$$

This equation will be used as the basis for all calculations in this chapter concerning permeation through metals.

4.1.2 Tritium Transport Through Fluids

The diffusive transport of tritium through a fluid (e.g., the helium coolant) is given by the following general expression

$$J_{fluid} = A\ h\left[C_1 - C_2\right] \qquad (4.4)$$

where J_{fluid} = rate of diffusion of tritium through the fluid
h = mass transfer coefficient for tritium in that fluid
A = area of transfer normal to flow
C_1 = concentration of tritium in bulk fluid
C_2 = concentration of tritium at the metal wall

* Kuehler and Axtmann[41] have obtained the following form of the permeation rate through metals at low driving pressures:

$$J_{metals} = \left[\frac{1}{k_{ads_1}} + \frac{1}{k_{ads_2}}\right]^{-1} (P_1 - P_2) \qquad (4.2)$$

where k_{ads} represents the number of molecules striking the surface per unit area, which includes a probability function of whether the molecules will dissociate and chemisorb as atoms.

If the resistance to mass transfer is assumed to be only that of the fluid*, then C_2 approaches zero, and

$$J_{fluid} \cong A \; h \; C_1 \tag{4.5}$$

The mass transfer coefficient is related to the mass transfer equivalent of the Nusselt Number, which is called the Sherwood Number:

$$Sh \equiv \frac{h \; d}{D_G(T_F)} \tag{4.6}$$

where d = characteristic length for mass transport (e.g., diameter of heat exchanger tubes)

$D_G(T_F)$ = tritium diffusivity in fluid as a function of the fluid temperature

Zarchy and Axtmann[9] used the following Gilliland coorelation[69,70] for turbulent flow inside round tubes to relate the Sherwood Number to the flow parameters:

$$Sh = 0.023 \; Re^{0.8} \; Sc^{1/3} \tag{4.7}$$

where Re = Reynolds Number $\equiv \frac{ud}{\nu}$

Sc = Schmidt Number $\equiv \frac{\nu}{D_G}$

For fluids like gaseous helium that dissolve tritium as molecules (T_2), the tritium concentration can be expressed in terms of Henry's Law[71]:

$$C = K_H(T_F) \; P \tag{4.8}$$

where K_H = Henry's Law constant for tritium in the fluid

P = tritium partial pressure in the fluid

* This assumption is valid when considering fluid-limited transport.

Substituting Equations (4.6), (4.7) and (4.8) into (4.5), the following expression for the tranport of tritium in the fluid is given by:

$$J_{fluid} \cong \frac{A}{x} D_G(T_F)\ K_H(T_F)\ \ 0.023\ Re^{0.8}\ Sc^{1/3}\ \ P_1 \qquad (4.9)$$

4.1.3 Determination of Rate-Limiting Step

Since the permeation through metals is proportional to the square root of the driving pressure (ref. Equation (4.3)) and transport through fluids is proportional to the first power of the pressure (ref. Equation (4.9)), it can be shown that at some low operating pressure, the overall permeation rate would be limited by that in the coolant. To determine the regimes in which each process is dominant, it is proposed to set the two permeation fluxes ($\equiv J/A$) equal as indeed they would be at the coolant/metal interface in steady-state, and solve for the corresponding tritium partial pressure. Equating Equations (4.3) and (4.9), and defining the pressure at which the transition from fluid-limited to metal-limited permeation as P_T, the result is:

$$P_T = \left[\frac{d\ K_D(T_M)}{x\ K_H(T_F)\ D_G(T_F)\ 0.023\ Re^{0.8}\ Sc^{1/3}} \right]^2 \qquad (4.10)$$

Assuming that the fluid and metal are in thermal equilibrium, then $T_F = T_M = T$. A plot of P_T versus temperature is given in Figure 4-1 where UWMAK-II system parameters are used in Equation (4.10) in conjunction with the coorelations suggested by Zarchy and Axtmann[9] which are repeated here in Table 4-1.

It is apparent that if the tritium partial pressure in the primary coolant loop falls in the range of P_T or lower, a careful look at the limitations to tritium transport afforded by the helium doolant might yield helpful results. It is possible that a higher tritium partial pressure could be maintained in the coolant without going above a certain maximum allowed leakage rate to the environment, if the resistance offered

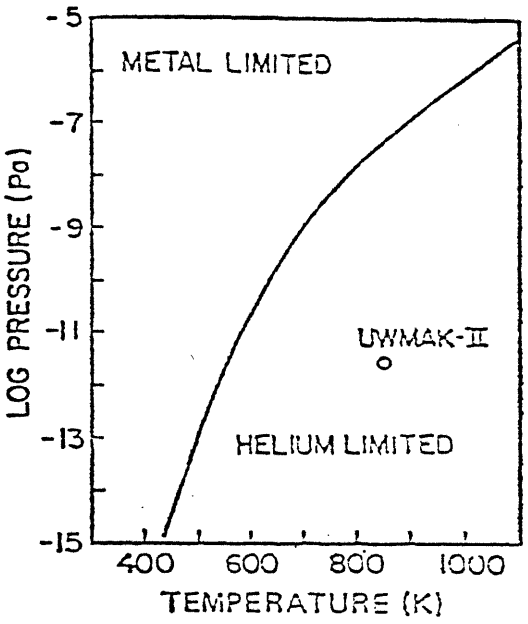

Figure 4-1

Plot of the System Temperature vs. Logarithm of the Driving Pressure Showing Regions of Metal-Limited and Helium-Limited Permeation

(Figure taken from Ref. (9))

Table 4-1

Physical Property Data for Use in Equation (4.10)

Fluid	Helium Coolant @ 50 atm	Ref. (10)
IHX Tube Material	Incoloy 800	Ref. (10)
Permeability[a]		
K_p^o $\frac{kg}{m\ day\ Pa^{\frac{1}{2}}}$	5.63×10^{-5}	Ref. (72)
Q_p kJ/mol	67.41	Ref. (72)
Viscosity		
$\mu(T_F)$ Pa sec	$\left[113 + 0.33\ T_F(^oK)\right] \times 10^{-7}$	Ref. (73)
Diffusivity		
$D_G(T_F)$ cm^2/sec	$0.012 \left[\frac{T_F(^oK)}{273}\right]^{1.5}$	Ref. (69)
Henry's Constant (ideal gas)		
$K_H(T_F)$ $\frac{kg}{m^3 Pa}$	$\frac{7.21 \times 10^{-4}}{T_F(^oK)}$	b

Note: a - Arrhenius form of the permeability is used:

$$K_p\ (T_M) = K_p^o \exp - (Q_p/RT_M)$$

b - Not given in report (Ref. (9))

by the coolant is considered.

4.2 Application of Fluid/Metal-Limited Permeation Model

The possibility of operating in the helium (fluid)-limited permeation region in Figure 4-1 is examined for the cases of General Atomic's Field-Reversed Mirror Fusion Reactor (FRM)[11] and ANL's STARFIRE Tokamak Reactor Design[8]. It must be understood that the permeation model developed in the preceding section can only be applied to the steady-state operating conditions of the fusion reactor designs. The time to reach a steady-state tritium concentration profile throughout the reactor system is not considered by this model.

4.2.1 GA FRM

A brief description of the Field-Reversed Mirror Fusion Reactor preliminary design is given in Appendix G. The system parameters presented in that appendix are used as input to the transport-limited model developed in Section 4.1.

4.2.1.1 Results of Steady-State Fluid/Metal-Limited Permeation Model

The transport of tritium in the helium coolant inside the mainstream generator is given by Equation (4.9) in conjunction with the input parameters determined in Appendix G for the GA FRM. Substituting the necessary values of Table G-2 into Equation (4.9) and a total surface area equal to 282.9 m^2, the specific equation for J_{fluid} ($\equiv J_F$) becomes:

$$J_F = 1.815 \times 10^{-1} \; P_1 \text{ (Pa)} \qquad \text{(kg/day)} \qquad (4.11)$$

Similarly, the permeation of tritium through the metal of the steam generator from the helium coolant into the steam cycle is given by Equation (4.3) in conjunction with the system values taken from Table G-2. The metal permeation equation for the GA FRM steam generator is thus:

$$J_M = 4.637 \times 10^{-5} \; P_1^{\frac{1}{2}} \; (Pa)^{\frac{1}{2}} \qquad (kg/day) \qquad (4.12)$$

A plot of the two medium-limited transport equations J_F and J_M is given in Figure 4-2. It is evident that at low tritium partial pressure in the coolant transport through the fluid is rate-limiting. At higher pressures, the tritium transport is given by the permeation through the metal. The pressure at which the transition between fluid-limited and metal-limited transport occurs is given by Equation (4.10). The value of P_T is obtained upon substitution of the GA FRM system parameters and/or a visual inspection of Figure 4-2. The result is:

$$P_T \approx 6.5 \times 10^{-8} \; Pa \qquad (4.13)$$

4.2.1.2 Comparison of Results with GA FRM Report[11]

The GA FRM preliminary design report only considered the permeation resistance offered by the metal of the steam generator when determining the maximum allowable tritium inventory in the helium coolant corresponding to a maximum tritium release rate to the environment. The metal permeation equation used for this calculation is given by (Equation (3.8) of Ref. (11)):

$$R = 2.15 \left[\frac{P}{600}\right]^{1.0} \qquad (\mu Ci/hr) \qquad (4.14)$$

where the units of the tritium partial pressure are $\mu Ci/std\text{-}m^3$. Equation (4.14) can be restated in terms of the gaseous tritium inventory of the coolant by making use of the ideal gas law:

$$p \; V = n \; R \; T \qquad (4.15)$$

where V = helium loop volume (= 16 m^3 from Table G-1)

T = average helium temperature (= 710 ^oK from Table G-1)

The tritium release rate as a function of the helium loop tritium inventory

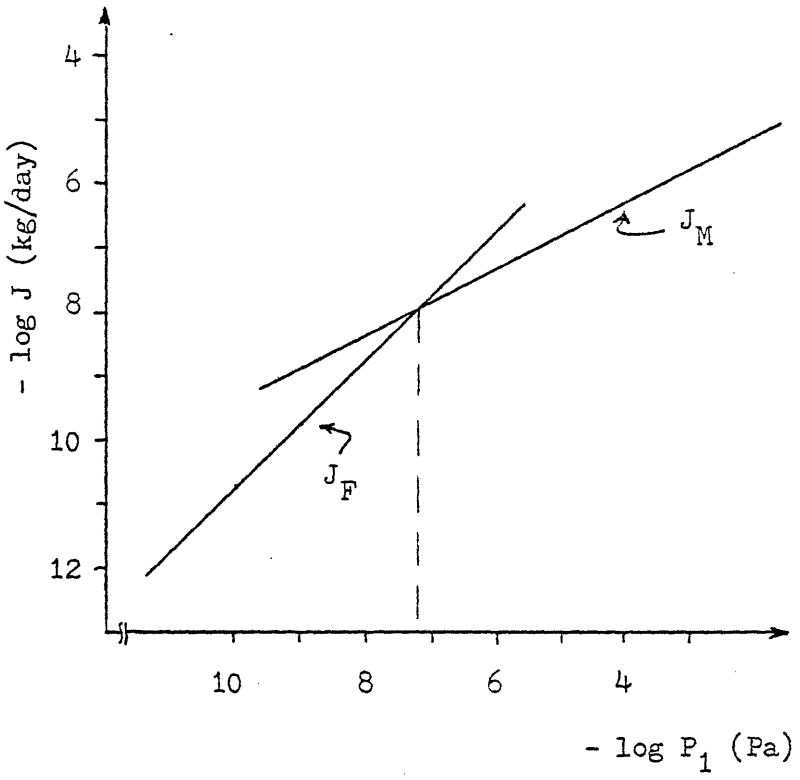

Figure 4-2

Tritium Transport Rates Showing Fluid-Limited (J_F) and Metal-Limited (J_M) Pressure Regimes for the GA FRM Design Parameters

I (in Curies) is thus:

$$R = 1.4 \times 10^{-2} \; I_c \qquad \text{(Ci/day)} \qquad (4.16)$$

Assuming the fusion reactor is operating in steady-state, the GA FRM report then goes on to equate the production of tritium in the breeding material (S) with the tritium clean-up and tritium loss through the steam generator:

$$S = I_c \, f_c + 1.4 \times 10^{-2} \; I_c \quad \text{(Ci/day)} \qquad (4.17)$$

where f_c is the helium clean-up system flow rate in inventories per day. The source term for a FRM blanket tritium breeding ratio of 1.03 is 6.2×10^4 Ci/day. The report chose 0.13 Ci/day as the maximum allowable tritium release rate. Thus, from Equation (4.16) the tritium inventory must be kept below 9.3 Ci in order to keep within the allowable release to the environment. Substituting $I_{c,max} = 9.3$ Ci and $S = 6.2 \times 10^4$ Ci/day into Equation (4.17), the required clean-up rate is 6.7×10^3 inventories/day. Since there are 54.7 kg in the helium loop ($= V_c \cdot \rho(710\ ^{o}K)$) this corresponds to a clean-up flow rate of 1.5×10^4 kg/hr. The total helium flow rate is 26.3 kg/sec given in Table G-1. Thus the clean-up is approximately 16% of the main helium loop flow rate.*

The effect on the clean-up rate deduced by GA by using the results of Section 4.2.1.1 are now discussed. Equations (4.11) and (4.12) must first be put in the form of Equation (4.16). Using the helium average temperature of 710 ^{o}K, the ideal gas law gives:

* The actual figure given in the GA FRM Report (11) is approximately 12% of the main helium flow rate. The value for the clean-up rate (6.7×10^3 inventories/day) is the same as that quoted above. The discrepancy is due to the value of P used in the calculation. The value for the density was not specified in the design report so it was calculated from the data presented in Appendix C. That value is given in Table G-2 of Appendix G, and is consistently used throughout this comparison between the GA FRM results and that calculated from the model of Section 4.1.

$$J_F = 3.9 \times 10^3 \; I_c \text{ (Ci)} \qquad \text{(Ci/day)} \qquad (4.18A)$$

$$J_M = 2.15 \times 10^1 \; I_c^{\frac{1}{2}} \text{ (Ci)} \qquad \text{(Ci/day)} \qquad (4.18B)$$

With a maximum release rate of 0.13 Ci/day as stipulated by the design report, the corresponding maximum allowable tritium inventories in the coolant are:

$$I_{c,max_F} = 3.3 \times 10^{-5} \text{ Ci} \qquad (4.19A)$$

$$I_{c,max_M} = 3.7 \times 10^{-5} \text{ Ci} \qquad (4.19B)$$

Both of these are a lot less than the previously reported 9.3 Ci inventory, and will necessarily adversely affect the clean-up rate. Following the same procedure as that used by GA, and the same value for the source term, the clean-up flow rates are found to be:

$$w_F = 4.2 \times 10^9 \text{ kg/hr} \qquad (4.20A)$$

$$w_M = 3.6 \times 10^9 \text{ kg/hr} \qquad (4.20B)$$

Since the required clean-up flow rates are much greater than the main helium flow rate itself ($\sim 9.5 \times 10^4$ kg/hr) this analysis proves the tritium inventory cannot be kept at an acceptable level using only the rudimentary permeation barriers offered by the helium fluid and metal resistances. A possible explanation for the wide disagreement between the GA results, namely that a 12% by-pass flow is all that is required to keep tritium releases below 0.13 Ci/day, and the results of this permeation model, that no amount of clean-up can keep the releases below 0.13 Ci/day without the use of some sort of auxiliary permeation barrier, is given in Section 4.2.1.3.

The GA FRM report also includes the addition of oxygen to the main helium loop as a means of reducing the required clean-up flow rate below their previously calculated 6.7×10^3 inventories/day. The tritium inventory in the coolant was assumed to be 0.15 gm, equal to that in the solid. An oxygen partial pressure of 10^{-2} torr (1.3 Pa) would make most of this

tritium be present in the form of T_2O due to a large value of the equilibrium constant* for the reaction $T_2 + \frac{1}{2} O_2 \rightleftharpoons T_2O$. The partial pressure of tritium (T_2) in the helium coolant in which this much oxygen has been added is now 1.24×10^{-2} torr (1.7×10^{-10} Pa). This partial pressure is the driving force for tritium losses to the environment. The partial pressure of T_2O present in the system, although high (10.35 Pa), is inconsequential for release considerations since T_2O is assumed to be a non-permeating species.

With P_1 equal to 1.7×10^{-10} Pa, the tritium partial pressure falls below that of the transition pressure ($= 6.5 \times 10^{-8}$ Pa). Thus the addition of oxygen to the helium loop has placed the system in a regime where the fluid is the rate-limiting step to tritium transport. The implications of this result are given in the next section.

Without the added effect of the presence of oxygen, the tritium partial pressure would have been 9.1×10^{-1} Pa (corresponding to the tritium inventory of 9.3 Ci). This would have placed the system in a regime where permeation was metal-limited as was assumed by GA in the beginning. But, of course, this assumption was vital for the determination of the tritium partial pressure. It is as though their final answer justified their original assumption. Although the clean-up rate does not seem to benefit from the inclusion of the fluid resistance (ref. Equation (4.20A)), the fact that GA's results with their metal permeation equation is so different from the results (ref. Equation (4.20B)) obtained with the metal permeation equation of Section 4.1 (ref. Equation (4.3)) deserves special attention. This problem is addressed in the following Section 4.2.1.3.

4.2.1.3 Conclusions

There are two reasons for the discrepancy for the tritium losses due to permeation through metals between the GA FRM Report and that calculated

* The design report uses a value of 6.3×10^{11} torr$^{-\frac{1}{2}}$ for the equilibrium constant, which was calculated at a system temperature of 525 °C (798 °K). This is <u>not</u> the same temperature used for the average helium temperature in the permeation equations.

from the model presented in Section 4.1: the first is the expression for the tritium permeability in Incoloy 800, and the second is the pressure dependency of the permeation rate.

Regarding the first reason, the GA FRM Report states[11] that the permeation of tritium through oxide-covered Incoloy 800 is "described by"

$$P(T) = 93.1 \exp -\left[\frac{6.67 \times 10^3}{T}\right] \qquad (\mu Ci/m^2) \qquad (4.21)$$

at a pressure of 600 $\mu Ci/std\text{-}m^3$. Although P(T) does not have units of permeability, it is possible to compare a "quasi" permeation coefficient from their report with that used by Zarchy and Axtmann[9] and subsequently used in Equation (4.3):

$$K_p(T) = 5.63 \times 10^{-5}\left(\frac{kg}{mday Pa^{\frac{1}{2}}}\right) \exp -\left[\frac{8.103 \times 10^3}{T}\right] \qquad (4.22)$$

At a common pressure of 600 $\mu Ci/std\text{-}m^3$ (2.44×10^{-5} Pa) and temperature of 798 °K, the permeation coefficients from the GA FRM Report* and the model are thus 6.1×10^{-2} $\mu Ci\text{-}mm/m^2\text{-}hr$ and 3.86×10^3 $\mu Ci\text{-}mm/m^2\text{-}hr$ respectively. Thus, the GA report relied upon a much lower (5 orders of magnitude) permeability than the present model did in using Equation (4.22). This would account for a much lower tritium release value for permeation through the metal. The lower permeability is attributed to GA's assumption of an oxide-coated metal for use in the steam generator. This has already been shown (in Section 2.3.4) to be an effective permeation barrier in steady-state after the oxide layer has been formed in situ by steam oxidation.

The second reason for the discrepancy in the effectiveness of the metal barrier is that the GA FRM design report assumed a linear dependency on pressure for the metal permeation rate, while the model assumed the usual square-root power of the pressure. In the design report it was

* Value taken from the first line of Table 3-1 in Ref. (11).

stated that:

> "The pressure dependence of tritium permeation can be approximated . . . by $P \alpha p^{y}$ where y is 0.79 at 700 °C and 1.04 at 400 °C. Since we will be extrapolating . . . (the) data upward from 600 $\mu Ci/m^3$ (2.44×10^{-5} Pa), y = 1.0 can be used as a conservative estimate."

Their assumption is not really conservative because at pressures below $\sim 10^{-2}$ Pa, the pressure dependency returns to the square root ($J_M \alpha P^{\frac{1}{2}}$ for $P \leq 10^{-2}$ Pa) [37] where the defects (holes or cracks) in any surface film (e.g., oxide coating) are rate-limiting. Only for extreme low pressures, where dissociative chemisorption is rate-limiting[41] or from 10^{-2} Pa to 10^{0} Pa where transport through the oxide film is rate-limiting, is the pressure dependency linear. Therefore, a conservative estimate of the pressure dependency for pressures above 10^{-5} Pa would be to take $J_M \alpha P^{\frac{1}{2}}$ as is usually done.

With oxygen added to the helium coolant, it was shown that the transport of tritium by the fluid finally becomes important. The intentional introduction of oxygen made the tritium partial pressure drop within the regime of fluid-limited transport. Thus, it is possible that although the tritium is being carried around the primary coolant loop by the helium, it is also being prevented from diffusing out of the coolant by the favorable transport properties provided by the helium. If the tritium is inhibited from ever dissolving into the metal, then this brings to mind some interesting consequences. First of all, the tritium transport properties of the primary coolant cannot be overlooked when the choice of coolant is being made. Secondly, the overall permeation rate would be correspondingly less than for metal permeation-based calculations at the same pressure. Thus, it is possible that grosser pathways for tritium leakage, e.g., via pinholes and leaky valves, would become more important tritium release terms than permeation losses.

4.2.2 STARFIRE-Interim Design[8]

A detailed description of the STARFIRE-Interim Reference Design is given in Appendix F and also in Section 3.1 and thus will not be repeated here. The system parameters presented in Appendix F are needed as input to

the transport-limited model developed in Section 4.1.

4.2.2.1 Results of Steady-State Fluid/Metal-Limited Permeation Model

The STARFIRE-Interim parameters that are used as input to the transport-limited permeation model of Section 4.1 is given in Column I of Table 4-2. Substituting the necessary values of Table 4-2 into Equation (4.9), the corresponding fluid-limited transport equation becomes:

$$J_F = 1.495 \times 10^{1} \quad P_1(\text{Pa}) \qquad (\text{kg/day}) \qquad (4.23)$$

The metal permeation equation for the STARFIRE heat exchanger is given by*

$$J_M = 1.632 \times 10^{-1} \quad P_1^{\frac{1}{2}} (\text{Pa}) \qquad (\text{kg/day}) \qquad (4.24)$$

A plot of these two tritium transport equations is given in Figure 4-3. The pressure at which the transition between fluid-limited and metal-limited transport occurs is calculated by equating Equations (4.23) and (4.24), or from the intersection of the lines in Figure 4.3. The result is:

$$P_T \sim 1.2 \times 10^{-4} \text{ Pa} \qquad (4.25)$$

4.2.2.2 Comparison of Results with Transient Permeation Model Steady-State Results

The application of the transient permeation model to the STARFIRE-Interim design has already been completed in Chapter 3. The steady-state tritium partial pressure in the helium coolant was found to be approxi-

* The permeability of Croloy is used instead of Incoloy 800 that was used in Ref. (9) because the steam generator tubes are made out of Croloy.

Table 4-2

STARFIRE-Interim Steam Generator Parameters

			I[a] Input to Permeation Model, Section 4.1	II[b] Input to Transient Permeation Model, Section 2.4
STEAM GENERATOR TUBE MATERIAL			(Incoloy 800)	Croloy
*Permeability	K_p	($kg/mday Pa^{\frac{1}{2}}$)	3.323×10^{-10}	1.0×10^{-8}[c]
**Heat Transfer Area	A		- - - -	3.264×10^{8}
Thickness	x		- - - -	0.2
PRIMARY COOLANT			Helium	Helium
Average Temperature		(^{o}K)	- - -	673
Pressure		(atm)	- - -	50
Flow Area	A_f	(cm^2)	- - -	1.709×10^{5}
Equivalent Diameter	d	(cm)	- - -	138.4
Mass Flux	G	($gm/cm^2 sec$)	- - -	1.855
*Viscosity	μ	(gm/cm-sec)	3.35×10^{-4}	3.85×10^{-2}
*Diffusivity	D_G	(cm^2/sec)	4.65×10^{-2}	1.26×10^{-1}
*Henry's Constant	K_H	(kg/m^3 Pa)	1.07×10^{-6}	- - - -
*Density	ρ	(gm/cm^3)	- - -	3.616×10^{-3}
Reynolds Number	Re		7.66×10^{5}	7.57×10^{5}
Schmidt Number	Sc		1.99	0.745

Note: a - Property values calculated from equations in Table 4-1

b - STARFIRE-Interim system parameters and property values given in Appendix F

c - Permeability of Croloy given in STARFIRE-Interim Reference Design

* - Evaluated at T = 673 ^{o}K

** - Total heat transfer area of all six heat exchangers for the plant

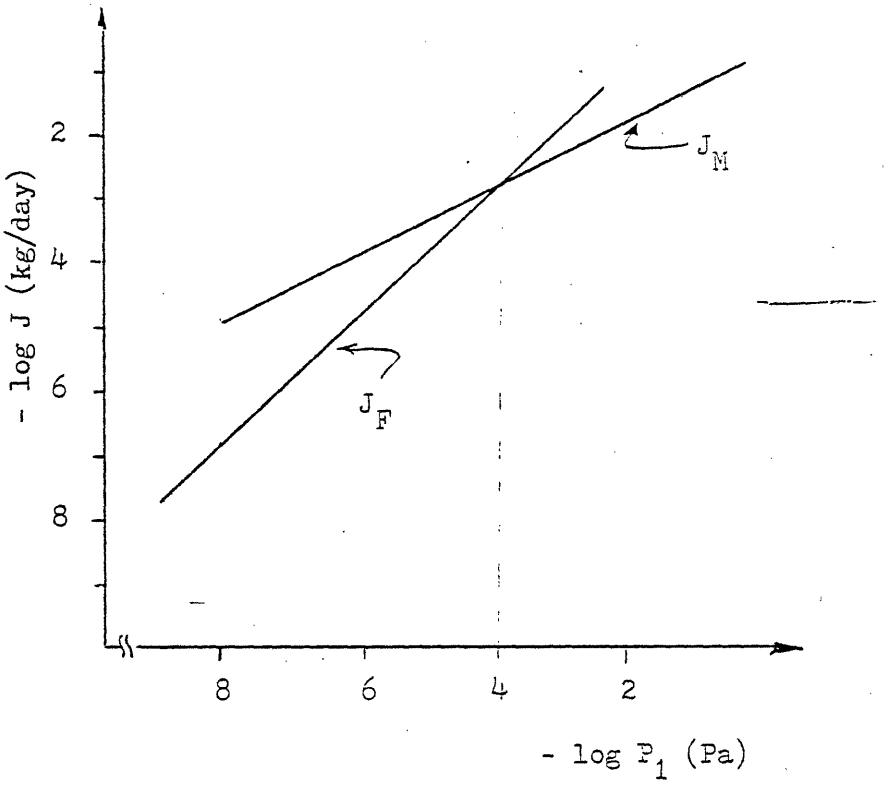

Figure 4-3

Tritium Transport Rates Showing Fluid-Limited (J_F) and Metal-Limited (J_M) Pressure Regimes for the STARFIRE-Interim Design Parameters

mately 3×10^3 torr when no effort was made to control the tritium losses except via the "clean" metal primary containment. Even with the addition of oxygen to the helium coolant, the resulting reduction in tritium partial pressure is on the order of 10^6. From Section 3.2.4, the "corrected" tritium partial pressure is only 3×10^{-3} torr (4×10^{-1}Pa). This is still above the transition pressure of 1.2×10^{-4} Pa calculated in the previous section, implying that permeation through the metal is the rate-limiting step for tritium transport in the steam generator.

This is in accordance with the relative magnitudes of the resistances offered by the coolant and metal inside the heat exchanger, as calculated in Chapter 3. From Table 3-1 these resistances are given by:

$$R_F = \frac{1}{A_{HX}\, h_{HX}} \tag{4.26A}$$

and,

$$R_M = \frac{x_{HX}}{A_{HX}\, D_{HX}} \tag{4.26B}$$

Substituting the input parameters derived for STARFIRE in Appendix F into Equations (4.26A) and (4.26B):

$$R_F = 2.198 \times 10^{-9} \quad \text{sec/cm}^3 \tag{4.27A}$$

and,

$$R_M = 3.501 \times 10^{-4} \quad \text{sec/cm}^3 \tag{4.27B}$$

The metal resistance is indeed much larger than that of the fluid, thus the system can be expected to operate in a metal-limited mode if the final, steady-state tritium partial pressure is not inappreciable. Thus, the medium-limited model developed in this chapter is in agreement with the steady-state results of the transient permeation model developed in Section 2.4.

It must be pointed out that the mass transfer coefficient h that went into calculating the fluid-limited transport (Equation (4.9)) used the helium property values calculated from Table 4-1 (from Ref. (9)) and the

following Sherwood coorelation

$$Sh = 0.023\ Re^{0.8}\ Sc^{1/3} \tag{4.28}$$

The mass transfer coefficient used in the calculation of the fluid resistance (Equation (4.26A)) was determined from the general expressions for the helium property values given in Appendix C and the following Gilliland correlation for the mass transfer analogy of the Nusselt Number:

$$Sh = 0.023\ Re^{0.83}\ Sc^{0.44} \tag{4.29}$$

Substituting the property values deterimined from the Zarchy and Axtmann's equations[9] (ref. Column I, Table 4-2) into Equation (4.28) and the corresponding property values used in Chapter 3 and listed in Column II of Table 4-2, into Equation (4.29), the respective mass transfer coefficients are:

$$h_I = 0.5 \quad cm/sec \tag{4.30A}$$

$$h_{II} = 1.4 \quad cm/sec \qquad (ref.\ Equation\ (F.27)) \tag{4.30B}$$

This implies that the fluid/metal-limited permeation model is underestimating the diffusive transport of tritium, with respect to the transient permeation model of Chapter 2. The transition pressure of Equation (4.25) is therefore higher than the STARFIRE operating conditions would predict. To make a more reasonable assessment of the fluid/metal-limited permeation model results, the transition pressure can be adjusted according to Equation (4.10):

$$P'_T = \left[\frac{h_I}{h_{II}}\right]^2 P_T \tag{4.31}$$

Substitution of Equations (4.30) and (4.25) into (4.31) yields a more accurate value for the transition pressure, 1.5×10^{-5} Pa. Again, both the uncorrected and corrected (with O_2 added) steady-state tritium partial

pressures determined by the transient permeation model of Chapter 2 fall above this value of the transition pressure.

Although the tritium permeation through the metal is the rate-limiting step to tritium transport inside the steam generator when the operating tritium partial pressure is kept above 1.5×10^{-5} Pa (1.1×10^{-7} torr), the hindrance to tritium transport offered by the coolant may be of some merit. This would require proper adjustment of the flow parameters and system temperature in order to optimize (i.e., minimize) the transport properties of the coolant. Only after significant changes to these variables (D, d, Re and Sc) will the fluid resistance become as equally important as the metal resistance. However, optimization of the tritium control aspects of a fusion reactor design could interfere with other just as critical design choices regarding heat transfer and plant reliability concerns.

CHAPTER 5 CONCLUSIONS AND RECOMMENDATIONS

5.1 Conclusions

5.1.1 Transient Permeation Model

A transient permeation model of tritium transport within a conceptual fusion reactor was developed in this study as a first step in assessing tritium flows through critical reactor components. The model attempts to predict tritium concentrations in these system components as they evolve in time from reactor start-up. (Initial tritium concentrations are set equal to zero.) This transient permeation model is perhaps the first attempt in following the unintentional transport of tritium in a fusion plant until steady-state operating conditions and concentrations are obtained. Most investigations into tritium control have focused on the steady-state mode and thus, while admitting this is the more conservative approach, do not know when it is reached and may indeed be overly conservative. This transient model has provided the mechanism for estimating the time to reach steady-state tritium concentrations in various components throughout the plant, and thus provide basic information used in the design of the systems that are most affected (notably, the tritium recovery and refuelling system, and the heat transfer loop).

The criteria for the applicability of the transient permeation model to the fusion reactor designs proposed by other authors (e.g., those at ANL, ORNL, GA, U. of Wisconsin and INTOR) are not too stringent. Basically the reactor designs must include a solid breeder, a (helium) purge-gas sweeping the breeder and a helium primary coolant. From thermal hydraulic and heat transfer considerations, the helium purge gas and coolant must necessarily be operating at low and high pressures, respectively. Although this model assumes a helium/steam generator as the primary loss mechanism for tritium release to the environment, this could be used as an intermediate heat exchanger if a design proposes a secondary coolant loop. Losses through the model's steam generator can then be used as a source term for another differential equation describing tritium build-up in the secondary coolant. Other possible changes (i.e., improvements) to the

existing model are given in Section 5.2.1.

The model as it stands is a "quasi" steady-state representation of the system dynamics with respect to tritium transport. Assuming that the tritium behavior in each reactor component is correctly described, the fusion plant dynamics, when modelled as a hierarchy of consecutive differential equations, was found to be very "stiff". The relatively fast dynamics of the breeder and purge gas system necessitated the de-coupling of that part of the system from the rest of the plant. However, time-dependent solutions for the tritium concentrations in various reactor components were retained by making several assiduous assumptions in the model formulation which capitalized on the inherent disparity in response times.

The inclusion in this model's formulation of both diffusion and solubility effects on the build-up of tritium in the solid breeder deserves special mention. Since both the diffusive hold-up and solubility of tritium in the lithium compound are known [17, 26] to be two of the major contributors to the breeder tritium inventory, it was important to include both effects. The model treats the build-up of tritium from both effects concurrently in order to obtain an effective time to reach a steady-state breeder concentration. This is just a first attempt at modelling the time evolution of the breeder concentration when both diffusion and solubility are taken into account; most analyses compare the two inventories (which were determined separately) only at steady-state. Obviously the time to reach a steady-state breeder concentration is of interest for both radiological hazards and refuelling considerations. The inclusion of solubility effects necessarily lengthens this time if calculated from diffusive hold-up times alone.

Although tritium permeation through the heat exchanger into the steam cycle is by far the most important tritium loss mechanism for release to the environment, and as such was included in the model, the model also provided the means to calculate the losses to the secondary containment (reactor building). This can be used as an estimate of the amount of tritium gas escaping from the helium coolant piping into the building atmosphere, and as such, the operating load that a continuous air detritiation system has to contend with. Since other tritium-containing devices

and piping runs (e.g., processing and injection systems) were not included in this model and would otherwise contribute significantly to the tritium leakage into the secondary containment, this amount is necessarily a bare minimum. The detritiation system would be sized from more information than is provided by this model.

5.1.2 STARFIRE Case Study

The transient tritium permeation model was successfully applied to the STARFIRE-Interim Reference Design[8] and the results given in Chapter 3. A brief summary of the major conclusions drawn from that case study will be given here.

The transient behavior of the system components in the STARFIRE design was characterized by the time to reach a steady-state tritium concentration in the breeder and purge gas ($\sim$ 18 days) and in the coolant system (an additional 118 days). This has numerous implications for the design of the tritium processing and storage systems and in the tritium releases from the plant. As a rough estimate, the (maximum) steady-state releases will not occur until 120 days after reactor start-up, considerably longer than the "worst-case" estimate of almost instantaneous tritium leakage, yet within the time frame of a fusion reactor operating cycle (eleven months per year).

Although a more complete reference design description would have given more accurate results, there are several important results of this case study which are true even if some of the input parameters used in the model (ref. Appendix F) were only "best" values. First, the breeder concentration in solution with that in the purge gas dominated the tritium inventory in the breeding blanket. It was also the cause for a much-delayed time to reach steady-state (18 days vs $\sim$ 7 hours for a diffusive hold-up time). The relatively low equilibrium tritium pressure for the breeder, Li_2O, hence a high tritium solubility, accounts for the large solubility-determined inventory (breeder inventory due to solubility effects $\sim$ 4.47 kg vs inventory due to diffusion effects $\sim$ 7 gms). Increasing the purge gas flow rate Q_{pg} if possible from thermal-hydraulic considerations, would serve to reduce the purge gas tritium concentration.

In so doing, the total breeder inventory would be decreased substantially since it is heavily dependent on the solubility-determined concentration which in turn depends on the purge gas concentration. In the other direction, a reduced stead-state purge gas concentration would mean less tritium diffusing into the coolant and thus less tritium leaking into the steam cycle and eventually, the environment. It is interesting to note this possibility of reduced breeder inventory and tritium releases resulting from a change in one variable, Q_{pg}. Whether this can in fact be implemented, can be determined from a detailed assessment of the advantages mentioned previously versus the increased pumping and processing requirements resulting from an increased flow rate and decreased tritium purge gas concentration.

The last major conclusion of this case study was that, after all the effort was made to properly characterize the helium film coefficient, the fluid resistance was found to be almost negligible in comparison with that offered by the metal (ref. Table 3-1). For this conceptual design at least, control of tritium transport must come from a proper choice of metal structural materials (those exhibiting a very low tritium permeability), the use of special permeation barriers (e.g., oxide films, surface coatings, bonded-metal composites) and/or the introduction of oxygen into the main helium coolant loop in order to reduce the driving T_2 pressure. All of these or some combination of them, will have to be used to some extent in all currently proposed fusion reactor designs since, on the basis of this case study on the STARFIRE design, the helium coolant cannot be expected to seriously impede the transport of tritium.

5.1.3 Steady-State Fluid/Metal - Limited Permeation Model

The permeation model presented in Chapter 4 was developed with the intent of characterizing the regimes in which transport through the coolant and permeation through the metal are rate-limiting. For purposes of this model, the reactor is operating in a steady-state mode and the conditions of interest are those inside the main steam generator where losses to the environment are assumed to originate. The main consideration given to this model is that it recognizes the possibility of the

fluid resistance being significant, and it provides the means to calculate the tritium partial pressure at the transition from fluid-limited to metal-limited tritium transport. Since transport through a fluid is linearly dependent on the pressure and permeation through a metal is assumed to have a square root pressure dependence, this means the fluid would be rate-limiting over some range of low pressures.

The addition of oxygen to the helium coolant could reduce the tritium gas (T_2) pressure to within this fluid-limited regime of tritium transport. This was shown to be true for the case of the GA Field-Reversed Mirror Fusion Reactor[11]. However, because a very low tritium permeability for the steam generator tube metal was chosen in the design report, the permeation loss through the metal calculated by GA was less than the tritium transported by the fluid as determined from the model. For the STARFIRE-Interim reference design, the operating tritium partial pressure in the helium coolant was found to be higher than the corresponding transition pressure with and without oxygen present in the helium. Since this means that the steam generator is operating in a metal-limited tritium transport regime, it is consistent with the results from the transient permeation model of Chapter 2, that of a very low mass transfer coefficient evaluated for the helium flowing through the heat exchanger.

The main conclusion from this model's application, even though it did not always result in a fluid-limited transport prediction, is that the tritium transport properties of a candidate coolant for potential use in fusion reactors should be evaluated along with its heat transfer and thermal hydraulic properties. For fusion plant primary coolant systems designed to operate at a low tritium partial pressure, these coolant transport properties become significant. A closer examination of the helium flow characteristics and temperature distribution in the steam generator, as well as a more accurate appraisal of the tritium diffusivity in helium is required before further analyses based on these results can proceed. (The temperature dependence of D_G is different for those expressions given in Ref. (9) and in Appendix C.) Thus, the implications of fluid-limited tritium transport on the choice of coolant are obvious. What this means with respect to tritium release to the environment is not so clear; although leaks under normal operating conditions and

during regular maintenance procedures could become the major loss mechanism, quantifying those losses is very difficult to do since the details of the piping and vessel structure are usually not well specified in the reference designs[6].

5.2 Recommendations

5.2.1 Improvements to Transient Permeation Model

The tritium behavior in the various reactor components is assumed to be well described by the various temperature dependent property values (diffusivity, solubility, permeability) and also the equations used in the model (Fick's diffusion equation, Sieverts' Law, Richardson's Equation). Any results calculated from the model are only as good as the data that were used to calculate them. There is considerable uncertainty in the data base for most materials when dealing with tritium, thus their use gives rise to an error in the results that is unavoidable until better data are available. More specific suggestions for what improvements in the data base are necessary is given in Section 5.2.2.

A modest design change to the modelling of the blanket section of the simplified fusion reactor design could be implemented to more accurately describe the tritium transport in a blanket scheme such as that proposed in the final STARFIRE design and depicted in Figure 5-1. That design was developed under the assumption that enhancement of the diffusion of tritium in solid breeders is made possible by a special preparation of the breeder such that the purge gas channel is formed within the packed bed. Tritium that diffuses to the edge of the pellet can still be carried away by the purge gas it comes in contact with. But for those pellets resting against the tube wall (assuming the pellets are not suspended in the helium gas stream which would contradict the notion of a packed bed), the tritium might be able to permeate through the tube metal and directly into the helium coolant, foregoing the previous intermediate step of being part of the purge gas.

It would be improper to state whether the total tritium inventory in the coolant would be greater for this model than in the blanket design

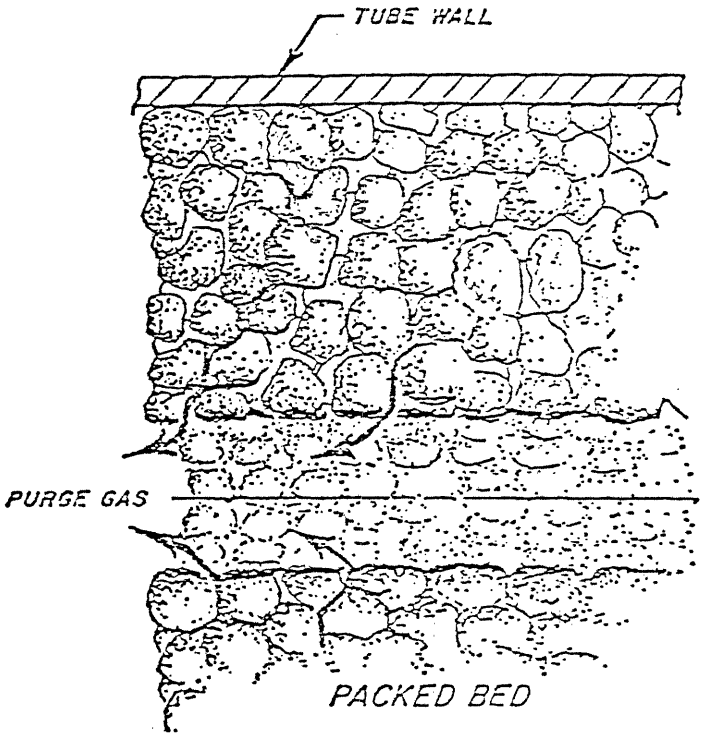

Figure 5-1

Schematic Diagram of STARFIRE Blanket Concept
Showing Tritium Removal Scheme

(Figure taken from Ref. (17))

used in the original model because there are two relevant aspects which have differing effects on the amount of tritium reaching the coolant. They are:

(1) a significantly higher tritium concentration in the pellet than in the surrounding purge gas, thus giving rise to a greater permeation rate for those pellets in contact with the tube wall,

and (2) a lower purge gas concentration near the wall surface than the "average" value calculated for the channel, since only the tritium diffusing into the purge gas from the pellets next to the tube wall contributes to this concentration.

It would be a formidable task to estimate the breeder tube surface area covered by pellets and therefore, the area exposed to a low purge gas concentration. The effect on the coolant inventory is unclear, and the average purge gas concentration may or may not increase depending on the relative magnitudes of the reduction in the effective tritium source and permeation loss. Therefore the complications arising from this design change should be weighed against the benefits of a more realistic representation of the breeder and tritium recovery scheme.

The transient model could be modified to permit a non-zero initial tritium concentration in all parts of the plant as a specified input. The motivation for this improvement is to be able to model off-normal operating conditions and their effect on tritium transport and distribution. Of particular interest is a sudden over-power condition which results in a rapid rise in the temperature of the breeder pellets. The proper initial tritium concentrations to be used as input for this case would be the steady-state values calculated previously. The relevant question to ask for this particular transient would be if the tritium gets out of the pellets at the same rate as before, assuming the tritium generated rate is unaffected by the temperature spike. (This assumption is valid over short times, if the cross-section of the reaction Li(n,p)T is weakly dependent on temperature over the range of interest.)

It is possible to speculate on the immediate effects of this transient assuming all property values (diffusivity, solubility) respond instantaneously to the temperature. Because of its Arrhenius dependence on temperature, the diffusivity D_b would necessarily increase with increasing temperature. This translates into a faster diffusion rate out of the pellet. But the solubility effects must also be considered. Since the purge gas concentration C_{pg} is weakly dependent on the diffusivity (ref. Equations (2.29) and (2.34)), then for the purposes of this brief analysis, C_{pg} is assumed constant. There is evidence[29] that for Li_2O at least the solubility is approximately constant at 100 wppm @ 10^{-1} Pa over a wide temperature range, 600 - 1000 ^{o}K. However, most other lithium compounds experience an enhanced solubility for a temperature increase (ref. Appendix A.3). Thus a potential increase in the solubility-determined inventory in the breeder could offset the reduction in the diffusive inventory. However, more information about the solid breeder properties is required before any quantitative decision can be made.

A third possible addition to the transient permeation model would be the inclusion of a means to calculate the tritium solubility in all the modelled reactor components. This requires a more extended data base than that given in Appendix B because the solubility (or Sieverts' Constant) of tritium in metals is the proportionality factor needed in the calculation. The other part of the equation (Sieverts' Law) demands knowledge of the tritium partial pressure in contact with the metal. This can be calculated from the permeation model as it now stands, and the results from this additional work would increase the overall plant inventory. But, there would be much better insight into the radiological hazard that personnel would be exposed to during a maintenance operation, once the amount of tritium dissolved in the metal is known.

The last and perhaps the most easily implemented improvement to the present permeation model would be to include a variation in the temperature profile across the breeder zone for use in the tritium inventory calculations. The temperature gradient could result from two causes: a radial dependence (from the center of the torus) away from the plasma, and an angular dependence (around the blanket torus) between coolant

tubes. Since the two major contributors to the breeder tritium inventory (diffusivity and solubility) are not linearly dependent on the temperature, calculations based on a single average temperature would misrepresent the true breeder inventory. Those pellets operating in the coldest regions in the blanket would, in fact, have a larger tritium inventory that more than offsets the decreased inventory calculated for regions operating above $\overline{T}_{b,avg}$.

Since one pellet operating at $T_{b,avg}$ may not give a good indication of the true breeder tritium inventory (in fact, may seriously underestimate it), a more detailed account of the number of pellets operating at various temperatures would yield a more accurate value. Greater confidence in the final value for the inventory would be gained when more temperature zones are used. Of course, the accuracy of any such inventory calculation is only as good as its input: breeder volume per temperature zone description and the diffusivity and solubility data. Presently, the lack of reliable data for solid lithium compounds under fusion reactor conditions is the major weakness in the design calculations. This problem is addressed in the next section.

5.2.2 Extension of Data Base

Three broad areas of investigation can be identified as being particularly important to fusion reactor design:

1 - Advances of basic data: influence of alloying elements and of bulk and surface impurities on the solubility, diffusivity and permeability with emphasis on low tritium concentrations in the temperature range 600 - 1000 °C.

2 - Simulations of reactor effects: studies of the influence of fusion reactor conditions (neutron irradiation, thermal gradients, transients) on the concentration and movement of tritium in the breeder.

3 - Permeation-reistant films: development of stable oxide films for the conditions of a helium/steam heat exchanger.

Area #2 can be expanded to include the effects of neutron damage on tritium dissolution in, and permeation through, metals and on the integrity of permeation barriers. The recommended approach to a better understanding of tritium migration through all fusion reactor materials, and for a definitive verification of permeation barrier performance in particular, is to conduct studies with tritium under realistic reactor conditions.

Extension of the data base specific to the transient permeation model and its application would involve studies on the solubility (K_{S,T_2}) and diffusion coefficients (D_b) for the candidate lithium solid breeders. Experimental data on tritium solubility in most lithium compounds are limited as was demonstrated in Chapter 3. Determination of the Sieverts' Constant for each of the lithium compounds instead of making an analogy with the solubility data from ZnO would be crucial for any further consideration of their being used as breeders. Although more data exists for the tritium diffusivity in lithium solids, it should be extended over a broader temperature range and for many more particle sizes and distribution of particle sizes. The effect of the sweep gas flow rate and protium partial pressure on the extraction characteristics for the lithium compounds should be adequately quantified so that design optimization of the sweep gas processing methods can ultimately be completed. Considerable experimental work clearly remains to be done, requiring at a minimum the confirmation of tritium release characteristics of candidate solid breeder materials with an emphasis on the establishment of diffusion and solubility parameters, and the investigation of the behavior of these materials under intense neutron irradiation. Eventually, in-reactor testing of candidate solid breeder materials under realistic conditions (including simultaneous breeding and tritium extraction) should be made, as proposed for the ANL TEPR[74].

APPENDIX A PHYSICAL PROPERTY DATA: SOLID LITHIUM COMPOUNDS

A.1 Thermodynamic Data for Several Lithium Compounds

Table A-1

Thermodynamic Data

Lithium Compound	Molecular Weight	Melting Point (°C)	Density ρ (gm/cm^3)	Lithium Atom Density (gm/cm^3)	Thermal Conductivity k (W/m°K)	Specific Heat C_p (J/gm°K)	Thermal Diffusivity $\alpha=k/\rho C_p$ (cm^2/sec)
LiAl	33.92[a]	718[b]	1.76[c]	0.37[c]	30[c]	1.84[c]	9.3×10^{-2}
$LiAlO_2$	65.91[a]	1610[d]	α - 3.40[d] γ - 2.56[d]	0.27[d]	3[e]	1.6[d]	5.5×10^{-3} 7.3×10^{-3}
Li_2O	29.88[a]	1697[e]	2.01[e]	0.93[e]	3[e]	*1.47[c]	1.0×10^{-2}
Li_7Pb_2	463.0[a]	726[d]	4.59[d]	0.49[d]	20[e]	0.59[c]	7.4×10^{-2}
Li_2SiO_3	89.94[a]	1200[d]	2.52[d]	0.36[d]	3[e]	1.91[a] (est)	6.2×10^{-3}
Li_4SiO_4	150.1[a]	1250[d]	2.5[a]	0.54[d]	3[e] (est)	2.26[a] (est)	5.3×10^{-3}

Note: a - Ref. (75)
b - Ref. (23)
c - Ref. (76)
d - Ref. (17)
e - Ref. (8)

* The specific heat for Li_2O, as a function of temperature, is also given by:[77]

$$C_p \text{ (J/mol)} = 75.24 + 9.95 \times 10^{-3} T - 25.05 \times 10^{5} T^{-2}$$

A.2 Tritium Diffusion Coefficients For Several Lithium Compounds

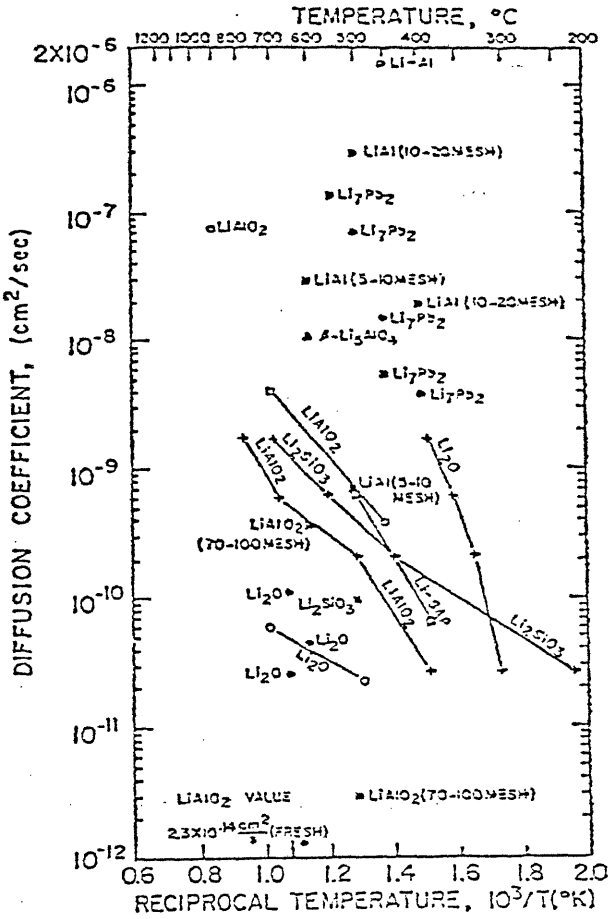

Figure A-1

Arrhenius Form for Experimentally-determined Diffusion Coefficients for Tritium in Seven Lithium Solid Breeders

(Figure taken from Ref. (26); key to above figure on next page)

Table A-2

Key for Figure A-1

Marker #	Symbol		Material Description	Reference
1	■	LiAl:	crushed and sieved solidified melts midpoint of mesh interval used	(22,23)
2	■	Li_2SiO_3:	sieved powder fractions mesh midpoint used	(22,23)
3	■	$LiAlO_2$:	sieved powder fractions mesh midpoint used	(22,23)
4	■	Li_7Pb_2:	crushed and sieved solidified melts mesh midpoint used	(22)
5	•	$LiAlO_2$:	$\frac{1}{4}$" x $\frac{1}{4}$" pellets	(21)
6	°	Li_2O:	sieved powder fractions	(21)
7	•	Li_7Pb_2:	crushed and sieved solidifed melts mesh midpoint used	(21)
8	□	$LiAlO_2$:	powders	(78)
9	○	γ-$LiAlO_2$:	fused samples	(79)
10	○	Li_2O:	powders	(79)
11	△	β-Li_5AlO_4:	ground solidified melts	(80)
12	▨	LiAl:	wafers, enriched in ^6Li	(81)
13	▨	Li-SAP:	wafers, enriched in ^6Li	(81)
14	+	Li_2O:	powders[a]	(82)
15	+	$LiAlO_2$:	powders[a]	(82)
16	+	Li_2SiO_3:	powders[a]	(82)

Note: a - midpoint of 0.05 - 0.15 mm interval used

Crosses (+) are 95, 75, 50 and 20 % fractional release points from curves given in reference.

Table A-3

Tabulated Experimental Diffusion Parameters from References Cited in Table A-2

Marker #	Lithium Compound	Condition	Average r_p (cm)	Temperature (°C)	D_o (cm²/sec)	τ^a	C^b_{He} (10^4) (gm/cm³sec)
1	LiAl	5-10 mesh	1.11×10^{-1}	500	7.0×10^{-10}	τ_1 = 1500 hrs	1.03
				600	3.0×10^{-8}	τ_1 = 14 hrs	1.03
		10-20 mesh	5.55×10^{-2}	400	2.0×10^{-8}	τ_1 = 6 hrs	1.03
				500	3.0 x 10-7	τ_1 = 0.3 hrs	1.03
2	Li_2SiO_3	70-100 mesh	9.0×10^{-3}	500	1.0×10^{-10}	τ_1 = 13.9 hrs	1.03
3	$LiAlO_2$	70-100 mesh	9.0×10^{-3}	500	3.0×10^{-12}	τ_1 = 500 hrs	1.03
				600	3.8×10^{-10}	τ_1 = 3.9 hrs	1.03
		80-120 mesh	7.6×10^{-3}	650	1.1×10^{-9}	τ_1 = 1 hr	1.03
4	Li_7Pb_2	20-40 mesh	2.78×10^{-2}	450	5.5×10^{-9}	τ_1 = 3.3 hrs	1.03
				550	1.4×10^{-9}	τ_1 = 1.3 hrs	1.03
5	$LiAlO_2$	pellets	3.5×10^{-5} (est.)	650	2.3×10^{-14}	τ_1 = 1 hr	1.03
6	Li_2O	powders	1.39×10^{-3}	500	4.5×10^{-12}	τ_1 = 8 hrs	1.03
			9.0×10^{-4}	600	2.0×10^{-11}	τ_1 = 0.75 hrs	1.03
			7.88×10^{-4}	650	5.0×10^{-11}	τ_1 = 0.23 hrs	1.03
7	Li_7Pb_2	20-30 mesh	3.1×10^{-2}	400	3.8×10^{-9}	τ_1 = 5.5 hrs	1.03
				450	1.5×10^{-8}	τ_1 = 2.6 hrs	1.03
				500	7.0×10^{-8}	τ_1 = 0.29 hrs	1.03
				550	1.4×10^{-7}	τ_1 = 0.13 hrs	1.03
8	$LiAlO_2$	powders	3.5×10^{-3}	$\log D = \frac{-(2.875 \pm 0.06) \times 10^3}{T} - (5.43 \pm 0.07)$			c
9	γ-$LiAlO_2$	fused	$r_g \sim 650\ \mu$	900	7.5×10^{-8}		0.086
	α-Li_5AlO_4	low temp phase	$r_g \sim 5\ \mu$	$\ln(\frac{1}{\tau_a}) = \frac{-(4430 \pm 720)}{T} - (1.13 \pm 0.14)$			0.086
		(Transition temperature 750 - 860°C)					
	β-Li_5AlO_4	high temp phase	$r_g \sim 5\ \mu$	$\ln(\frac{1}{\tau_a}) = \frac{-(9000 \pm 1200)}{T} + (6.06 \pm 0.13)$			0.086
10	Li_2O	powders	1.0×10^{-3}	$\ln(\frac{1}{\tau_a}) = \frac{-(2460 \pm 470)}{T} - (2.48 \pm 0.12)$			0.086
11	β-Li_5AlO_4	melts	7.5×10^{-3}	600	1.1×10^{-8}		0.086
12	LiAl	wafers	- - - -	450	1.5×10^{-6}		d
13	Li-SAP	wafers	- - - -	$D = 2.275 \times 10^{-4} \exp -(\frac{19.53\ kcal}{R\ T})$			d

Table A-3
(continued)

Note: a - Time constant used to calculate D is defined in two ways, for different references

$\tau_1 = r_p^2 / 15\,D$

$\tau_2 = r_p^2 / \pi\,D$

b - Helium sweep gas flowrate over lithium compound samples during tritium extraction experiments

c - Argon sweep gas used, at a flowrate of 20 cc (STP)/min

d - Preheated argon flushes the released tritium at a flow rate of 2 l/min

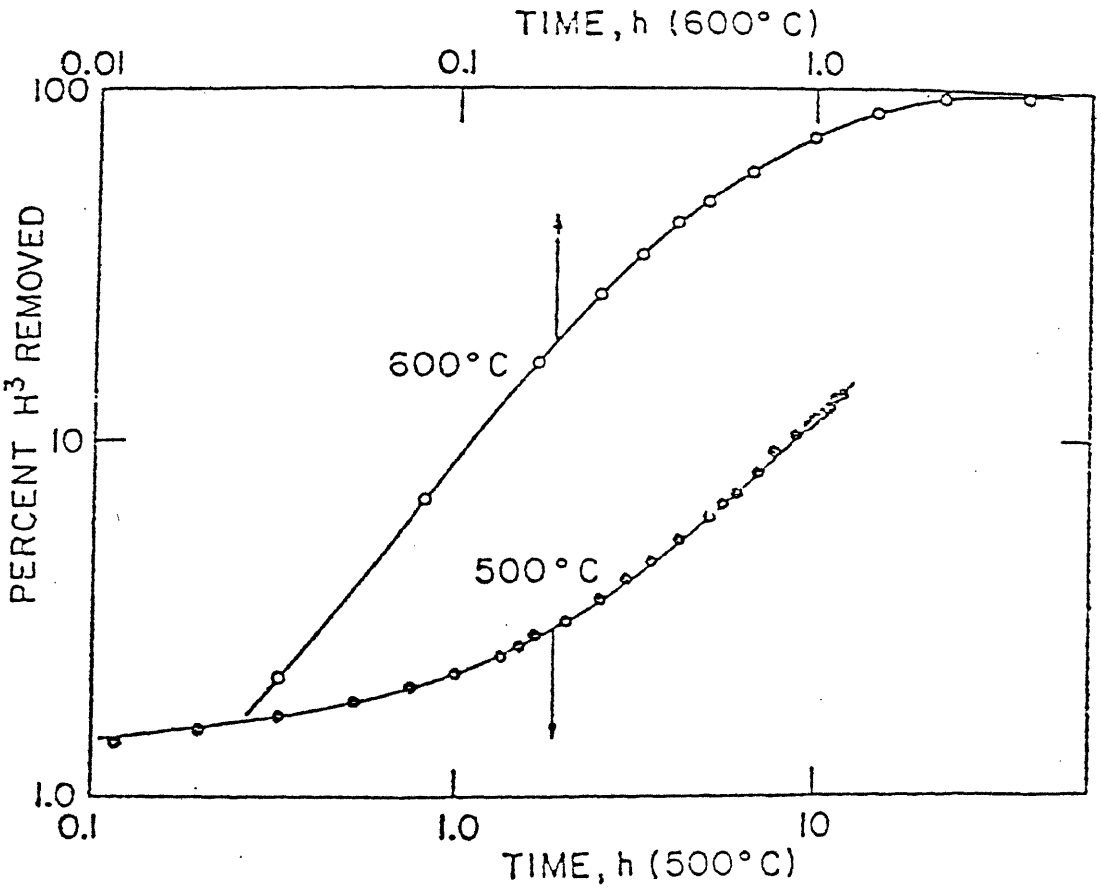

Figure A-2

Removal of Tritium from LiAl of 5-10 mesh

(Marker #1 in Table A-2)

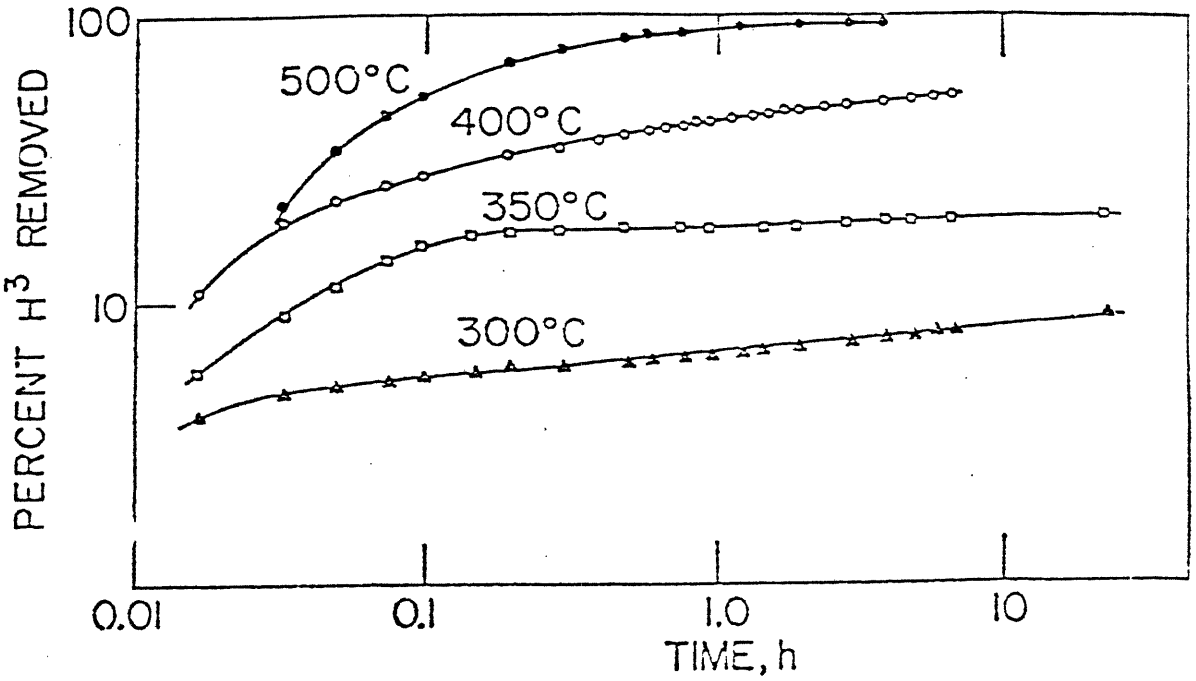

Figure A-3

Removal of Tritium from LiAl of 10-20 mesh

(Marker #1 in Table A-2)

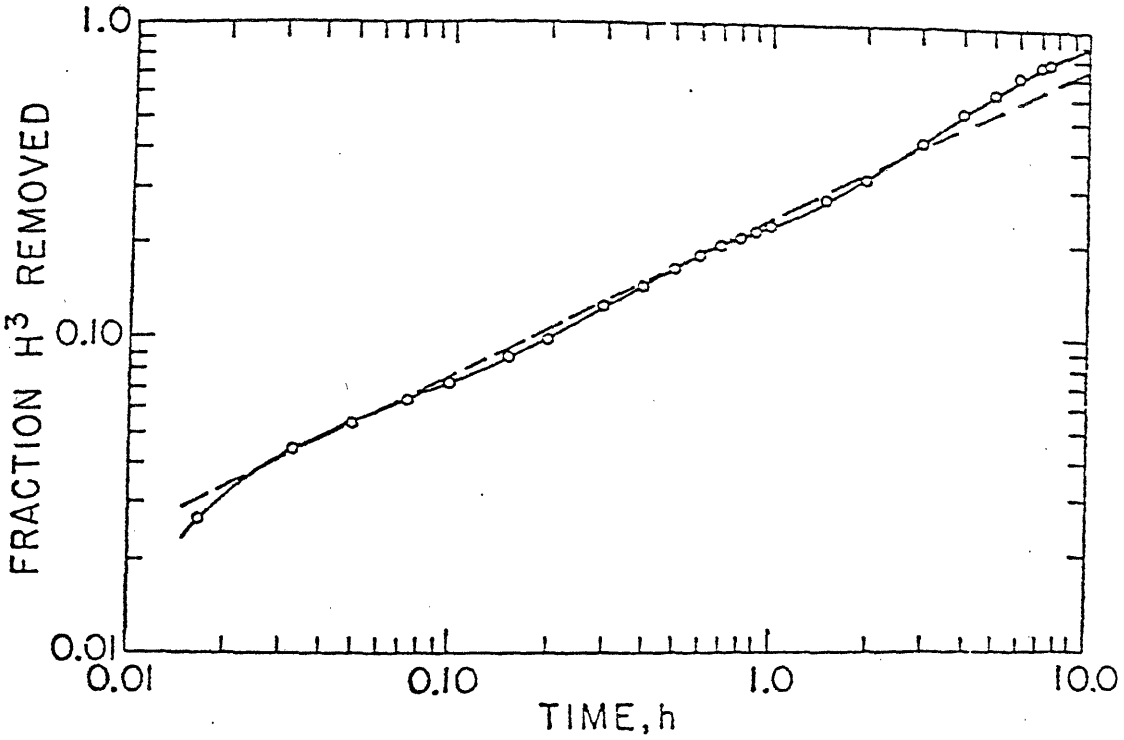

Figure A-4

Removal of Tritium from Li_2SiO_3 of 70-100 mesh

(Marker #2 in Table A-2)

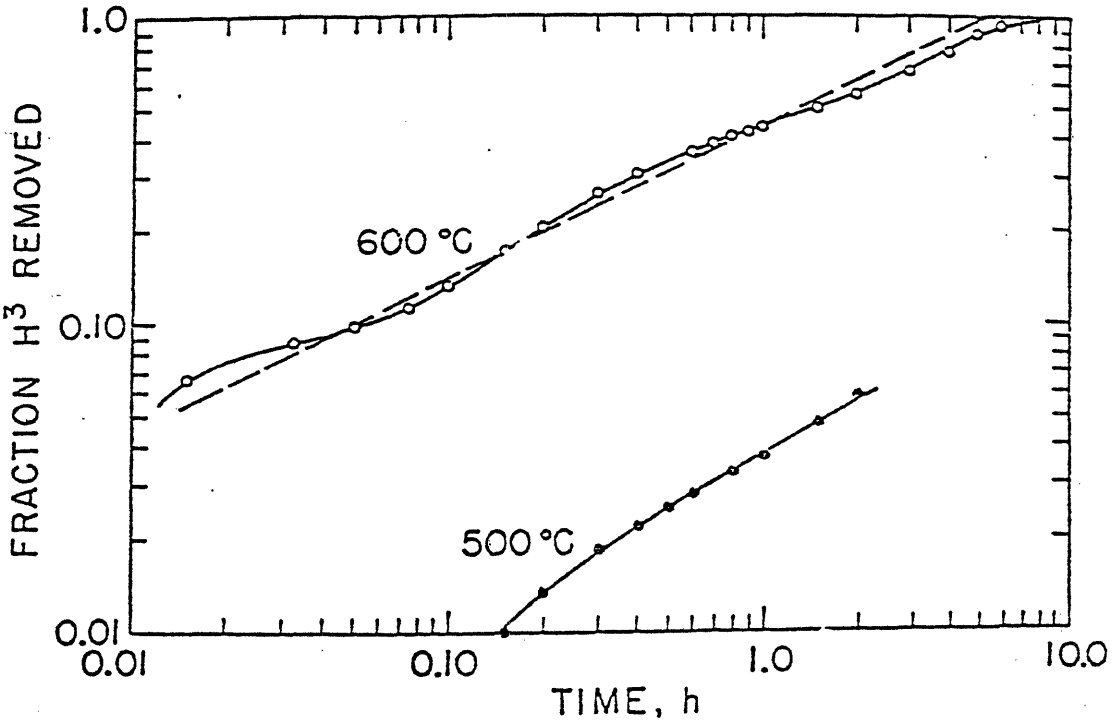

Figure A-5

Removal of Tritium from $LiAlO_2$ of 70-100 mesh

(Marker #3 in Table A-2)

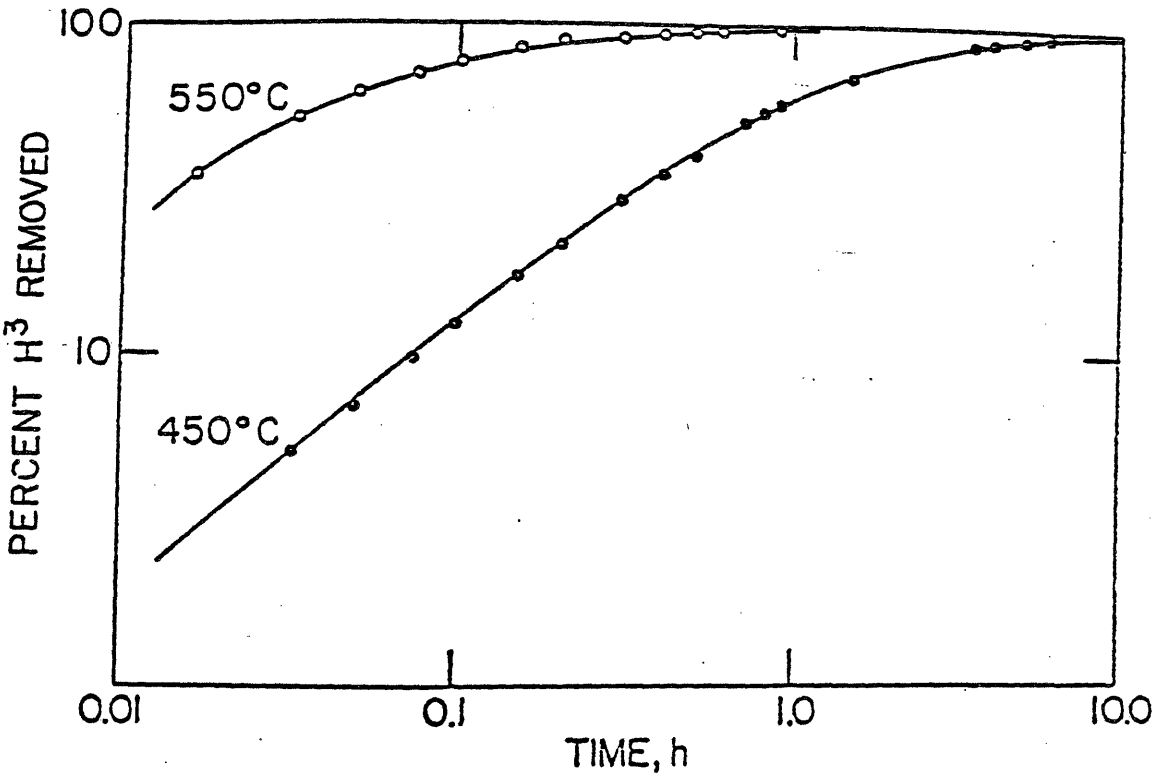

Figure A-6

Removal of Tritium from Li_7Pb_2 of 20-40 mesh

(Marker #2 in Table A-2)

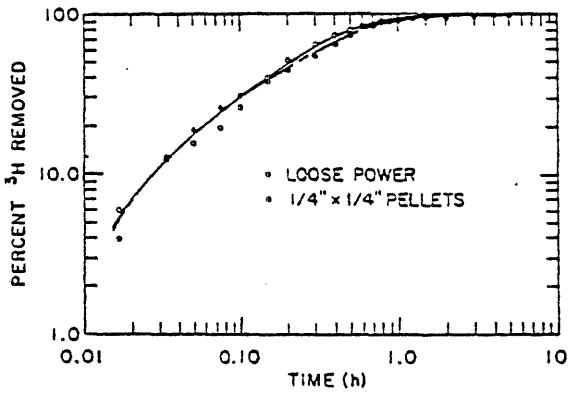

Figure A-7

Removal of Tritium from $LiAlO_2$ Pellets

(Marker #5 in Table A-2)

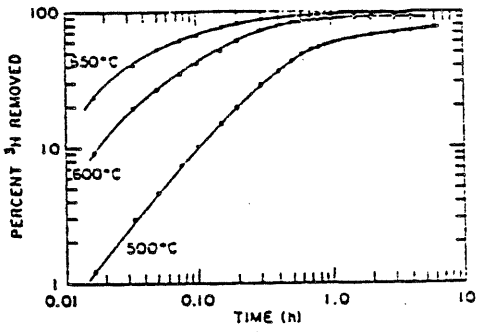

Figure A-8

Removal of Tritium from Li_2O Powders

(Marker #6 in Table A-2)

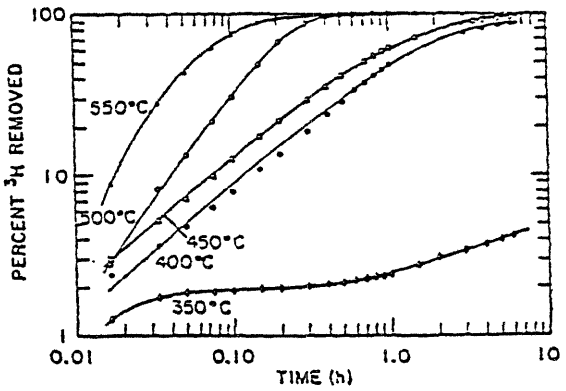

Figure A-9

Removal of Tritium from Li_7Pb_2 of 20-30 mesh

(Marker #7 in Table A-2)

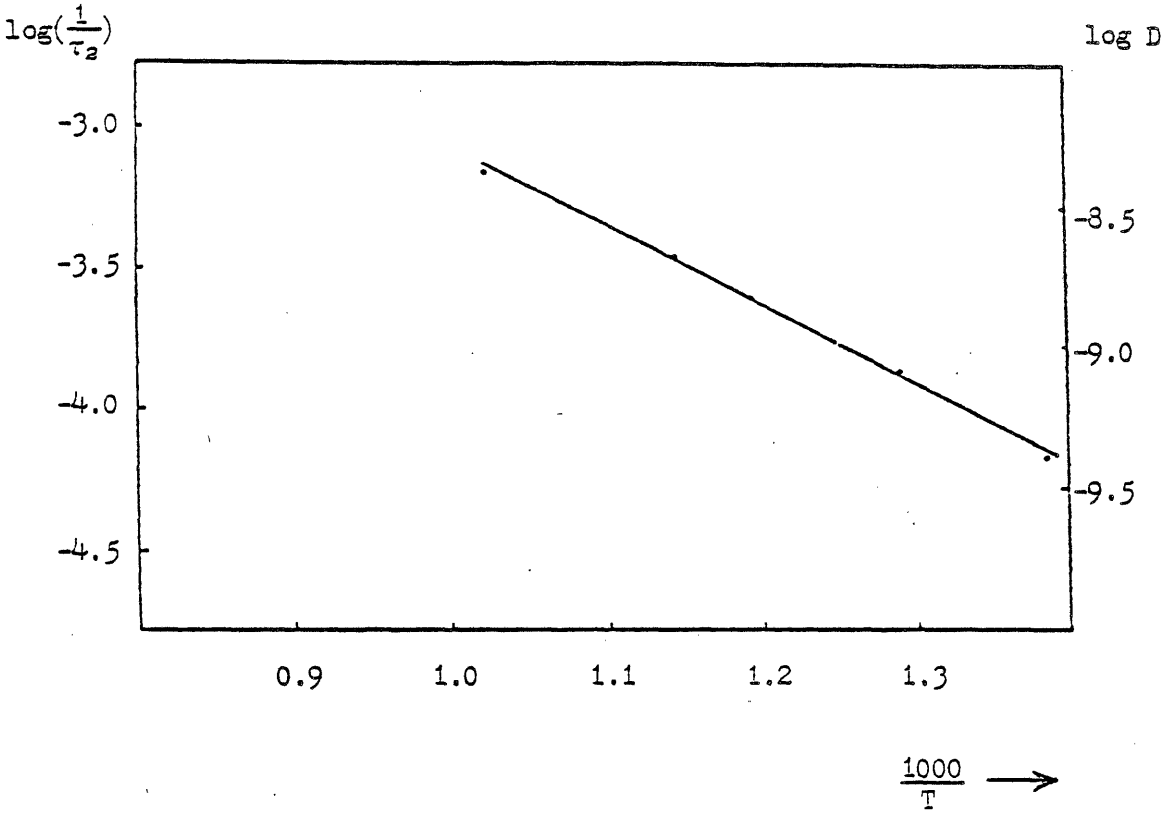

Figure A-10

Temperature Dependence of Reciprocal Time Constant $1/\tau_2$ and Diffusion Coefficient for Tritium in $LiAlO_2$ Powders

(Marker # 8 in Table A-2)

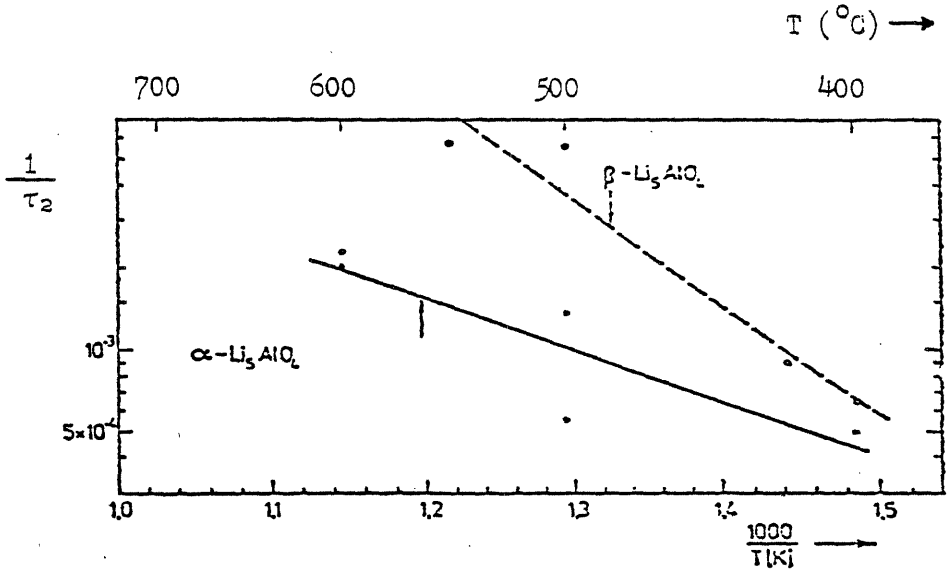

Figure A-11

Temperature Dependence of Reciprocal Time Constant $1/\tau_2$ for Tritium Release from α- and β- Li_5AlO_4

(Marker #9 in Table A-2)

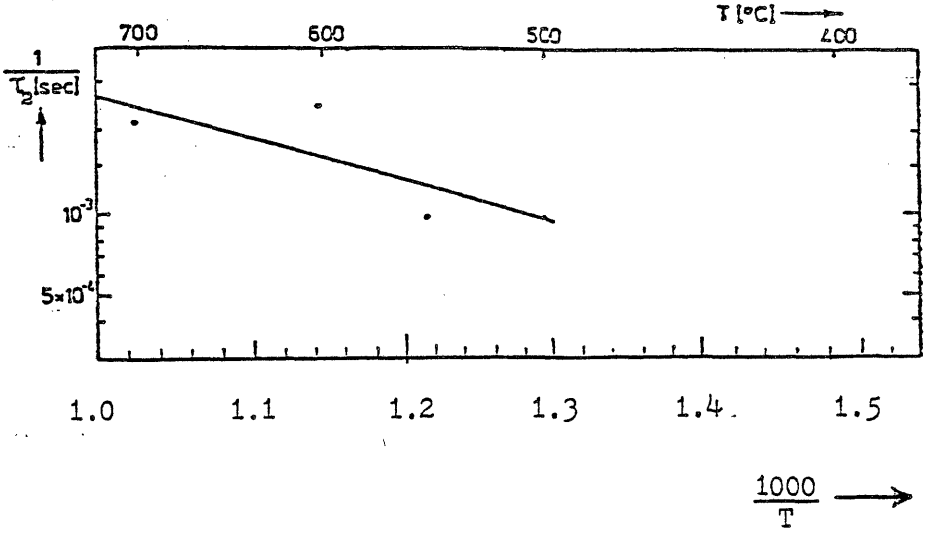

Figure A-12

Temperature Dependence of Reciprocal Time Constant $1/\tau_2$ for Tritium Release from Li_2O Powders

(Marker #10 in Table A-2)

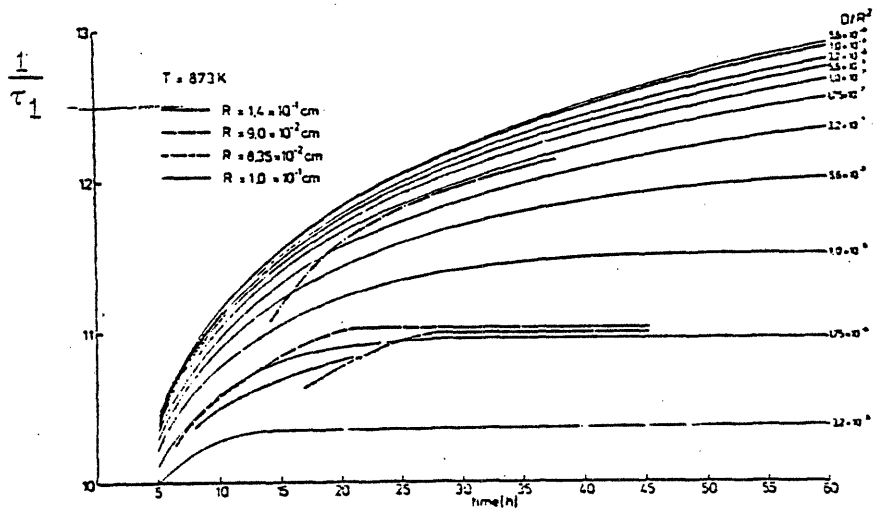

Figure A-13

Reciprocal Time Constant $1/\tau_1$ vs. Time for

β- Li_5AlO_4 melts

(Marker #11 in Table A-2)

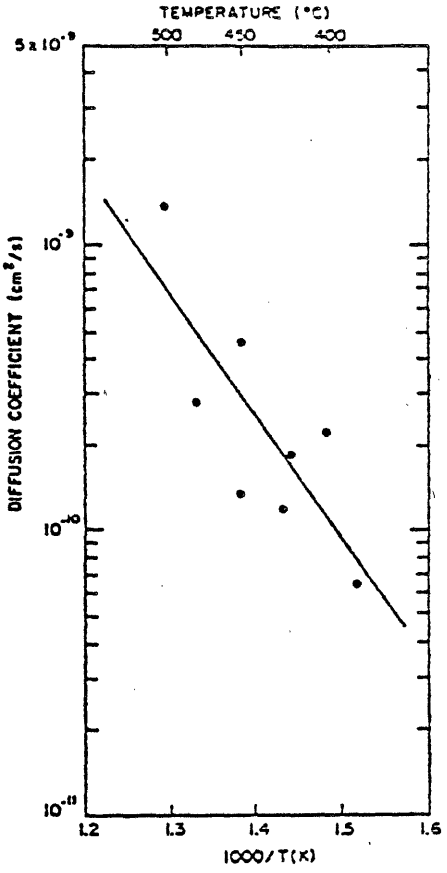

Figure A-14

Temperature Dependence of the Diffusion Coefficient for Tritium in Solid Li-SAP Alloy

(Marker #13 in Table A-2)

Table A-4

Conversion Table for Interpreting Mesh Size Intervals

Used in Tritium Extraction Curves

Mesh Size	Corresponding Particle Diameter (μ)	Average r_p at Mesh Midpoint (cm)
5 - 10	1500 - 2940	1.11×10^{-1}
10 - 20	750 - 1470	5.55×10^{-2}
20 - 30	500 - 735	3.08×10^{-2}
20 - 40	375 - 735	2.78×10^{-2}
70 - 100	150 - 210	9.0×10^{-3}
80 - 120	125 - 180	7.6×10^{-3}

A.3 Sieverts' Constants For Several Lithium Compounds

At thermodynamic equilibrium, the partial pressure of tritium P_{T_2}, in the helium purge gas is related to the atomic concentration of tritium in the solid breeder particles by

$$P_{T_2} = K_s^2 \; X_T^2 \qquad (A.1)$$

where K_s = Sieverts' Constant ($torr^{\frac{1}{2}}$/atomic fraction)
X_T = atom fraction of T in solid

Therefore, the tritium concentration at the pellet surface in equilibrium solution with that in the purge gas can be determined from the Sieverts' Constant for the lithium compound.

A.3.1 Complex Oxides -- $LiAlO_2$, Li_2SiO_3, Li_4SiO_4

The solubility of hydrogen has been measured for one oxide, ZnO, over a range of temperatures and pressures, and was found to be quite small[24]. The data are approximately represented by the equation

$$K_s \; (cm^3\text{-}T_2/cm^3 atm^{\frac{1}{2}}) = 2.1 \times 10^6 \exp - \left[\frac{36.7 \text{ kcal/mole}}{R\,T}\right] \qquad (A.2)$$

or,

$$K_s \; (cm^3\text{-}T_2/cm^3 torr^{\frac{1}{2}}) = 7.6 \times 10^4 \exp - \left[\frac{36.7 \text{ kcal/mole}}{R\,T}\right]$$

From chemical considerations, it is predicted that the solubility of hydrogen in an aluminate or silicate should be no greater than that in ZnO, so that Equation (A.2) can be used as a maximum value of K_s for H_2 in $LiAlO_2$, Li_2SiO_3 and Li_4SiO_4.

The problem of relating the Sieverts' Constant for tritium in lithium compounds to that given for hydrogen is addressed here. For a pure lithium system, the decomposition pressures in the two-phase region (Li-H, Li-T) (ref. Figure A-15) are related by:

$$P_{T_2} > P_{D_2} > P_{H_2} \tag{A.3}$$

where

$$\frac{P_{T_2}}{P_{H_2}} \sim 3^{\frac{1}{2}} \tag{A.4}$$

Veleckis et al.[83] have observed that essentially no isotope effects exist for the solubilities of hydrogen and deuterium in lithium. If it is assumed, therefore, that hydrogen and tritium have the same solubility in solid lithium compounds, meaning $C_T^S = C_H^S$ where C^S denotes concentration due to solubility, then[84]:

$$K_{s,T_2} = 3^{-\frac{1}{4}} K_{s,H_2} \tag{A.5}$$

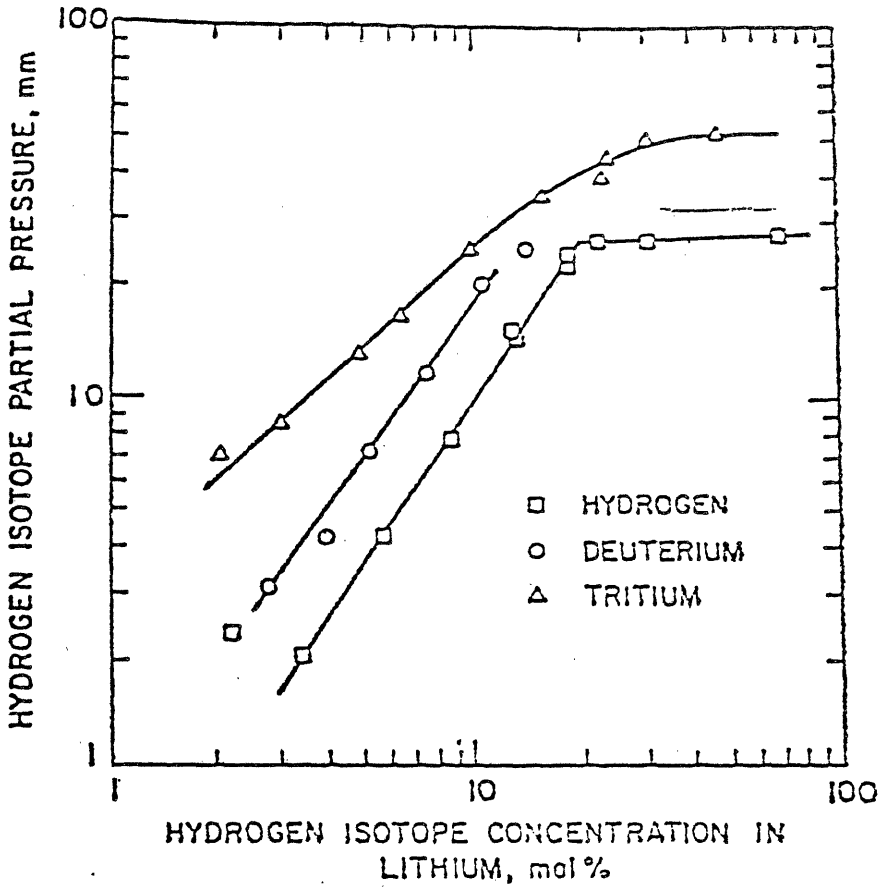

Figure A-15

Isotopic Dependence of the Hydrogen Pressure vs. Composition Curves for the Lithium-Hydrogen System at 700 °C.

(Figure taken from Ref. (85))

A.3.2 Lithium Lead Alloys -- Li_7Pb_2 , LiPb

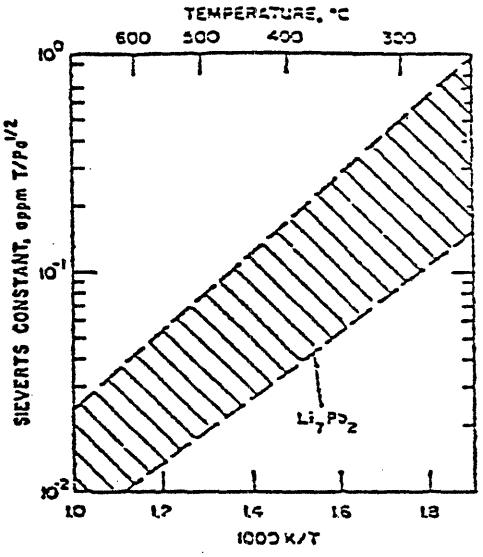

Figure A-16

Sieverts' Constant for Tritium in Li_7Pb_2

(Figure taken from Ref.(25))

A.3.3 Lithium-Aluminum Alloy -- LiAl

Experimental measurements regarding the release of tritium from irradiated LiAl pellets at temperatures from 300 - 600 °C, and concentrations in the range of 1 appm, indicate[24] that the Sieverts' Constant is no larger than 2×10^7 torr/(atom fraction)^2.

$$\therefore\ K_s^2\ (500^\circ C) \leq\ 2 \times 10^7\ \ \frac{\text{torr}}{(\text{atom fraction})^2} \qquad (A.6)$$

Wiswall and Wirsing[23] give a value for the Sieverts' Constant for T_2 in LiAl of:

$$K_s\ (500^\circ C)\ = 1.22 \times 10^4\ \ \frac{\text{torr}^{\frac{1}{2}}}{\text{atom fraction}} \qquad (A.7)$$

Sieverts' Constant for T_2 in LiAl at 500 °C was also measured by those at ORNL[87]. An average value for K_s is quoted here:

$$K_s\ (500^\circ C)\ = 1.9\ (\pm 0.1) \times 10^4\ \ \frac{\text{torr}^{\frac{1}{2}}}{\text{atom fraction}} \qquad (A.8)$$

An estimate of K_s for the temperature range ~ 380 - 550 °C, is given in the following Figure A-18. The solubility of hydrogen in lithium and aluminum is shown for comparison. A similar comparison is given in Figure A-19, where the range of tritium solubility in LiAl(solid) is more well-defined[88]. The Sieverts' Constant for LiAl can also be estimated from available data on Li and LiAl:[34]

$$K_s^2\big|_{T_2 \text{ in LiAl}} = K_s^2\big|_{T_2 \text{ in Li}}\ \ \frac{P_{H_2}\big|^*_{\text{LiAl}}}{P_{H_2}\big|^*_{\text{Li}}} \qquad (A.9)$$

where $P_{H_2}\big|^*_{\text{LiAl}}$ and $P_{H_2}\big|^*_{\text{Li}}$ are the plateau pressures (in two phase region) for H_2 in LiAl and Li. $K_s\big|_{T_2 \text{ in Li}}$ is given as a function of temperature by Maroni[85] in Table A-5. The plateau pressure for hydrogen in lithium ($P_{H_2}\big|^*_{\text{Li}}$) is also presented by Maroni[85] in Figure A-20.

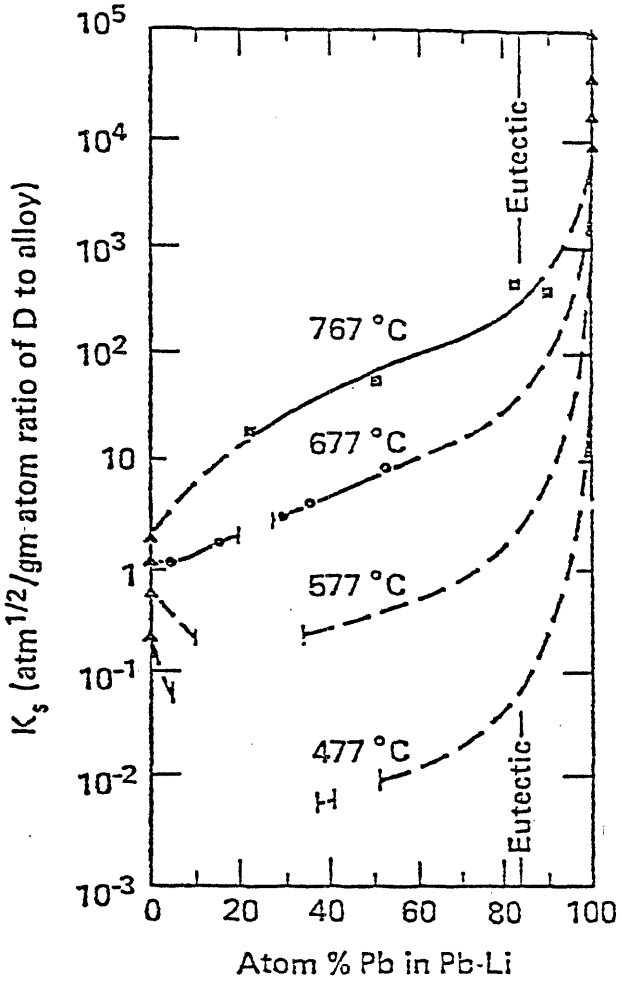

Figure A-17

Sieverts' Constant for Deuterium in

Li - Pb

(Figure taken from Ref.(86))

Table A-5

Estimated Sieverts' Constants for Dilute Solutions of Tritium in Lithium

Temperature (°C)	Sieverts' Constant ($torr^{\frac{1}{2}}$/atom fraction)
1000	243
900	157
800	93
700	51

The equilibrium H_2 pressure over 2-phase mixtures of the system β-LiAl-H_2 is quoted from Owen et al.:[89]

$$\ln P \text{ (torr)} = 20.46 - \frac{11,600}{T\ (^{\circ}K)} \qquad (A.10)$$

A sample of Owen's data for $P_{H_2}\big|^{*}_{LiAl}$ is given in Figure A-21. Combining the data of Maroni with that of Aronson and Salzano[91], the three variables on the right hand side of Equation (A.9) are plotted together in Figure A-22. $K_s\big|_{T_2 \text{ in LiAl}}$ can then be calculated according to Equation (A.9).

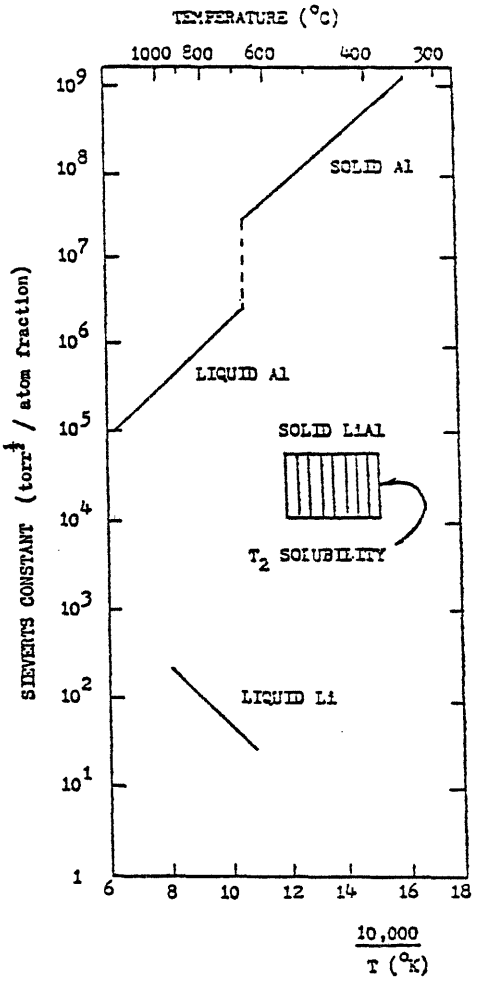

Figure A-18

Sieverts' Constant for Tritium in LiAl, for Comparison with the Hydrogen Solubility in Aluminum and Lithium

(Figure taken from Ref.(87))

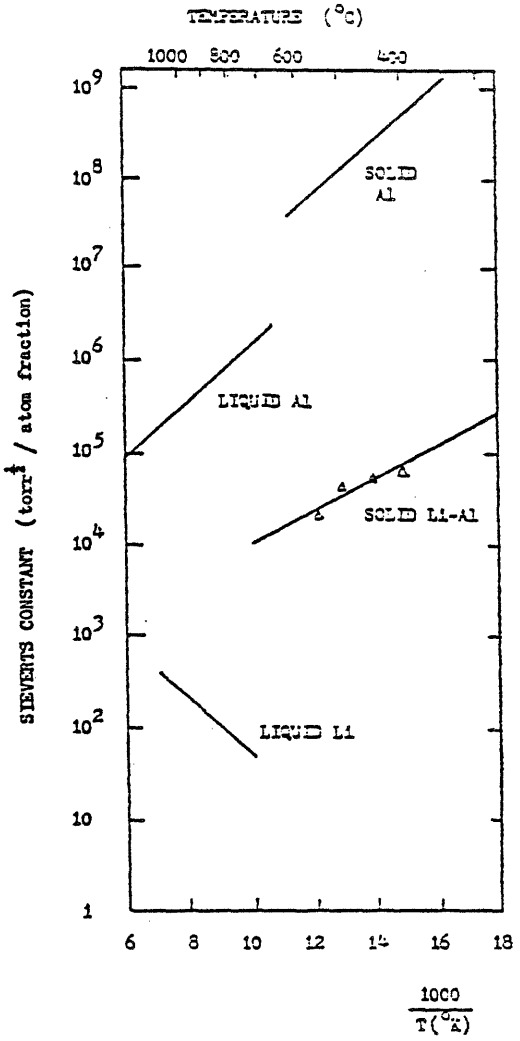

Figure A-19

A Comparison of the Sieverts'

Constants for Aluminum, Lithium and Li-Al Alloy

(Figure taken from Ref. (88))

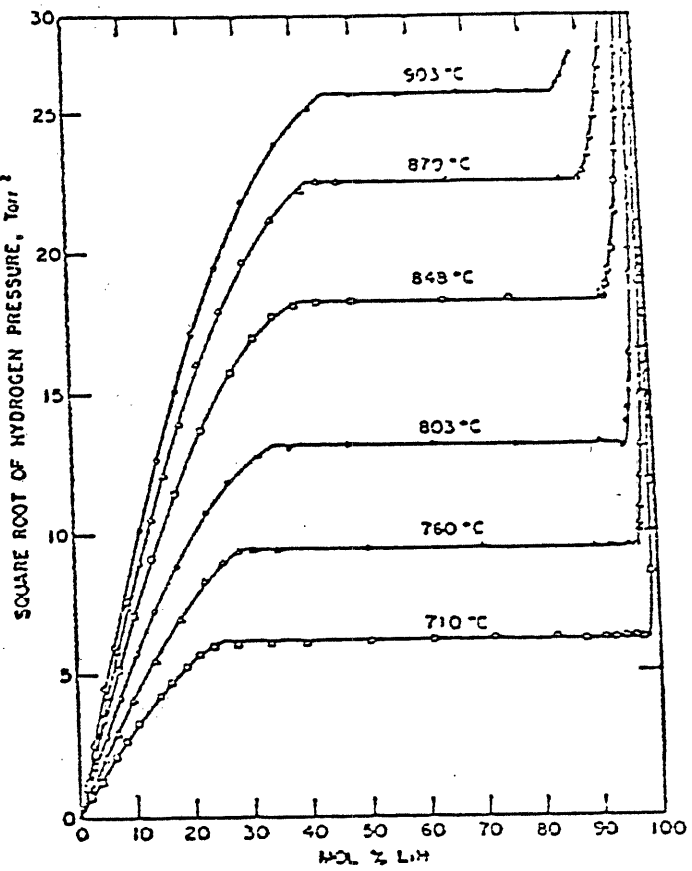

Figure A-20

$P^{*}_{H_2\ Li}$ -- Plateau Pressure of Hydrogen in the Lithium-Hydrogen System, at Various Temperatures

(Figure taken from Ref. (85))

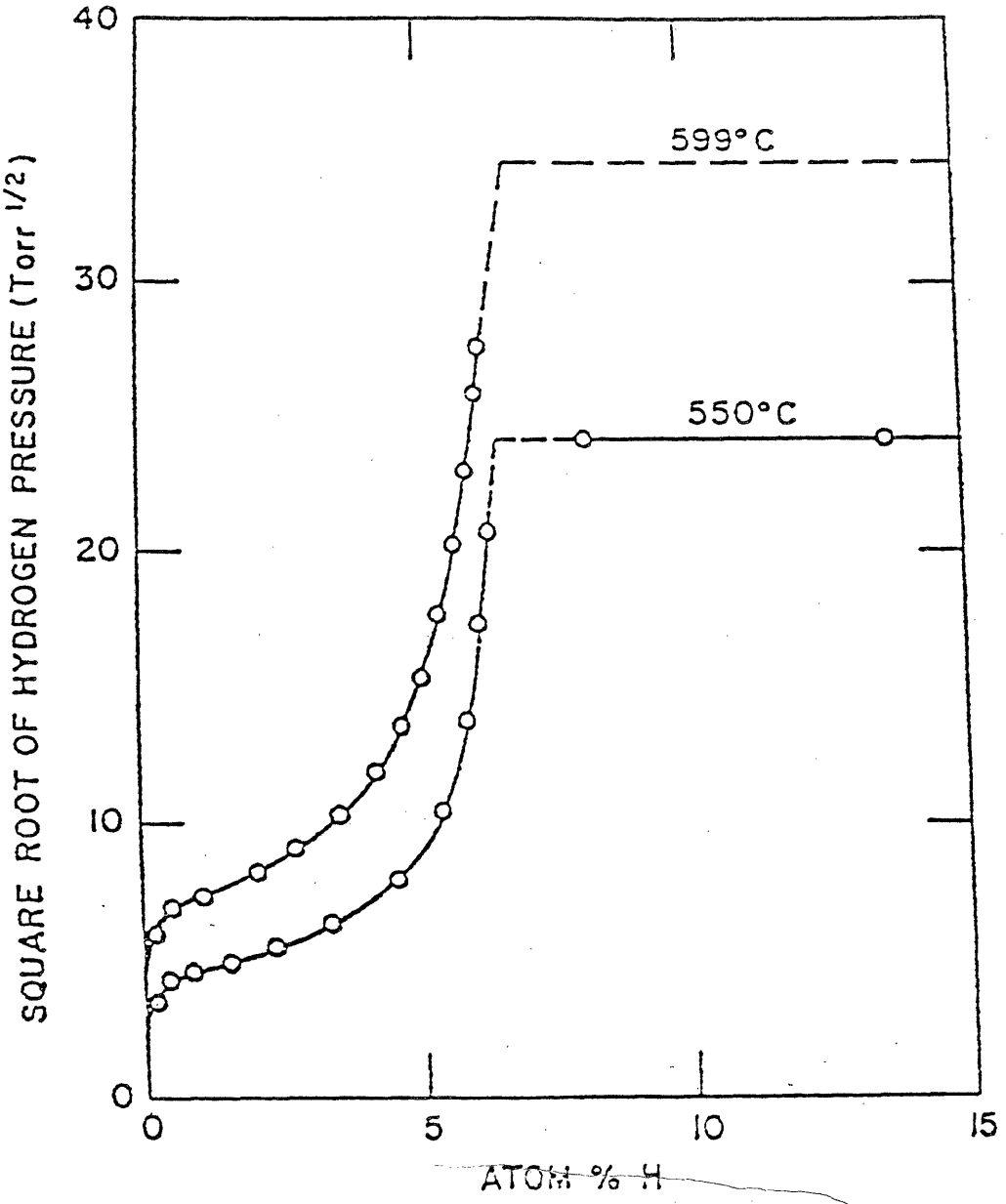

Figure A-21

$P^{*}_{H_2,\ LiAl}$ -- Plateau Pressure of Hydrogen in the LiAl-Hydrogen System, at Two Temperatures

(Figure taken from Ref. (89))

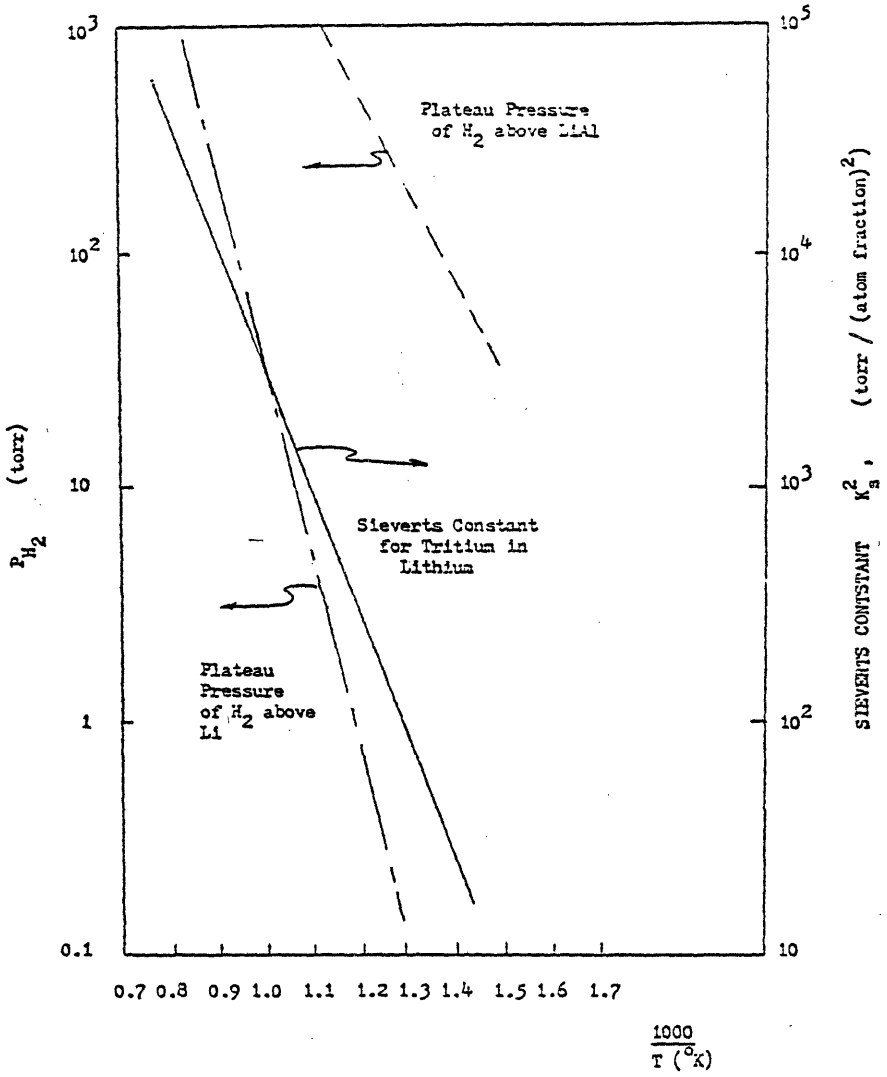

Figure A-22

Sieverts' Constant for Tritium in Lithium

(Figure taken from Ref. (13))

APPENDIX B PHYSICAL PROPERTY DATA: METALS

B.1 Tritium Diffusion Coefficients for Several Metals: Experimentally-Determined

Table B-1

Tritium Diffusion Coefficients for Metals:

$$D = D^{o} \exp - (Q_d/RT)$$

Metal	Condition	Temperature Range (°C)	D^{o} (cm²/sec)	Q_d (cal/mole)	Reference
Aluminum Oxide (Al_2O_3)	single crystal	600-1000	$3.26\ ^{+9.86}_{-1.08} \times 10^{-2}$	57200 ± 2400	(91)
	sintered	600- 900	$7.35\ ^{+0.247}_{-2.19} \times 10^{-2}$	43800 ± 2500	(91)
	powder	250- 600	$3.23\ ^{+3.36}_{-3.10} \times 10^{-8}$	23300 ± 3000	(91)
	BEST FIT	300-1000	6.4×10^{-5}	31500	(91)
Copper (Cu)	- - - - - - -	200- 440	$*1.06 \pm 0.05 \times 10^{-2}$	9180 ± 60	(92)
Iron (Fe)	- - - - - - -	70- 402	$*3.1 \times 10^{-4}$	1100	(93)
Inconel 625	- - - - - - -	- - - -	7.6×10^{-3}	11500	(94)
Molybdenum (Mo)	- - - - - - -	- - - -	$*2 \times 10^{-2}$	14700	(36)
	(1 atm)	466- 850	$*6.31 \times 10^{-4}$	5900	(95)
		850-1750	$*4.8 \times 10^{-3}$	9000	(96)
	(1 atm)	1280-1700	$*5.9 \times 10^{-2}$	14700	(95)
Nickel (Ni)	(1 atm)	200- 420	$*5.2 \times 10^{-3}$	9600	(96)
Niobium (Nb)	- - - - - - -	- - - -	$*1.8 \times 10^{-2}$	10000	(36)
	- - - - - - -	- - - -	$*2.15 \times 10^{-2}$	9370 ± 600	(97)
Palladium (α-Pd)	10^{-7}-10^{-5} atm	25- 440	$*4.7 \times 10^{-3}$	5740	(96)
	0.04-0.66 atm	260- 640	$*2.9 \times 10^{-3}$	5260	(96)
Stainless Steel (SS) 304-SS	- - - - - - -	- - - -	1.8×10^{-2}	14000	(42)
	- - - - - - -	- - - -	2.3×10^{-6}	8153	(98)
	(1 atm)	100- 300	1.24×10^{-2}	13600	(96)
	- - - - - - -	- - - -	1.8×10^{-2}	14000	(99)
304L	- - - - - - -	- - - -	$*4.7 \times 10^{-3}$	12900	(94)
316-SS	- - - - - - -	20- 222	$1.80\ ^{+1.1}_{-0.7} \times 10^{-2}$	14000 ± 230	(100)
347-SS	- - - - - - -	550- 700	1.29×10^{-2}	14020	(101)

Table 3-1

(continued)

Tantalum (Ta)	- - - - - - -	- - - -	$^{*}4.4 \pm 0.4$	$\times 10^{-4}$	3210 ± 100	(102)
Tungsten (W)	- - - - - - -	- - - -	$^{*}4.1$	$\times 10^{-3}$	9000	(36)
	- - - - - - -	- - - -	$^{*}2.4$	$\times 10^{-3}$	9000	(99)
Vanadium (V)	- - - - - - -	- - - -	$^{*}4.4 \pm 1.5$	$\times 10^{-4}$	1350 ± 160	(103)
	- - - - - - -	- - - -	$^{*}3.5 \pm 1$	$\times 10^{-4}$	1150 ± 100	(104)
	- - - - - - -	- - - -	$^{*}2.4$	$\times 10^{-3}$	1790	(105)
Zircaloy-2	- - - - - - -	-78- 204	$2.1 \, ^{+15}_{-1.8}$	$\times 10^{-4}$	8500 ± 230	(100)
Zirconium (α-Zr)	- - - - - - -	149- 240	1.53	$\times 10^{-3}$	9070	(106)

Note: * values for hydrogen diffusion in metals given
$\therefore$ Multiply by a factor of $3^{\frac{1}{2}}$ for D of T_2 in metal
to recover isotopic dependence

B.2 Tritium Diffusion Coefficients for Several Alloys: Determined from the Relation $D = K_p/K_s$

Table B-2

Tritium Diffusion Coefficients for Metals:

$$D = K_p/K_s^{\,a}$$

Metal	Temperature Range (°C)	D^o (cm²/sec)	Q_d (cal/mole)	Reference
Croloy (2¼Cr,1Mo)	- - - -	*3.05×10^{-3}	9810	K_s^b: (94) K_p: (53)
	400-500	*1.88×10^{-3}	37740	K_s^b: (94) K_p: (84)
	350	1.75×10^{-6}		K_s^b: (94) K_p: (8)
Incoloy 800	- - - -	*2.36×10^{-3}	14270	K_s: (4) K_p: (4)
	- - - -	1.03×10^{-2}	17851	K_s: (4) K_p: (61)
	- - - -	8.57×10^{-4}	14290	K_s: (4) K_p: (53)
Inconel 600	- - - -	2.32×10^{-3}	13970	K_s^c: (4) K_p: (95)
PE-16	- - - -	*2.36×10^{-4}	14270	K_s: (4) K_p: (4)

Note: a - D = diffusivity (cm²/sec)
K_p = permeability (cm³(STP)/cm-sec-torr$^{\frac{1}{2}}$)
K_s = solubility (cm³(STP)/cm³-torr$^{\frac{1}{2}}$)

b - for 304L-SS

c - for Incoloy 800

* values for hydrogen diffusion in metals given

∴ Multiply a factor of $3^{\frac{1}{2}}$ for D of tritium in metal to recover isotopic dependence

APPENDIX C PHYSICAL PROPERTY DATA: HELIUM

C.1 Thermodynamic Properties of Gaseous Helium

For the temperature range 400 - 1600 ^{o}K and the pressure range 0.1 to 10.0 MPa[107]:

$$\rho_{He}\ (g/cm^3) = 4.80 \times 10^{-7}\ \frac{P_{He}}{T_{He}} \qquad (C.1)$$

$$\mu_{He}\ (g/cmsec) = 8.33 \times 10^{-5} + 4.16 \times 10^{-7}\ T_{He} - 5.30 \times 10^{-11}\ T_{He}^2 \qquad (C.2)$$

$$C_{p_{He}}\ (J/g^{o}K) = 5.190 \times 10^{3} \qquad (C.3)$$

$$\nu_{He}\ (cm^2/sec) = \frac{1.735 \times 10^{2} T_{He} + 0.8667\ T_{He}^2 - 1.104 \times 10^{-4}\ T_{He}^3}{P_{He}} \qquad (C.4)$$

Note: For the above four equations the units for temperature and pressure are:

$$[T_{He}] = {}^{o}K \quad \text{and} \quad [P_{He}] = Pa$$

C.2 Diffusion Coefficient for Tritium in Helium

The mass diffusivity of tritium gas (T_2) in helium gas, D_G, is given by an optimized Gilliland-type equation:[108]

$$D_G\ (cm^2/sec) = \frac{10^{-3}\ \left[T\ (^oK)\right]^{1.75}\left[\frac{1}{M_1}+\frac{1}{M_2}\right]^{\frac{1}{2}}}{P\ (atm)\ \left[(\Sigma v_1)^{\frac{1}{3}}+(\Sigma v_2)^{\frac{1}{3}}\right]^2} \qquad (C.5)$$

where: M = molecular weight

$M_1 = M_{T_2} = 3.0227672$

$M_2 = M_{He} = 4.0026033$

Σv = diffusion volume

$\Sigma v_1 = \Sigma v|_{T_2} \cong 6.40$

$\Sigma v_2 = \Sigma v|_{He} \cong 2.88$

$$\therefore \quad D_{T_2 \text{ in } He}\ (cm^2/sec) \cong 7.0856 \times 10^{-5}\ \frac{\left[T_{He}(^oK)\right]^{1.75}}{P_{He}(atm)} \qquad (C.6)$$

$$\cong 7.7054 \times 10^{-10}\ \frac{\left[T_{He}(^oK)\right]^{1.75}}{P_{He}(Pa)} \qquad (C.7)$$

APPENDIX D EQUILIBRIUM CONSTANT K_{T_2O} (T)

The addition of oxygen to a high-pressure helium system which includes a trace of tritium gas, T_2, will necessarily involve the following reaction:

$$T_2 + \tfrac{1}{2}\, O_2 \rightleftharpoons T_2O \qquad (D.\ )$$

The equilibrium constant for this reaction, K_{T_2O}, is defined by:

$$K_{T_2O} \equiv \frac{P\,(T_2O)}{P\,(T_2)\;\; P^{\frac{1}{2}}\,(O_2)} \qquad (D.2)$$

Although the exact value for K_{T_2O} is unavailable for this report, it is assumed that it can be approximated by the value of the equilibrium constant for the following similiar reaction:

$$H_2 + \tfrac{1}{2}\, O_2 \rightleftharpoons H_2O \qquad (D.3)$$

whose equilibrium constant K_{H_2O} is defined as:

$$K_{H_2O} \equiv \frac{P\,(H_2O)}{P\,(H_2)\;\; P^{\frac{1}{2}}\,(O_2)} \qquad (D.4)$$

If isotope and pressure effects are negigible, then K_{T_2O} is approximately equal to K_{H_2O}, and is then only a function of temperature. A temperature-dependent expression for K_{H_2O} is given by Maroni[71]:

$$\ln\left[K_{T_2O}\right] \sim \ln\left[K_{H_2O}\right] = -3.7675 + \frac{30{,}428}{T(^{\circ}F)} \qquad (D.5)$$

where K_{T_2O} is in $\text{torr}^{\frac{1}{2}}$.

APPENDIX E SENSITIVITY STUDIES FOR STEADY-STATE APPLICATION OF PERMEATION MODEL

Given a function of the form

$$F = fn\,(a,b,c) \tag{E.1}$$

The ln can be taken of both sides:

$$\ln F = \alpha_a \ln a + \alpha_b \ln b + \alpha_c \ln c \tag{E.2}$$

Recognizing that $\frac{dF}{F} \equiv \ln F$, this can be reduced to the following:

$$\frac{dF}{F} = \alpha_a \frac{da}{a} + \alpha_b \frac{db}{b} + \alpha_c \frac{dc}{c} \tag{E.3}$$

The coefficients α are called the sensitivity coefficients because they relate a nondimensional change in one variable (keeping all other variables the same) to a percentage change in the function. The sensitivity coefficient α_a^F shall be read "the sensitivity of F to the variable a". Furthermore, if the variable a is itself a function of other variables such that

$$\frac{da}{a} = \alpha_x \frac{dx}{x} + \alpha_y \frac{dy}{y} + \alpha_z \frac{dz}{z} \tag{E.4}$$

Then the total sensitivity of the original function F to the specific variable x, will necessarily be:

$$\alpha_x^F = \alpha_a^F \; \alpha_x^a \tag{E.5}$$

It is possible to examine analytically the effect of a particular choice of a system parameter on certain steady-state tritium concentration values. Based on the permeation model presented in Section 2.4, the steady-state values for the tritium concentration in the purge gas

system and the helium coolant loop, and the tritium losses through the heat exchanger: $C_{pg}(SS)$, $C_c(SS)$ and $J_{HXL}(SS)$ respectively, are given below:

$$C_{pg}(SS) = \frac{S}{Q_{pg}} \tag{E.6}$$

$$C_c(SS) = \frac{\tau_c}{V_c R_{pgc}} C_{pg}(SS) = \frac{S}{Q_{pg}} \frac{R_{CL}}{R_{pgc} + R_{CL}} \tag{E.7}$$

$$J_{HXL}(SS) = \frac{1}{R_{HXL}} C_c(SS) = \frac{S}{Q_{pg}} \frac{R_{CL}}{R_{HXL}} \frac{R_{CL}}{R_{pgc} + R_{CL}} \tag{E.8}$$

Since the steady-state value for the purge gas concentration depends on only two variables, the sensitivity analysis is simple.

$$\ln C_{pg}(SS) = \ln S - \ln Q_{pg}$$

or,

$$\frac{d\, C_{pg}(SS)}{C_{pg}} = \frac{dS}{S} - \frac{dQ_{pg}}{Q_{pg}} \tag{E.9}$$

It is clear that for this case, the sensitivity coefficients are:

$$\alpha_S^{C_{pg}(SS)} = 1 \tag{E.10A}$$

$$\alpha_{Q_{pg}}^{C_{pg}(SS)} = -1 \tag{E.10B}$$

meaning an x % drop in helium purge gas volumetric flow rate would cause an x % increase in the purge gas tritium concentration at steady-state, for example.

Similiar sensitivity analyses for the steady-state coolant concentration and tritium losses from the heat exchanger are complicated by their functional dependence on additional system variables. Taking the ln of Equations (E.7) and (E.8),

$$\ln C_c(SS) = \ln S - \ln Q_{pg} + \ln R_{CL} - \ln (R_{pgc} + R_{CL}) \tag{E.11}$$

$$\ln J_{HXL}(SS) = \ln S - \ln Q_{pg} + \ln R_{CL} - \ln R_{HXL} - \ln (R_{pgc} + R_{CL}) \tag{E.12}$$

or,

$$\frac{dC_c(SS)}{C_c(SS)} = \frac{dS}{S} - \frac{dQ_{pg}}{Q_{pg}} + \frac{dR_{CL}}{R_{CL}} - \frac{d(R_{pgc} + R_{CL})}{R_{pgc} + R_{CL}} \tag{E.13}$$

$$\frac{dJ_{HXL}(SS)}{J_{HXL}(SS)} = \frac{dS}{S} - \frac{dQ_{pg}}{Q_{pg}} + \frac{dR_{CL}}{R_{CL}} - \frac{dR_{HXL}}{R_{HXL}} - \frac{d(R_{pgc} + R_{CL})}{R_{pgc} + R_{CL}} \tag{E.14}$$

Since $d(R_{pgc} + R_{CL}) = dR_{pgc} + dR_{CL}$, the above expressions become:

$$\frac{dC_c(SS)}{C_c(SS)} = \frac{dS}{S} - \frac{dQ_{pg}}{Q_{pg}} + \left[\frac{1}{R_{CL}} - \frac{1}{R_{pgc} + R_{CL}}\right] dR_{CL} - \frac{dR_{pgc}}{R_{pgc} + R_{CL}} \tag{E.15}$$

and,

$$\frac{dJ_{HXL}(SS)}{J_{HXL}(SS)} = \frac{dS}{S} - \frac{dQ_{pg}}{Q_{pg}} + \left[\frac{1}{R_{CL}} - \frac{1}{R_{pgc} + R_{CL}}\right] dR_{CL} - \frac{dR_{HXL}}{R_{HXL}} - \frac{dR_{pgc}}{R_{pgc} + R_{CL}} \tag{E.16}$$

The resistances R_{HXL} and R_{CL} are related by

$$R_{CL} = R_{HPL} + R_{HXL} + R_{CPL} \tag{E.17}$$

$$dR_{CL} = d(R_{HPL} + R_{HXL} + R_{CPL}) = dR_{HPL} + dR_{HXL} + dR_{CPL} \tag{E.18}$$

Substitution of this relationship into Equations (E.15) and (E.16) yields the expanded form for the sensitivity equations:

$$\begin{aligned}\frac{dC_c(SS)}{C_c(SS)} = {} & \frac{dS}{S} - \frac{dQ_{pg}}{Q_{pg}} + \frac{R_{HPL}}{R_{CL}}\left[1 - \frac{R_{CL}}{R_{pgc} + R_{CL}}\right]\frac{dR_{HPL}}{R_{HPL}} \\ & - \frac{R_{HXL}}{R_{CL}}\left[1 - \frac{R_{CL}}{R_{pgc} + R_{CL}}\right]\frac{dR_{HXL}}{R_{HXL}} \\ & + \frac{R_{CPL}}{R_{CL}}\left[1 - \frac{R_{CL}}{R_{pgc} + R_{CL}}\right]\frac{dR_{CPL}}{R_{CPL}} \\ & - \frac{R_{pgc}}{R_{pgc} + R_{CL}}\frac{dR_{pgc}}{R_{pgc}}\end{aligned} \tag{E.19}$$

$$\begin{aligned}\frac{dJ_{HXL}(SS)}{J_{HXL}(SS)} = {} & \frac{dS}{S} - \frac{dQ_{pg}}{Q_{pg}} + \frac{R_{HPL}}{R_{CL}}\left[1 - \frac{R_{CL}}{R_{pgc} + R_{CL}}\right]\frac{dR_{HPL}}{R_{HPL}} \\ & + \left[\frac{R_{HXL}}{R_{CL}} - \frac{R_{pgc}}{R_{pgc} + R_{CL}} - 1\right]\frac{dR_{HXL}}{R_{HXL}} \\ & + \frac{R_{CPL}}{R_{CL}}\left[1 - \frac{R_{CL}}{R_{pgc} + R_{CL}}\right]\frac{dR_{CPL}}{R_{CPL}} \\ & - \frac{R_{pgc}}{R_{pgc} + R_{CL}}\frac{dR_{pgc}}{R_{pgc}}\end{aligned} \tag{E.20}$$

The sensitivity coefficients for the steady-state tritium concentration in the coolant and for the tritium loss out of the heat exchanger are determined from Equations (E.19) and (E.20). These coefficients are tabulated in Table E-1).

The resistances are themselves functions of the system parameters. The definitions of R_{HPL}, R_{HXL}, R_{CPL} and R_{pgc} are taken from Section 2.4, but are repeated here for convenience:

$$R_{HPL} = \frac{1}{A_{HP} h_{HP}} + \frac{x_{HP}}{A_{HP} D_{HP}} \qquad \text{(E.21A)}$$

$$R_{HXL} = \frac{1}{A_{HX} h_{HX}} + \frac{x_{HX}}{A_{HX} D_{HX}} \qquad \text{(E.21B)}$$

$$R_{CPL} = \frac{1}{A_{CP} h_{CP}} + \frac{x_{CP}}{A_{CP} D_{CP}} \qquad \text{(E.21C)}$$

$$R_{pgc} = \frac{1}{A_m h_{pg}} + \frac{x_m}{A_m D_m} + \frac{1}{A_m h_B} \qquad \text{(E.21D)}$$

These resistances for the coolant loop are of the form:

$$R_L = \frac{1}{A h} + \frac{x}{A D} \qquad \text{(E.22)}$$

Equation (E.22) can be used for any of the Equations (E.21A-C) with the understanding of using the proper subscripts. Rearranging Equation (E.22) and taking its ln:

$$R_L = \frac{1}{A} \left[\frac{D + xh}{h D} \right]$$

or,

$$\ln R_L = - \ln A - \ln h - \ln D + \ln (D + xh) \qquad \text{(E.23)}$$

Table E-1

Sensitivity Coefficients, α
for $C_c(SS)$ and $J_{HXL}(SS)$

	$C_c(SS)$	$J_{HXL}(SS)$
α_S^-	1	1
$\alpha_{Q_{pg}}^-$	- 1	- 1
$\alpha_{R_{HPL}}^-$	$\frac{R_{HPL}}{R_{CL}}\left[1 - \frac{R_{CL}}{R_{pgc} + R_{CL}}\right]$	$\frac{R_{HPL}}{R_{CL}}\left[1 - \frac{R_{CL}}{R_{pgc} + R_{CL}}\right]$
$\alpha_{R_{HXL}}^-$	$\frac{R_{HXL}}{R_{CL}}\left[1 - \frac{R_{CL}}{R_{pgc} + R_{CL}}\right]$	$\frac{R_{HXL}}{R_{CL}} - \frac{R_{pgc}}{R_{pgc} + R_{CL}} - 1$
$\alpha_{R_{CPL}}^-$	$\frac{R_{CPL}}{R_{CL}}\left[1 - \frac{R_{CL}}{R_{pgc} + R_{CL}}\right]$	$\frac{R_{CPL}}{R_{CL}}\left[1 - \frac{R_{CL}}{R_{pgc} + R_{CL}}\right]$
$\alpha_{R_{pgc}}^-$	$\frac{- R_{pgc}}{R_{pgc} + R_{CL}}$	$\frac{- R_{pgc}}{R_{pgc} + R_{CL}}$

Equation (E.23) can be rewritten:

$$\frac{dR_L}{R_L} = -\frac{dA}{A} - \frac{dh}{h} - \frac{dD}{D} + \frac{d(D + xh)}{D + xh} \qquad (E.24)$$

The total derivative of d(D + xh) can be written:

$$d(D + xh) = \frac{\partial(\ )}{\partial D} dD + \frac{\partial(\ )}{\partial x} dx + \frac{\partial(\ )}{\partial h} dh$$

$$= dD + h\,dx + x\,dh \qquad (E.25)$$

Rewriting Equation (E.24) with the help of Equation (E.25), one obtains

$$\frac{dR_L}{R_L} = -\frac{dA}{A} - \left[1 - \frac{xh}{D + xh}\right]\frac{dh}{h} - \left[1 - \frac{D}{D + xh}\right]\frac{dD}{D}$$

$$+ \left[\frac{xh}{D + xh}\right]\frac{dx}{x} \qquad (E.26)$$

Rearranging Equation (E.21D) and taking its ln:

$$R_{pgc} = \frac{1}{A_m}\left[\frac{D_m h_B + h_{pg} x_m h_B + h_{pg} D_m}{h_{pg} D_m h_B}\right]$$

then,

$$\ln R_{pgc} = -\ln A_m - \ln h_{pg} - \ln D_m - \ln h_B$$

$$+ \ln\left[D_m h_B + h_{pg} x_m h_B + h_{pg} D_m\right]$$

or,

$$\frac{dR_{pgc}}{R_{pgc}} = -\frac{dA_m}{A_m} - \frac{dh_{pg}}{h_{pg}} - \frac{dD_m}{D_m} - \frac{dh_B}{h_B} + \frac{d\left[D_m h_B + h_{pg} x_m h_B + h_{pg} D_m\right]}{D_m h_B + h_{pg} x_m h_B + h_{pg} D_m} \qquad (E.27)$$

The total derivative of $d(D_m h_B + h_{pg} x_m h_B + h_{pg} D_m)$ can be written

$$d(\quad) = \frac{\partial(\quad)}{\partial D_m} dD_m + \frac{\partial(\quad)}{\partial h_{pg}} dh_{pg} + \frac{\partial(\quad)}{\partial h_B} dh_B + \frac{\partial(\quad)}{\partial x_m} dx_m$$

$$= (h_{pg}+h_B)\, dD_m + (D_m+x_m h_B)\, dh_{pg} + (D_m+x_m h_{pg})\, dh_B + (h_{pg} h_B)\, dx_m \qquad (E.28)$$

Equation (E.27) can then be written:

$$\frac{dR_{pgc}}{R_{pgc}} = -\frac{dA_m}{A_m} - \left[1 - \frac{D_m(h_{pg}+h_B)}{D_m h_B + h_{pg} x_m h_B + h_{pg} D_m}\right] \frac{dh_{pg}}{h_{pg}}$$

$$- \left[1 - \frac{D_m(h_{pg}+h_B)}{D_m h_B + h_{pg} x_m h_B + h_{pg} D_m}\right] \frac{dD_m}{D_m}$$

$$- \left[1 - \frac{h_B(D_m+x_m h_{pg})}{D_m h_B + h_{pg} x_m h_B + h_{pg} D_m}\right] \frac{dh_B}{h_B}$$

$$+ \frac{x_m h_{pg} h_B}{D_m h_B + h_{pg} x_m h_B + h_{pg} D_m} \frac{dx_m}{x_m} \qquad (E.29)$$

Sensitivity coefficients for all resistances, R_L (R_{HPL}, R_{HXL}, R_{CPL}) and R_{pgc}, with proper attention to subscript, are given in Table E-2. The results from Tables E-1 and E-2 can be used to give the overall sensitivity coefficients, as outlined next in Table E-3.

Table E-2

Sensitivity Coefficients, α, for R_L and R_{pgc}

	R_L	R_{pgc}
α_A^-	-1	-1
α_h^-	$\frac{xh}{D + xh} - 1$	N.A.
α_D^-	$\frac{D}{D + xh} - 1$	$\frac{D\,(h_{pg} + h_B)}{Dh_B + h_{pg}xh_B + h_{pg}D} - 1$
α_x^-	$\frac{xh}{D + xh}$	$\frac{xh_{pg}h_B}{Dh_B + h_{pg}xh_B + h_{pg}D}$
$\alpha_{h_{pg}}^-$	N.A.	$\frac{h_{pg}\,(D + xh_B)}{Dh_B + h_{pg}xh_B + h_{pg}D} - 1$
$\alpha_{h_B}^-$	N.A.	$\frac{h_B\,(D + xh_{pg})}{Dh_B + h_{pg}xh_B + h_{pg}D} - 1$

Note: N.A. = Not applicable

Table E-3

Sensitivity Coefficients of $C_c(SS)$ and $J_{HXL}(SS)$ for the Various System Parameters

System Parameter	Total Sensitivity Coefficients for $C_c(SS)$	Total Sensitivity Coefficients for $J_{HXL}(SS)$
S	$\alpha_S^{C_c}$	$\alpha_S^{J_{HXL}}$
Q_{pg}	$\alpha_{Q_{pg}}^{C_c}$	$\alpha_{Q_{pg}}^{J_{HXL}}$
A_m	$\alpha_{R_{pgc}}^{C_c}\,\alpha_{A_m}^{R_{pgc}}$	$\alpha_{R_{pgc}}^{J_{HXL}}\,\alpha_{A_m}^{R_{pgc}}$
D_m	$\alpha_{R_{pgc}}^{C_c}\,\alpha_{D_m}^{R_{pgc}}$	$\alpha_{R_{pgc}}^{J_{HXL}}\,\alpha_{D_m}^{R_{pgc}}$
x_m	$\alpha_{R_{pgc}}^{C_c}\,\alpha_{x_m}^{R_{pgc}}$	$\alpha_{R_{pgc}}^{J_{HXL}}\,\alpha_{x_m}^{R_{pgc}}$
h_{pg}	$\alpha_{R_{pgc}}^{C_c}\,\alpha_{h_{pg}}^{R_{pgc}}$	$\alpha_{R_{pgc}}^{J_{HXL}}\,\alpha_{h_{pg}}^{R_{pgc}}$
h_B	$\alpha_{R_{pgc}}^{C_c}\,\alpha_{h_B}^{R_{pgc}}$	$\alpha_{R_{pgc}}^{J_{HXL}}\,\alpha_{h_B}^{R_{pgc}}$
A_{HP}	$\alpha_{R_{HPL}}^{C_c}\,\alpha_{A_{HP}}^{R_{HPL}}$	$\alpha_{R_{HPL}}^{J_{HXL}}\,\alpha_{A_{HP}}^{R_{HPL}}$
D_{HP}	$\alpha_{R_{HPL}}^{C_c}\,\alpha_{D_{HP}}^{R_{HPL}}$	$\alpha_{R_{HPL}}^{J_{HXL}}\,\alpha_{D_{HP}}^{R_{HPL}}$
x_{HP}	$\alpha_{R_{HPL}}^{C_c}\,\alpha_{x_{HP}}^{R_{HPL}}$	$\alpha_{R_{HPL}}^{J_{HXL}}\,\alpha_{x_{HP}}^{R_{HPL}}$
h_{HP}	$\alpha_{R_{HPL}}^{C_c}\,\alpha_{h_{HP}}^{R_{HPL}}$	$\alpha_{R_{HPL}}^{J_{HXL}}\,\alpha_{h_{HP}}^{R_{HPL}}$
A_{HX}	$\alpha_{R_{HXL}}^{C_c}\,\alpha_{A_{HX}}^{R_{HXL}}$	$\alpha_{R_{HXL}}^{J_{HXL}}\,\alpha_{A_{HX}}^{R_{HXL}}$
D_{HX}	$\alpha_{R_{HXL}}^{C_c}\,\alpha_{D_{HX}}^{R_{HXL}}$	$\alpha_{R_{HXL}}^{J_{HXL}}\,\alpha_{D_{HX}}^{R_{HXL}}$
x_{HX}	$\alpha_{R_{HXL}}^{C_c}\,\alpha_{x_{HX}}^{R_{HXL}}$	$\alpha_{R_{HXL}}^{J_{HXL}}\,\alpha_{x_{HX}}^{R_{HXL}}$
h_{HX}	$\alpha_{R_{HXL}}^{C_c}\,\alpha_{h_{HX}}^{R_{HXL}}$	$\alpha_{R_{HXL}}^{J_{HXL}}\,\alpha_{h_{HX}}^{R_{HXL}}$

Table E-3

(continued)

A_{CP}	$\alpha_{R_{CPL}}^{C_c} \alpha_{A_{CP}}^{R_{CPL}}$	$\alpha_{R_{CPL}}^{J_{HXL}} \alpha_{A_{CP}}^{R_{CPL}}$
D_{CP}	$\alpha_{R_{CPL}}^{C_c} \alpha_{D_{CP}}^{R_{CPL}}$	$\alpha_{R_{CPL}}^{J_{HXL}} \alpha_{D_{CP}}^{R_{CPL}}$
x_{CP}	$\alpha_{R_{CPL}}^{C_c} \alpha_{x_{CP}}^{R_{CPL}}$	$\alpha_{R_{CPL}}^{J_{HXL}} \alpha_{x_{CP}}^{R_{CPL}}$
h_{CP}	$\alpha_{R_{CPL}}^{C_c} \alpha_{h_{CP}}^{R_{CPL}}$	$\alpha_{R_{CPL}}^{J_{HXL}} \alpha_{h_{CP}}^{R_{CPL}}$

APPENDIX F STARFIRE SYSTEM PARAMETERS

The STARFIRE tokamak reactor reference design system parameters, as needed for input to the permeation model developed in Chapter 2, were taken from the Interim Report, Ref. (8). This appendix will include all the necessary parameters that were explicitly specified in Ref. (8). For those values not given in the report, the procedure for determining a "best" value is presented from which the unspecified system parameters were derived.

F.1 Blanket Parameters

STARFIRE-Interim has a continuous-burn plasma at a nominal thermal power rating of 3800 MW_t and an average breeding ratio of 1.05. The blanket breeding material is Li_2O, which breeds tritium at an average rate of 498 gm/day (57.64 Ci/sec) at full power. There are 24 blanket modules with the approximate dimensions: 1 m x 0.6 m x 0.6 m. The total blanket volume would therefore be 8.64×10^6 cm^3. According to their pressurized module design, the approximate volume percentages for the blanket are given below:

Structure (HT-9 Ferritic)	- 14.9 %
Li_2O	- 57.2 %
* Helium coolant and void	- 27.9 %

At an average density of 2.013 gm/cm^3 (see Appendix A, Table A-1), the Li_2O breeder has a total mass of 9.94×10^6 gm, corresponding to the volume percentage given above for Li_2O (i.e., $V_{Li_2O} = 4.94 \times 10^6$ cm^3).

Assuming 90 % of the zone marked * above is helium, then the total volume of helium in the blanket is 2.169×10^6 cm^3. One third of this amount is part of the low pressure (1 atm) helium purge gas system, and the rest of the helium is the high pressure (50 atm) coolant used to cool the entire blanket.

The Li_2O is assumed to be fabricable in 20 μ pellets; with uniform particle size this translates into an average pellet radius of 10 μ

(10^{-3} cm). An average operating temperature of 650 °C was chosen, as it was within the acceptable temperature range suggested by ANL for Li_2O (ref. Table F-1) and was close to the $T_{b,avg}$ (670 °C) specified for the $LiAlO_2$ breeder in the STARFIRE-Final Design Report[17]. The minimum operating temperature due to thermal effects for these solid breeders was determined from Figure F-1 (taken from Ref. (8)) where a maximum allowable inventory of 10 kg was assumed. Using a value of 650 °C for $T_{b,avg}$, an average value for the diffusion coefficient of tritium in Li_2O, D_b, determined from Figure A-1 in Appendix A, is 5×10^{-11} cm²/sec.

The solubility of gaseous tritium in solid Li O was approximated by using the data from Ref. (16). At 800 °K (assumed edge temperature of the Li_2O breeder), a tritium concentration of 1 wppm of tritium in Li_2O is in equilibrium with a T_2O vapor pressure of 10^{-8} torr. At 300 wppm, the T_2O equilibrium pressure is increased to 10^{-3} torr. Assuming the T_2 gas in the helium purge gas stream acts similarly, an equation relating surface concentration to purge gas tritium concentration is deduced:

$$\text{for } Li_2O: \quad \text{wppm} = 299/5 \left[8.017 + \log P_{pg}(\text{torr}) \right] \tag{F.1}$$

The partial pressure of tritium in the purge gas is directly related to the concentration, C_{pg}:

$$P_{pg} = \frac{1/6 \times 10^{-4} \; C_{pg} \; V_{pg} \quad RT_{pg}}{V_{pg}} \tag{F.2}$$

where $1/6 \times 10^{-4} \; C_{pg} V_{pg}$ is the number of gm-moles of T_2 gas in the purge gas. Therefore the surface concentration due to solubility effects, is determined by:

$$C_{sol} \; (\text{Ci/cm}^3) = \text{wppm} \; \frac{\rho_b}{10^2}$$

$$= \frac{\rho_b}{10^2} \frac{299}{5} \left[8.017 + \log \left[\frac{C_{pg} RT_{pg}}{6 \times 10^4} (\text{torr}) \right] \right] \tag{F.3}$$

Table F-1

Temperature Limits for Solid Breeders*

Breeder	Melting Point (°C)	Thermal Effects (°C)		Radiation Effects (°C)	
	T_m	T_{min} (1)	T_{max} (2)	T_{min} (3)	T_{max} (4)
Li_2O	1700	410	1000	460	910
$LiAlO_2$	1610	500	1000	550	850
Li_2SiO_3	1200	420	900	470	610
LiAl	700	300	500	350	380
Li_7Pb_2	726	320	530	370	390

Note: * Table taken from Ref. (8), p. 89.

(1) Set by diffusion-limited tritium inventory considerations (ref. Figure F-1) for the design criterion that the blanket inventory does not exceed 1 kg/GW_t

(2) Thermal sintering

(3) Radiation-induced trapping (factor of 10 degradation in tritium release estimated)

(4) Radiation-enhanced sintering limit relative to the breeder material melting temperature, T_m (0.6 T_m for oxides and 0.67 T_m for other compounds), leading to increased diffusion paths

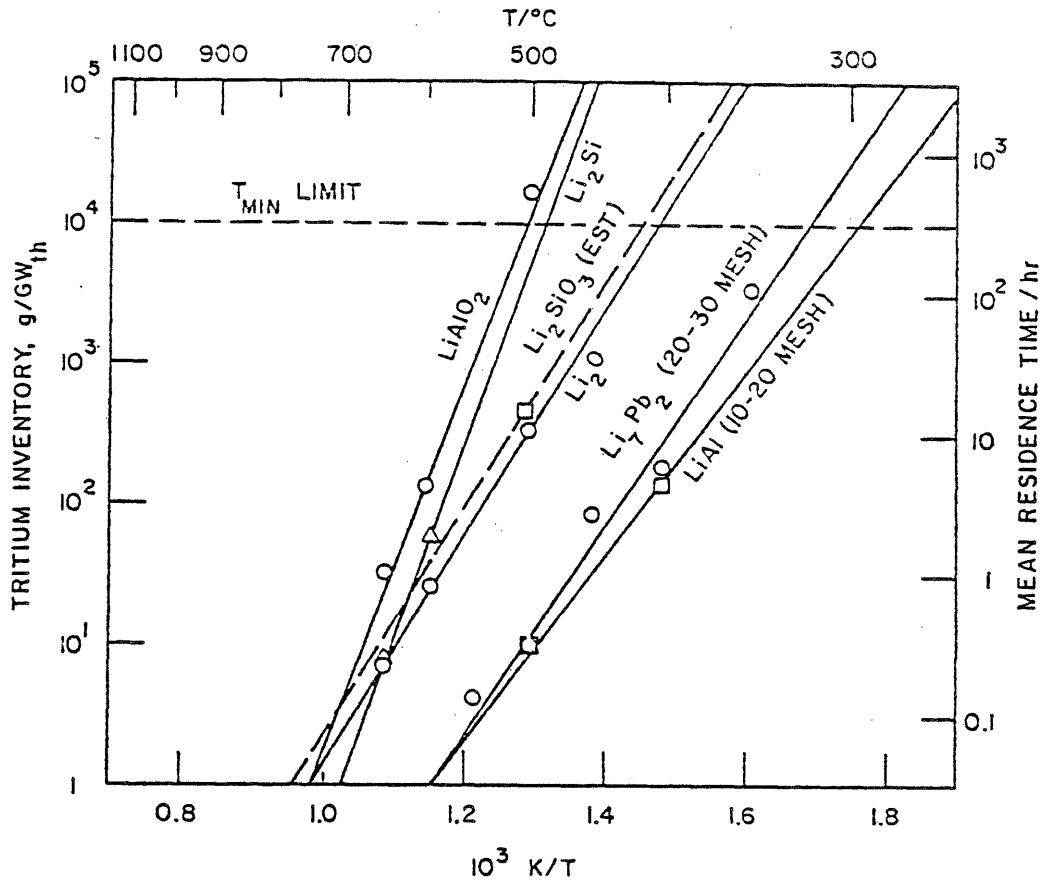

Figure F-1

Predicted Tritium Inventory in Candidate Solid Breeding Materials (20 Mesh) as a Function of Temperature. Solubility Effects not Included.

(Figure taken from Ref. (8))

It is particularly striking that Li_2O has a very high solubility for tritium. From previous experimental work[25], maintaining low ppm levels of tritium in Li_2O may be very difficult to do. The more complex oxides ($LiAlO_3$, Li_2SiO_3) appear to have comparatively low tritium solubilities (ref. Appendix A.3).

The parameters for the purge gas and coolant systems will be discussed next. The length of the coolant tubes in the blanket ranged from 1.1 m to 2.3 m depending on the position in the blanket. An average tube length of 170 cm was used in the ensuing calculations. (For simplicity, the length of the purge gas channel is the same as for a coolant tube.) The inside diameter of the coolant tube ranged from 1.27 cm to 0.8 cm for increasing raidal distance from the first wall. An average coolant tube inside diameter is $\frac{1}{2}$ (1.27 + 0.8) cm $\cong$ 1.035 cm. Since the diameter for the purge gas channel was not specified, the final STARFIRE design value was used: d_{pg} = 0.2 cm. The number of coolant tubes and purge gas channels are respectively:

$$N_c = \frac{V_{c_B}}{\frac{1}{4}\pi\, d_B^2\, L_{avg}} = \frac{\frac{2}{3}\ 2.169 \times 10^6}{\frac{1}{4}\pi\ (1.035)^2\ 170} = 1.01 \times 10^4 \qquad (F.4)$$

$$= \frac{V_{pg}}{\frac{1}{4}\pi\, d_{pg}^2\, L_{avg}} = \frac{1/3\ 2.169 \times 10^6}{\frac{1}{4}\pi\ (0.2)^2\ 170} = 1.35 \times 10^5 \qquad (F.5)$$

The helium coolant enters the blanket at 300 °C and exits at 500 °C. An average coolant temperature inside the blanket is therefore 400 °C. Being in direct contact with the breeding material, the average purge gas temperature is necessarily higher than that for the coolant, but not so high as the breeder edge temperature (approximately 525 °C). A value of 425 °C was chosen for the purge gas temperature. Given the following values for the pressure and temperature of the helium purge gas and helium coolant:

$$P_{He,pg} = 1 \text{ atm} \qquad T_{pg,avg} = 425\ ^\circ C \qquad (F.6)$$

$$P_{He,c} = 50 \text{ atm} \qquad T_{c,max} = 500\ ^{o}C$$
$$T_{c,avg} = 400\ ^{o}C$$
$$T_{c,low} = 300\ ^{o}C \qquad (F.7)$$

the helium property values were obtained from the formulas presented in Appendix C. The results are tabulated in Table F-2.

The STARFIRE-Interim Report stated a "low mass flow rate" for the purge gas system without specifying any vital parameters. A maximum flow rate of 1 ft/sec (30.48 cm/sec) for such a small channel was set, giving a total mass flow rate for the purge gas of

$$w_{pg} = N_{pg}\, \rho_{pg}\, u_{pg}\, \tfrac{1}{4}\pi\, d_{pg}^2 = 9.005 \text{ gm/sec} \qquad (F.8)$$

This corresponds to a total volumetric flow rate for the purge gas of:

$$Q_{pg} = N_{pg}\, u_{pg}\, \tfrac{1}{4}\pi\, d_{pg}^2 = 1.293 \times 10^{5} \text{ cm}^3/\text{sec} \qquad (F.9)$$

The total helium coolant mass flow into the blanket was given as 1900 kg/sec. From this, a value of u_B, the blanket helium coolant velocity, was determined:

$$u_B = \frac{w_B}{\rho_{B,avg}\, N_c\, \tfrac{1}{4}\pi\, d_B^2}$$

$$= \frac{1.9 \times 10^{6} \text{ g/sec}}{3.616 \times 10^{-3} \text{ g/cm}^3 \; 1.01 \times 10^{4}\, \tfrac{1}{4}\pi\, (1.035\text{cm})^2}$$

$$= 6.183 \times 10^{4} \text{ cm/sec} \qquad (F.10)$$

The Reynold's Number (Re) for the purge gas system and the helium coolant inside the blanket are respectively:

Table F-2

Helium Property Values

	PURGE GAS	COOLANT		
	@ T = 425 °C	@ T = 500 °C	@ T = 400 °C	@ T = 300 °C
ρ (gm/cm^3)	6.966×10^{-5}	3.366×10^{-3}	3.616×10^{-3}	4.247×10^{-3}
ν (cm^2/sec)	4.993	1.185×10^{-1}	9.382×10^{-2}	7.164×10^{-2}
D_G (cm^2/sec)	6.716	1.61×10^{-1}	1.26×10^{-1}	9.51×10^{-2}

$$Re_{pg} = \frac{u_{pg}\, d_{pg}}{\nu_{pg}} = 1.221 \qquad (F.11)$$

$$Re_{B,avg} = \left.\frac{u_B\, d_B}{\nu_B}\right|_{T=400^{\circ}C} = 6.82 \times 10^5 \qquad (F.12)$$

Because the purge gas flow is laminar, and the coolant flow is turbulent within the blanket two different correlations for the Nusselt Number (and hence, the mass transfer coefficient for helium gas) must be used[64]:

for laminar flow (uniform surface concentration):

$$Nu_{\infty} \equiv \frac{h\, d}{D_G} = 3.66 \qquad (F.13)$$

for turbulent flow:

$$Nu \equiv \frac{h\, d}{D_G} = 0.023\, Re^{0.83}\, Sc^{0.44} \qquad (F.14)$$

where $Sc \equiv \frac{\nu}{D_G}$.

Using the helium property values from Table F-2 and the aforementioned system parameters, the mass transfer coefficients for the purge gas and helium coolant in the blanket are respectively,

$$h_{pg} = 122.9 \quad cm/sec \qquad (F.15)$$

$$h_B = 170.7 \quad cm/sec \qquad (F.16)$$

F.2 Coolant Loop Parameters

There are six primary coolant loops leading out of the blanket, each one containing one steam generator and one helium circulator. A total pipe length of 125 m per loop was given, as well as a typical pipe diame-

ter of 1.25 m. It was assumed that the pipe lengths for the "hot" and "cold" legs were equal (i.e., $L_{HP} = L_{CP} = \frac{1}{2}$ 125 m = 62.5 m) and the diameter was the same for both the "hot" pipe and "cold" pipe. The helium mass flow rate per loop is necessarily 317 kg/sec ($w_B/6$), with a corresponding helium velocity of 100 m/sec. The temperature of the "hot" leg segment of the coolant is 500 °C and that for the "cold" leg is 300 °C. The average temperature of the helium coolant flowing through the steam generator is therefore 400 °C.

A typical steam generator is the basic shell and tube heat exchanger, with the hot helium flowing in the shell side, and high pressure (1800 psig) water/steam flowing on the tube side (T_{in} = 204 °C, T_{out} = 427 °C). Preliminary sizing for the heat exchanger done in the Interim Report[8] has deduced an overall height of 9.2 m and overall diameter of 4.7 m. The total tube heat transfer area is 5440 m² consisting of 375 tubes (I.D. of 2.54 cm) carrying the water. The tubes have a 2.0 mm thickness, and an average wall temperature of 350 °C.

The rest of the helium coolant parameters for the heat transport loop are calculated based on the above information. The volum of helium in the "hot" and "cold" pipes (for one loop) are the same, and equal to:

$$V_{c_{HP,1}} = V_{c_{CP,1}} = \tfrac{1}{4}\pi d_P^2 L_P = 7.67 \times 10^7 \text{ cm}^3 \qquad (F.17)$$

The Reynolds and Schmidt Numbers for the helium in the "hot" and "cold" pipe segments of the coolant loop are determined with the assistance of the property values presented in Table F-2.

$$Re_{HP} = \left.\frac{u_P d_P}{\nu_{HP}}\right|_{T=500\,^\circ C} = 1.055 \times 10^7 \qquad (F.18)$$

$$Sc_{HP} = \left.\frac{\nu}{D_G}\right|_{T=500\,^\circ C} = 0.736 \qquad (F.19)$$

$$Re_{CP} = \left.\frac{u_P\, d_P}{\nu_{CP}}\right|_{T=300^\circ C} = 1.745 \times 10^7 \qquad (F.20)$$

$$Sc_{CP} = \left.\frac{\nu}{D_G}\right|_{T=300^\circ C} = 0.753 \qquad (F.21)$$

These flow parameters are then used in Equation (F.14) for determining the mass transfer coefficient in a turbulent flow regime.

$$h_{HP} = 17.473 \quad cm/sec \qquad (F.22)$$

$$h_{CP} = 15.833 \quad cm/sec \qquad (F.23)$$

Next, the helium flow parameters unside the steam generator are calculated. The flow area for the helium flowing past a bark of tubes is:

$$A_f = A_{SG} - (\#\ of\ tubes)\, A_{tube}$$

$$= \tfrac{1}{4}\pi \left[d_{SG}^2 - N_t (OD)_t^2 \right] \qquad (F.24)$$

where $d_{SG} = 470$ cm

$N_t = 375$

$OD_t = ID + 2\,(thickness) = (2.54 + 2(0.2))$ cm

The wetted perimeter is just $\pi(d_{SG} + N_t OD_t)$. The hydraulic diameter for helium flow within the steam generator (or, heat exchanger) is

$$d_{HX} = \frac{4A_f}{P_w} = \frac{4\ (1.709 \times 10^5)\ cm^2}{4.940 \times 10^3\ cm}$$

$$= 1.384 \times 10^2 \quad cm \qquad (F.25)$$

The average velocity of helium in the steam generator is

$$u_{HX} = \left.\frac{w_{HX}}{\rho_{HX} A_f}\right|_{T=400^\circ C} = 5.130 \times 10^2 \quad \text{cm/sec} \qquad (F.26)$$

where the mass velocity is the same as before for flow around one loop (317 kg/sec). The average Reynolds and Schmidt Numbers for the helium are thus

$$Re_{HX} = \left.\frac{u_{HX}\, d_{HX}}{\nu_{HX}}\right|_{T=400^\circ C} = 7.568 \times 10^5 \qquad (F.27)$$

$$Sc_{HX} = \left.\frac{\nu_{HX}}{D_G}\right|_{T=400^\circ C} = 0.7446 \qquad (F.28)$$

Again, substituting these values into the turbulent coorelation for the Nusselt Number, one obtains the average mass transfer coefficient for the helium inside the heat exchanger:

$$h_{HX} \cong 1.394 \quad \text{cm/sec} \qquad (F.29)$$

The volume of helium inside one heat exchanger is $V_{c_{HX}} = V_{HX} - V_{H_2O} - V_{tubes}$. This can be written:

$$V_{c_{HX,1}} = L_{SG} \tfrac{1}{4} \pi \left[d_{SG}^2 - N_t (OD)_t^2 \right]$$

$$= 1.572 \times 10^8 \quad \text{cm}^3 \qquad (F.30)$$

The volume of helium in one loop is therefore $V_{c_{HP}} + V_{c_{HX}} + V_{c_{CP}} = 3.104 \times 10^8$ cm^3. The total amount of helium coolant in this reference design is six times $V_{c,loop} + V_{c,blanket}$. Using the value for $V_{c,blanket}$ calculated previously, the total helium coolant volume is

$$V_c = 1.865 \times 10^9 \quad \text{cm}^3 \qquad (F.31)$$

F.3 System Structure Parameters

The system parameters for the metal composing the breeder tube wall, the "hot" and "cold" pipes and that for the heat transfer surface wall will now be considered. The breeder tube wall metal was chosen to be a ferritic steel. For a stainless stell operating at a maximum structure temperature of 560 °C, the tritium diffusion coefficient from Appendix B is 3.82×10^{-6} cm²/sec. The thickness of the blanket metal wall was not specified in the Interim Report, so the value designated by the STAR-FIRE Final Design was used: $x_m = 0.15$ cm. The area available for tritium permeation from the breeding zone into the blanket coolant is calculated from

$$A_m = N_c \pi (d_B + 2x_m) L_{\text{coolant tube}}$$

$$= 7.201 \times 10^6 \quad \text{cm}^2 \qquad \text{(F.32)}$$

The volume of breeder tube metal is just $V_m = A_m x_m$, or 1.080×10^6 cm³.

The metal for the helium coolant piping system was assumed to be the same for both the "hot" and "cold" legs: 347-SS. Assuming that in steady-state, the pipe metal operates at a temperature approaching that of the fluid being carried within it, then

$$T_{HP} \cong T_{c,HP} = 500 \ ^\circ\text{C} \qquad \text{(F.33)}$$

$$T_{CP} \cong T_{c,CP} = 300 \ ^\circ\text{C} \qquad \text{(F.34)}$$

Using the tritium diffusivity data for 347-SS presented in Appendix B, the corresponding diffusion coefficients for the "hot" and "cold" pipe metals are respectively:

$$D_{HP} = 1.40 \times 10^{-6} \quad \text{cm}^2/\text{sec} \qquad \text{(F.35)}$$

$$D_{CP} = 5.79 \times 10^{-8} \quad \text{cm}^2/\text{sec} \qquad \text{(F.36)}$$

The inside surface area of both the "hot" and "cold" legs are equivalent, and equal to:

$$A_{HP,1} = A_{CP,1} = \pi\, d_P\, L_P = 2.454 \times 10^6 \text{ cm}^2 \qquad \text{(F.37)}$$

Assuming a typical metal thickness of 4 inches (10.16 cm) for such a large diameter pipe (125 cm) carrying high pressure gas (50 atm), the volume of metal for one segment is:

$$V_{HP,1} = V_{CP,1} = A_{HP,1}\, x_{HP} = 2.494 \times 10^7 \text{ cm}^3 \qquad \text{(F.38)}$$

Since there are six primary coolant loops, the total areas and volumes represented in the STARFIRE-Interim Design are:

$$A_{HP} = A_{CP} = 6\ (2.454 \times 10^6)\ \text{cm}^2 = 1.472 \times 10^7\ \text{cm}^2 \qquad \text{(F.39)}$$

$$V_{VP} = V_{CP} = 6\ (2.494 \times 10^7)\ \text{cm}^3 = 1.496 \times 10^8\ \text{cm}^3 \qquad \text{(F.40)}$$

The steam generator is constructed of Croloy (Fe-2¼Cr-1Mo). At the designated average tube temperature of 350 °C, the value for the tritium diffusion coefficient calculated from Appendix B, is $D_{HX} \cong 1.75 \times 10^{-6}$ cm²/sec. With a tube heat transfer area of 5.440×10^7 cm² and tube thickness of 0.2 cm, the volume of Croloy metal per heat exchanger is equal to 1.088×10^7 cm³. Again, because there are a total of six helium/water heat exchangers for the plant, the values used in the permeation model for the heat transfer area and metal volume are

$$A_{HX} = 6\ (5.440 \times 10^7)\ \text{cm}^2 = 3.264 \times 10^8\ \text{cm}^2 \qquad \text{(F.41)}$$

$$V_{HX} = 6\ (1.088 \times 10^7)\ \text{cm}^3 = 6.528 \times 10^7\ \text{cm}^3 \qquad \text{(F.42)}$$

A summary of the system parameters for the STARFIRE-Interim Reference Design is given in Tables F-3 through F-5 for easy reference. Some of these values are required for input to the permeation model developed in Chapter 2.

Table F-3

STARFIRE-Interim Design System Parameters:

Plasma and Breeding Zone

PLASMA	
continuous burn *	
nominal power level	3800 MW_t *
BREEDING ZONE	
breeder	Li_2O *
breeding ratio	1.05 *
S	57.64 Ci/sec *
ρ_b	2.013 gm/cm^3
V_b	4.94×10^6 cm^3
m_b	9.94×10^6 gm
$S_b \equiv S/V_b$	1.167×10^{-5} $Ci/cm^3 sec$
$T_{b,avg}$	650 °C
T_{edge}	525 °C
D_b	5×10^{-11} cm^2/sec
r_p	1.0×10^{-3} cm
$N_p \equiv 3V_b/4\pi r_p^3$	1.18×10^{15}

* denotes parameters that were explicitly specified in Ref. (8)

Figure F-4

STARFIRE-Interim Design System Parameters:
Helium Purge Gas System and Coolant Loop

	Helium Purge Gas System	Helium Coolant in: Blanket	"Hot" Pipe	HX	"Cold" Pipe
Pressure (atm)	1 *	50 *	50 *	50 *	50 *
T_{avg} (°C)	425	400	500 *	400	300 *
D_G (cm²/sec)	6.716	1.26×10^{-1}	1.61×10^{-1}	1.26×10^{-1}	9.51×10^{-2}
ρ (gm/cm³)	6.966 x 10^{-5}	3.616×10^{-3}	3.366×10^{-3}	3.616×10^{-3}	4.247×10^{-3}
ν (cm²/sec)	4.993	9.382×10^{-2}	1.185×10^{-1}	9.382×10^{-2}	7.164×10^{-2}
d (cm)	0.2	1.035 *	1.25×10^{2} *	1.384×10^{2} *	1.25×10^{2} *
w (gm/sec)	9.005	1.90×10^{6} *	3.17×10^{5} *	3.17×10^{5} *	3.17×10^{5} *
u (cm/sec)	30.48	6.183×10^{4}	1.0×10^{4} *	5.130×10^{2}	1.0×10^{4} *
V (cm³)	7.23×10^{5}	1.446×10^{6} †	4.602×10^{8} †	9.432×10^{8} †	4.602×10^{8} †
Q (cm³/sec)	1.293×10^{5}	5.254×10^{8}	9.417×10^{7}	8.767×10^{7}	7.464×10^{7}
Re	1.221	6.82×10^{5}	1.055×10^{7}	7.568×10^{5}	1.745×10^{7}
h (cm/sec)	122.9	170.7	17.473	1.394	15.833

Note: * denotes parameters that were explicitly specified in Ref. (8)

† The total helium coolant volume for this plant is $V_c = V_{c_B} + V_{c_{HP}} + V_{c_{HX}} + V_{c_{CP}}$, or $V_c = 1.865 \times 10^{9}$ cm³.

Table F-5

STARFIRE-Interim Design System Parameters:
Metal Structure Property Values

		Breeder Tube	"Hot" Pipe	HX	"Cold" Pipe
Type		Ferritic Steel*	347-SS	Croloy *	347-SS
T_{avg}	(^{o}C)	560 †	500	350 *	300
D	(cm^2/sec)	3.82×10^{-6}	1.40×10^{-6}	1.75×10^{-6}	5.79×10^{-8}
A	(cm^2)	7.201×10^{6}	1.472×10^{7}	3.264×10^{8}*	1.472×10^{7}
x	(cm)	0.15	10.16	0.2 *	10.16
V	(cm^3)	1.080×10^{6}	1.496×10^{8}	6.528×10^{7}*	1.496×10^{8}
L_{loop}	(cm)	- - -	6.25×10^{3}	- - -	6.25×10^{3}

Note: * denotes parameters that were explicitly specified in Ref. (8)

† maximum metal temperature

APPENDIX G GA FRM - SYSTEM PARAMETERS

The reference design reported in Ref. (11) is a preliminary conceptual design of a small ($\sim$ 100 MW_e) pilot plant fusion reactor based on a beam-sustained field-reversed mirror confinement scheme. General Atomic Company had responsibility for the blanket, shield and power conversion system design as reported in Ref. (11) for the joint (GA/LLL/PG&E) project on the Definition and Conceptual Design of a Small Fusion Reactor.

Since this design was chosen for application of the steady-state fluid/metal- limited tritium permeation model presented in Section 4.1, only those system parameters of use in the model's equations will be presented here. A summary of these parameters is given in Table G-1. Since the model concentrates on the operating conditions within the steam generator, those parameters are used to calculate the flow parameters.

Hot helium flows to the steam generator through a single lower duct and flows up through the central steam generator duct (ID $\sim$ 61 cm). The gas turns 180° and flows across a flow distribution screen and then downward over the helical coil EES* bundle in cross-counterflow to the steam and water. The cold helium then exits the steam generator through a lower single return duct. This arrangement is depicted in Figure G-1.

The helium flow area in the main steam generator is calculated according to the following:

$$A_f = \frac{1}{4}\pi\left[OD_b^2 - ID_b^2 - N_t\left[ID_t + 2t\right]^2\right] \qquad (G.1)$$

The wetted perimeter experienced by the helium inside the steam generator is given by

$$P_w = \pi\left[OD_b + ID_b + N_t\left[ID_t + 2t\right]\right] \qquad (G.2)$$

The equivalent diameter d is defined by the following equation:

* EES is the acronym for the economizer-evaporator-superheater.

Table G-1

System Parameters for the GA FRM

PRIMARY COOLANT LOOP		Helium
Coolant Volume		16 m^3
Average Temperature		710 ^oK
MAIN STEAM GENERATOR		Incoloy 800
Shell Side (Helium)		
Flow rate	(w_{He})	26.3 kg/sec
Temperature	(In/Out)	558 ^oK / 858 ^oK
Pressure		5.58 MPa (55 atm)
Tube Side (Water/Steam)		
Flow rate		15.5 kg/sec
Temperature	(In/Out)	445 ^oK / 755 ^oK
Pressure		5.96 MPa (59 atm)
Tubes		
Number of tubes	(N_t)	50
Tube size	(ID_t,t)	2.54 cm x 0.38 cm
Tube bundle ID_b		61 cm
Tube bundle OD_b		142 cm
Tube bundle height	(L_b)	371 cm
Heat transfer surface area	(A_{HX})	282.9 m^2
Overall Height		518 cm

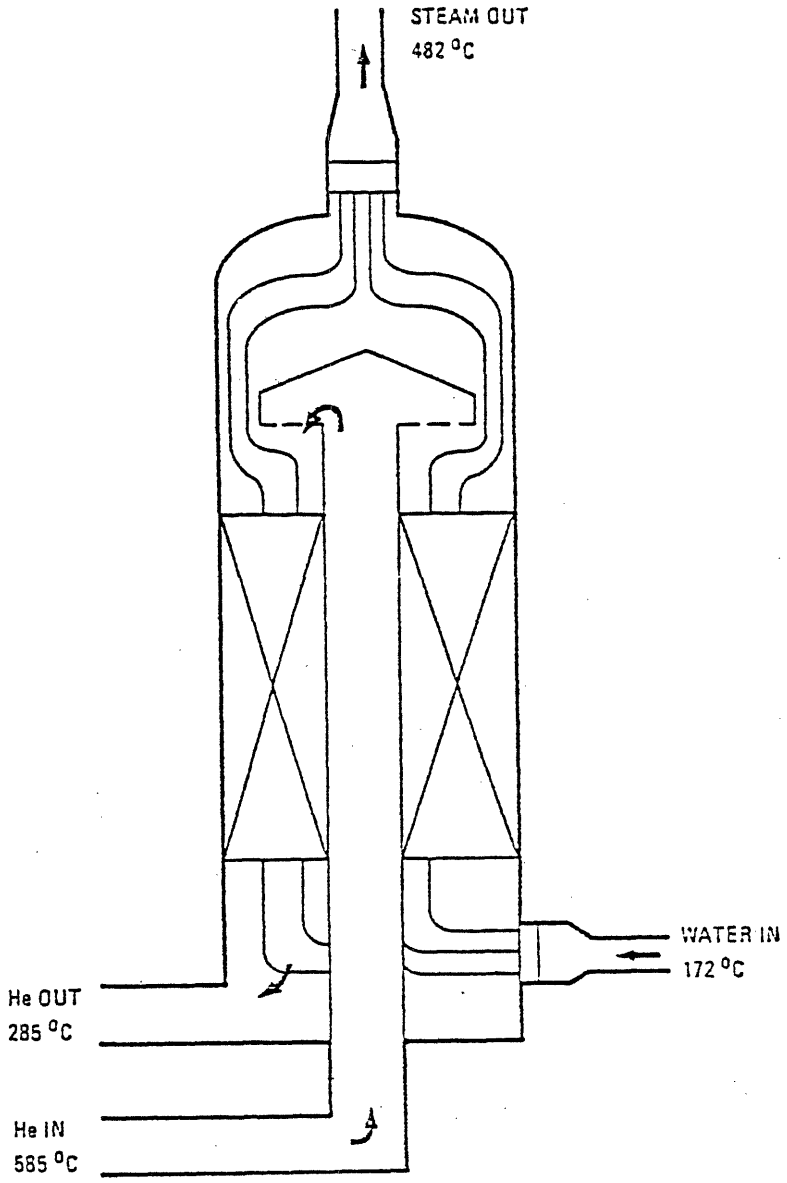

Figure G-1

GA FRM[11] Main Steam Generator

(Figure taken from Ref. (11))

$$d = \frac{4 A_f}{P_w} \qquad (G.3)$$

The mass flux of helium in the steam generator is given by:

$$G_{He} = \frac{w}{A_f} \qquad (G.4)$$

The dimensionless flow parameters, Reynolds Number and Schmidt Number, are given by the following relationships:

$$Re = \frac{G\,d}{\mu} \qquad (G.5)$$

$$Sc = \frac{\mu}{\rho\, D_G}$$

The helium property values are functions of the temperature and pressure. However only the functional dependence on temperature is retained for the equations given by Zarchy and Axtmann[9] which are evaluated at 50 atm. Repeating those helium property equations from Zarchy and Axtmann[9] for the viscosity μ, the tritium diffusivity D_G, and the Henry's Constant K_H, and from Appendix C for the density ρ:

$$\mu\,(50\ \text{atm}, T) = 113 + 0.33\ T(^{\circ}K) \times 10^{-6} \quad (\text{gm/cm-sec}) \qquad (G.6)$$

$$D_G\,(50\ \text{atm}, T) = 0.012 \left(\frac{T\,(^{\circ}K)}{273}\right)^{1.5} \quad (\text{cm}^2/\text{sec}) \qquad (G.7)$$

$$K_H\,(50\ \text{atm}, T) = \frac{7.21 \times 10^{-4}}{T\,(^{\circ}K)} \quad (\text{kg/m}^3\text{-Pa}) \qquad (G.8)$$

$$\rho\,(50\ \text{atm}, T) = \frac{2.428}{T\,(^{\circ}K)} \quad (\text{gm/cm}^3) \qquad (G.9)$$

Substitution of the system parameters in Table G-1 into Equations (G.1) through (G.10) yield the parameters of interest for use as input to the model described in Section 4.1. The results are summarized in Table G-2.

Table G-2

Input Parameters for GA FRM

A_f	(cm^2)	1.249×10^{4}
d	(cm)	43.22
x	(cm)	0.38
G_{He}	(gm/cm^2-sec)	2.106
μ (710°K)	(gm/cm-sec)	3.473×10^{-4}
D_G(710°K)	(cm^2/sec)	5.033×10^{-2}
ρ (710°K)	(gm/cm^3)	3.42×10^{-3}
K_H(710°K)	(kg/m^3-Pa)	1.015×10^{-6}
Re		2.62×10^{5}
Sc		2.02
K_p(710°K)[a]	(kg/m-day-$Pa^{\frac{1}{2}}$)	6.23×10^{-10}

Note: a - Expression for the tritium permeability in Incoloy 800 is that given by Zarchy and Axtmann[9].

REFERENCES

(1) W.M. Stacey Jr. et al., "Tokamak Experimental Power Reactor Conceptual Design", ANL/CTR-76-3 (1976).

(2) R.G. Mills et al., "A Fusion Power Plant", Princeton Plasma Physics Laboratory, MATT-1050 (August 1974).

(3) B. Badger et al., "Wisconsin Tokamak Reactor Design", University of Wisconsin, UWFDM-68 (March 1974).

(4) V.A. Maroni, "An Analysis of Tritium Distribution and Leakage Characteristics for Two Fusion Reactor Reference Designs", in Proc. 5th Symp. on Engineering Problems of Fusion Research (November 1973) pp. 206-211.

(5) V.A. Maroni, "Control of Tritium Permeation Through Fusion Reactor Structural Materials", Environmental Control Symp., CONF-781109-12 (1978)

(6) T.J. Kabele, A.B. Johnson and L.K. Mudge, "Tritium Source Terms for Fusion Power Plants", BNWL-2018 (September 1976).

(7) J.M. Mintz, T.S Elleman and K. Verghese, "Tritium Diffusion in Fusion Reactor Blankets", Nuclear Technology, 31(November 1976)172-182.

(8) "STARFIRE, A Commercial Tokamak Reactor: An Interim Report", Argonne National Laboratory, McDonnell Douglas Astronautics Company, General Atomic Company, The Ralph M. Parsons Company, ANL/FPP/TM-125 (December 1979)

(9) A. Zarchy and R. Axtmann, "Limitations on Tritium Transport Through Fusion Reactors", Nuclear Technology, 39(August 1978)258-265.

(10) B. Badger et al., "UWMAK-II, A Conceptual Tokamak Reactor Design", University of Wisconsin, UWFDM-112 (October 1975).

(11) General Atomic Company Project Staff, "Blanket, Shield and Power Conversion System for a Small Field-Reversed Mirror Fusion Reactor", GA-A15533 (July 1979).

(12) A.P. Fraas, "Conceptual Design of the Blanket and Shield Region and Related Systems for a Full Scale Toroidal Fusion Reactor", ORNL-TM-3096 (1973).

(13) J.R. Powell et al., "Studies of Fusion Reactor Blankets with Minimum Radioactive Inventory and with Tritium Breeding in Solid Lithium Compounds: A Preliminary Report", BNL-18236 (June 1973).

(14) K. Sako et al., "Conceptual Design of JAERI Demonstration Fusion Reactor" Japanese Atomic Energy Research Institute, in Proc. Second Topical Meeting on the Technology of Controlled Nuclear Fusion, Richland, WA (September 1976).

(15) U.S. Contribution to International Tokamak Reactor Workshop, "INTOR, Phase-1", USA INTOR/80-1 (June 1980).

(16) D.L. Smith, R.G. Clemmer and J.W. Davis, "Assessment of Solid Breeding Blanket Options for Commercial Tokamak Reactors", in Proc. 8th Symp. on Engineering Problems of Fusion Research (1979) pp. 433-438.

(17) "STARFIRE - Final Design", Argonne National Laboratory, McDonnell-Douglas Astronautics Company, General Atomic Company, The Ralph M. Parsons Company, ANL/FPP-80-1 (October 1980).

(18) C.G. Bathke, R.A. Krakowski and H.S. Cullingford, " Tritium Transport in a Packed-Bed Li_2O Fusion Blanket", LASL, ANS Transactions, 33 (1979) 72.

(19) D.R. Olander, Fundamental Aspects of Nuclear Reactor Fuel Elements, TID-26711-P1, ERDA (1976).

(20) J.R. Powell, "Tritium Recovery from Fusion Blankets Using Solid Lithium Compounds - I: Design and Minimization of Tritium Inventory", in Proc. of International Conference on Radiation Effects and Tritium Technology for Fusion Reactors, CONF-750989, Vol. III (March 1976) pp. 197-231.

(21) R. Wiswall and E. Wirsing, "The Removal of Tritium From Fusion Reactor Blankets", BNL-50748 (October 1977).

(22) R.H. Wiswall and E. Wirsing, "Tritium Recovery from Fusion Blankets Using Solid Lithium Compounds - II: Experiments on Tritium Removal and Absorption", in Proc. of International Conference on Radiation Effects and Tritium Technology for Fusion Reactors, CONF-750989, Vol. III (March 1976) pp. 232-252.

(23) R.H. Wiswall and E. Wirsing, "The Removal of Tritium from Solid CTR Blanket Materials: A Progress Report", BNL-19766 (February 1975).

(24) M.A. Abdou, L.J. Wittenberg and C.W. Maynard, "A Fusion Design Study of Nonmobile Blankets with Low Lithium and Tritium Inventories", Nuclear Technology, 26(August 1975)400-419.

(25) E.H. Van Deventer et al., "A Review of Fusion-Related Experimentation on Blanket/Tritium Processing and Hydrogen Isotope Migration at the Argonne National Laboratory", in Proc. of Tritium Technology in Fission, Fusion and Isotopic Applications, American Nuclear Society National Topical Meeting (April 1980).

(26) K. Okula and D.K. Sze, "Tritium Recovery from Solid Breeders: Implications of Existing Data", in Proc. of Tritium Technology in Fission, Fusion and Isotopic Applications, American Nuclear Society National Topical Meeting (April 1980)

(27) W.A. Stark, Jr., "Diffusion Analyses For Systems of Spherical Particles", Nuclear Technology, 26(May 1975)35-45.

(28) General Atomic Company Project Staff, "Conceptual Design Study of a Noncircular Tokamak Demonstration Fusion Reactor", GA-A13992 (November 1976).

(29) D.L. Smith, R.G. Clemmer, V.Z. Jankus and J. Rest, "Analysis of In-Situ Tritium Recovery from Solid Fusion Reactor Blankets" ANL, in Proc. Fourth Topical Meeting on the Technology of Controlled Nuclear Fusion (October 1980).

(30) D. Steiner et al., "ORNL Fusion Power Demonstration Study: Interim Report", ORNL/TM-5813 (March 1977).

(31) R.G. Clemmer, E.M. Larsen and L.J. Wittenberg, "Tritium Handling, Breeding and Containment in Two Conceptual Fusion Reactor Designs: UWMAK-II and UWMAK-III", Nuclear Engineering and Design, 39(1976) 85-98.

(32) E.F. Johnson, "Fusion Reactor Fuel Processing", in The Chemistry of Fusion Technology, D.M. Gruen ed., (Plenum Press, New York, 1972) pp. 199-213.

(33) J. Darvas, "Tritium Technology in Fusion Devices", in Proc. of International Conference on Radiation Effects and Tritium Technology for Fusion Reactors, CONF-750989, Vol. III (March 1976) pp. 1-31.

(34) J.R. Powell et al., "Minimum Activity Blankets for Commercial and Experimental Power Reactors", in Proc. 5th Symp. on Engineering Problems of Fusion Research (November 1973) pp. 163-174.

(35) A. Sieverts, Z. Physik. Chem., 60(1907)129.

(36) R.E. Stickney, "Diffusion and Permeation of Hydrogen Isotopes in Fusion Reactors: A Survey", in The Chemistry of Fusion Technology, D.M. Gruen ed., (Plenum Press, New York, 1972) pp. 241-319.

(37) V.A. Maroni and E.H. Van Deventer, "Materials Considerations in Tritium Handling Systems", Journal of Nuclear Materials, 85 & 86(1976) 257-269.

(38) R.C. Weast ed., Handbook of Chemistry and Physics, 51st Edition, The Chemical Rubber Co., publishers, Cleveland, OH (1971) pp. F-80.

(39) O. Richardson, Phil. Mag. Serv. 6, 7(1904)266.

(40) R.L. Levin and R.E. Stickney, "Permeation of Hydrogen Isotopes Through Fusion Reactor Materials", in Proc. 5th Symp. on the Engineering Problems of Fusion Research (November 1973) pp. 212-216.

(41) C.W. Kuehler and R.C. Axtmann, "Tritium Permeation Through Metals and Alloys", in Proc. of 6th Symp. on the Engineering Problems of Fusion Research (1975) pp. 1154-1158.

(42) T.S. Elleman and K. Verghese, "Tritium Diffusion in Fusion Reactor Materials", in Proc. of the Symp. on Tritium Technology Related to Fusion Reactor Systems, Mound Laboratory, ERDA-50 (October 1974).

(43) K. Verghese et al., "Hydrogen Permeation Through Non-metallic Solids", Journal of Nuclear Materials, 85 & 86(1979)1161-1164.

(44) C. Alexander et al., "Tritium Transport in Non-Metallic Solids", in Proc. of the CTR Insulator Conference, CONF-760558-6, Los Alamos, NM (June 1976).

(45) T.S. Elleman, L.R. Zumwalt and K. Verghese, "Hydrogen Transport and Solubility in Non-Metallic Solids", in Proc. of the Third Topical Meeting on the Technology of Controlled Nuclear Fusion, CONF-780508, (May 1978) pp. 763-770.

(46) E.H. Van Deventer, "Hydrogen Permeation Characteristics of Aluminum-coated and Aluminum-modified Steels", Journal of Nuclear Materials, 88(1980)168-173.

(47) V.A. Maroni, E. Veleckis and E.H. Van Deventer, "A Review of ANL Research on Lithium-Hydrogen Chemistry and Tritium-Containment Technology", in Proc. of the Symp. on Tritium Technology Related to Fusion Reactor Systems, Mound Laboratory, ERDA-50 (October 1974).

(48) W.F. Calaway et al., "Review of the ANL Program on Liquid Lithium Processing and Tritium Control Technology", ANL/FPP/TM-74 (November 1976).

(49) E.F. Johnson, "Fusion Reactor Fuel Processing", USAEC Report MATT-901 (June 1976).

(50) J.S. Watson, "An Evaluation of Methods for Recovering Tritium from the Blankets or Coolant Systems of Fusion Reactors", ORNL-TM-3794 (July 1972).

(51) J.T. Bell and J.D. Redman, "Tritium Permeation Through Metals Under Steam Conditions", in Proc. of 9th Symp. on Fusion Technology, EURATOM (1976) pp.345-350.

(52) A.S. Zarchy and R.C. Axtmann, "Tritium Permeation Through 304-Stainless Steel at Ultra-Low Pressures", Journal of Nuclear Materials, 79 (1979)110-117.

(53) J.T. Bell and J.D. Redman, "Tritium Permeation Through Steam Generator Materials", in Proc. 14th Intersociety Energy Conversion Engineering Conference (1979) pp. 1577-1582.

(54) R.A. Strehlow and H.C. Savage, "The Permeation of Hydrogen Isotopes Through Structural Metals at Low Pressures and Through Metals with Oxide Film Barriers", Nuclear Technology, 22(April 1974)127-137.

(55) J.S. Watson et al., "Current CTR-Related Tritium Handling Studies at ORNL", in Proc. Second Topical Meeting on the Technology of Controlled Nuclear Fusion, Richland, WA (September 1976).

(56) C.L. Huffine and J.M. Williams, Corrosion, 16(1960)430.

(57) E.H. Van Deventer, T.A. Renner, R.H. Pelto and V.A. Maroni, Journal of Nuclear Materials, 64(1977)241.

(58) H.D. Rohrig and R. Hecker, "In-Situ Formation of Protective Oxide Scales as Measured by Their Inhibiting Effect on High Temperature Hydrogen Permeability of Heat Exchanger Materials", in Proc. Second International Conference on Metallurgical Coatings, San Francisco, CA (March 1977).

(59) W.A. Swansiger, "Tritium Transport in Stainless Steels - Surface Effects", in Proc. of First Topical Meeting on Fusion Reactor Materials, Bal Harbour, FA (January 1979).

(60) T.S. Elleman and K. Verghese, "Surface Effects on Tritium Diffusion in Niobium, Zirconium and Stainless Steel", Journal of Nuclear Materials, 53(1974)299-306.

(61) J.T. Bell et al., "Tritium Permeation Through Incoloy 800 Oxidized In-Situ by Water Vapor", in Proc. of the Third Topical Meeting on the Technology of Controlled Nuclear Fusion, CONF-780508 (May 1978) pp. 757-762.

(62) V.A. Maroni et al., "Experimental Studies of Tritium Barrier Concepts for Fusion Reactors", in Proc. of International Conference on Radiation Effects and Tritium Technology for Fusion Reactors, CONF-750989, Vol. IV (March 1976) pp. 329-360.

(63) H.S. Carslaw and J.C. Jaeger, Conduction of Heat in Solids, Oxford at the Corendar Press (1959) pp. 243.

(64) W.M. Rohsenow and H. Choi, Heat, Mass and Momentum Transfer, Prentice Hall, Inc. (1961).

(65) H.D. Rohrig et al., "Studies on the Permeation of Hydrogen and Tritium in Nuclear Process Heat Installations", Nuclear Engineering and Design, 34(1975)157-167.

(66) A.B. Johnson and J.R. Young, "Environmental Considerations for Alternative Fusion Reactor Blanket Designs", in Proc. of the Symp. on Tritium Technology Related to Fusion Reactor Systems, Mound Laboratory, ERDA-50 (October 1974).

(67) A.P. Fraas, "Comparative Study of the More Promising Combinations of Blanket Materials", in Power Conversion Systems and Tritium Recovery and Containment Systems for Fusion Reactors, ORNL-TM-4999 (1975).

(68) P.W. Davison, "Environmental Compatibility" in "A Fusion Power Plant", Princeton Plasma Physics Laboratory, MATT-1050 (August 1974).

(69) R.B. Byrd et al., Transport Phenomena, John Wiley and Sons, Inc., New York (1960).

(70) R.E. Treybal, Mass Transfer Operations, McGraw-Hill Book Company, New York (1963).

(71) V.A. Maroni, "Tritium Distribution and Leakage" in "A Fusion Power Plant", Princeton Plasma Physics Laboratory, MATT-1050 (August 1974).

(72) R.W. Webb, "Permeation of Hydrogen in Metals", NAA-SR-10462, North American Aviation (1965).

(73) R.C. Weast and S.M. Selby, ed., Handbook of Chemistry and Physics, 48th Edition, The Chemical Rubber Company, Cleveland, OH (1967).

(74) W.M. Stacey et al., "Tokamak Experimental Power Reactor Studies", ANL/CTR-75-2 (June 1975).

(75) C.S. Caldwell et al., "A Survey of Lithium Compounds for Tritium Breeding Applications (Properties and References)", paper presented at the Fourth ANS Topical Meeting on the Technology of Controlled Nuclear Fusion (October 1980).

(76) P.J. Krane, "Safety Aspects of Thermonuclear Reactor Designs Employing Use of Lithium-Lead Alloys", S.M. Thesis, Nuclear Engineering, Massachusetts Institute of Technology (September 1980).

(77) T. Tanifuji et al., Journal of Nuclear Materials, 78-2(1978)422-424.

(78) D. Guggi, H. Ihle, A. Neubert and R. Wofle, "Tritium Release from $LiAlO_2$, Its Thermal Decomposition and Phase Relationship: γ-$LiAlO_2$ - Li_5AlO_8 -- Implications Regarding Its Use as a Blanket Material in FRT", in Proc. of International Conference on Radiation Effects and Tritium Technology for Fusion Reactors, CONF-750989, Vol. III (March 1976) pp. 416-432.

(79) D. Guggi, H.R. Ihle and U. Kurz, "Diffusion of Tritium in Neuton-Irradiated Lithium-Aluminum Oxides", in Proc. of the 9th Symp. on Fusion Technology, Pergamon Press (June 1976) pp. 337-344.

(80) D. Guggi, H.R. Ihle and U. Kurz, "Diffusion of Tritium in Neuton-Irradiated Microcrystalling β-Li_5AlO_4", in Proc. of the 10th Symp. on Fusion Technology (1978).

(81) J.B. Talbot and F.W. Wiffen, "Recovery of Tritium from Lithium-Sintered Aluminum Product (SAP) and Lithium-Aluminum Alloys", Journal of Inorganic Nuclear Chemistry, 41(1979)439.

(82) V.G. Vasiliev et al., "Investigation of the Physical-Chemical Properties of Irradiated Inorganic Compounds of Lithium Oxides, Aluminates and Silicates", US/USSR Workshop on Engineering and Economic Problems of ETF, Moscow and Leningrad (USSR) (September 1979).

(83) E. Veleckis, R.M. Yonco and V.A. Maroni, "Solubility of Lithium Deuteride in Liquid Lithium" Journal of Less-Common Metals, 55(1977) 85.

(84) T.A. Renner and D.J. Raue, "Tritium Permeation Through Fe-2¼Cr-1Mo Steam Generator Material", Nuclear Technology, 42(1979)312-319.

(85) V.A. Maroni et al., "Review of the Chemical, Physical and Thermal Properties of Lithium That Are Related to its Use in Fusion Reactors", ANL-8001 (March 1973).

(86) N.J. Hoffman, A. Darnell and J.A. Blink, "Properties of Lead-Lithium Solutions", UCRL-84273 (October 1980).

(87) F.J. Smith et al., "Chemical Equilibrium Studies of Tritium-Lithium and Tritium-Lithium Alloy Systems", in Proc. of International Conference on Radiation Effects and Tritium Technology for Fusion Reactors, CONF-750989, Vol. III (March 1976) pp. 539-553.

(88) J.B. Talbot, "Study of Tritium Removal from Fusion Reactor Blankets of Molten Salt and Lithium-Aluminum", ORNL/TM-5104 (March 1974).

(89) J.H. Owen et al., "Equilibrium and Kinetic Studies of Systems of H_2 Isotopes in Lithium Hydrides, Aluminum, $LiAlO_2$", in Proc. of International Conference on Radiation Effects and Tritium Technology for Fusion Reactors, CONF-750989, Vol. III (March 1976) pp.433-469.

(90) A. Aronson and F.J. Salzano, Inorganic Chemistry, 8(1969)1541.

(91) J.D. Fowler et al., Journal of the American Ceramic Society, 60(1977) no. 3-4, 155-161.

(92) J.W. Guthrie et al., "Properties of Hydride-Forming Metals and of Multilayer Hydrogen Permeation Barriers", Journal of Nuclear Materials, 53(1974)313-322.

(93) F. Waelbroek et al., "Hydrogen Solubilisation Into and Permeation Through Wall Materials", Journal of Nuclear Materials, 85 & 86(1979) 345-349.

(94) J.L. Cecchi, "Tritium Permeation and Wall Loading in the TFTR Vacuum Vessel", Journal of Vacuum Science Technology, 16(1979)no. 1, 58-70.

(95) "International Tokamak Reactor: Zero Phase", Report of the International Tokamak Reactor Workshop, International Atomic Energy Agency, Vienna (1980).

(96) W.G. Perkins, "Permeation and Outgassing of Vacuum Materials", Journal of Vacuum Science Technology, 10(1973)no. 4, 543-556.

(97) R.G. Hickman, "Tritium Problems in Fusion Reactor Systems", in Proc. of the Symp. on Tritium Technology Related to Fusion Reactor Systems, Mound Laboratory, ERDA-50 (October 1974).

(98) G.L. Downs, "Diffusion and Autoradiographic Investigations of the Tritium-304 Stainless Steel System", in Proc. of the Symp. on Tritium Technology Related to Fusion Reactor Systems, Mound Laboratory, ERDA-50 (October 1974).

(99) H.K. Perkins et al., "Tritium Holdup Due to Coatings on the First Wall of Fusion Reactors", in Proc. of the International Conference on the Radiation Effects and Tritium Technology for Fusion Reactors, CONF-750989, Vol. IV (March 1976) pp. 397.

(100) J. Austin et al., "Diffusion of Gases in Solids", ORO-3508-7 (December 1971).

(101) K.F. Chaney and G.W. Powell, "The Diffusivity of Tritium in 304 Stainless Steel in the Temperature Range 100°C - 300°C", Metallurgical Transactions, 1(1970)2356-2357.

(102) G. Schauman, J. Volkl and G. Alefield, "The Diffusion Coefficients of Hydrogen and Deuterium in Vanadium, Niobium, Tantalum by Gorsky-Effect Measurements", Physica Status Solidi, 42(1970)401-413.

(103) J. Volkl, and G. Schauman and G. Alefield, "Diffusional Relazation of H and D in V and Nb", Journal of Physical Chemical Solids, 31(1970) 1805-1809.

(104) R. Cantelli, F.M. Mazzolai and M. Nuovo, "Internal Friction Due to Long-Range Diffusion of H_2 and D_2 in Vanadium", Journal of Physical Chemical Solids, 31(1970)1811-1817.

(105) R.H. Doremus, "Delayed Elasticity Rsulting From Periodic Stress-Induced Atomic Diffusion", Journal of Physical Chemical Solids, 32 (1971)2211-2215.

(106) W.M. Mueller, J.P. Blackledge and G.G. Libowitz, Metal Hydrides, Academic Press, New York (1968) pp. 297.

(107) P. Gierszewski, B. Mikic and N. Todreas, "Property Coorelations for Lithium, Sodium, Helium, Flibe and Water in Fusion Reactor Applications", PFC-RR-80-12 (August 1980) pp. 8.

(108) R.H. Perry and C.H. Chilton, ed., Chemical Engineers' Handbook, 5th Edition, McGraw-Hill Inc. (1973) pp. 3-234.